



# D4.5 Floating Wind Installation Strategies

RAMBOLL / DTU / INNOSEA / JDR / UPC / COBRA / ESTEYCO

March 2023

#### Disclaimer:



This project has received funding from the European Union's Horizon 2020 Research and Innovation programme under grant agreement No 815083.

#### Project details:

Duration:  
1 Sep 2019 - 28 Feb 2023  
Grant agreement:  
No: 815083

## Document information

Deliverable number	D4.5
Deliverable name	Floating Wind Installation Strategies
Reviewed by	Pau Trubat Casal (UPC), Ignacio Romero de Ávila Senise (COBRA)
Date	31.03.2023
Work Package and Task	WP4, Task 4.5
Lead Beneficiary for this Deliverable	RAMBOLL

## Authors

Name	Organisation
Friedemann Borisade	RAMBOLL
Matti Schilling	RAMBOLL
Xiaoai Ren	RAMBOLL
Simon Tiedemann	RAMBOLL
Tom Bailey	RAMBOLL
Pierre Amiot	RAMBOLL
Jannis Espelage	RAMBOLL
Ron Scheffler	RAMBOLL
Jeff Davis	RAMBOLL
Sithik Aliyar	DTU
Henrik Bredmose	DTU

## Version control

Version	Date	Author	Description of Changes
1	2023-03-31	RAMBOLL	Final version for submission

# Table of Content

1	Nomenclature.....	5
2	Executive Summary .....	7
3	Introduction.....	10
4	Input Data and Baseline Conditions .....	11
4.1	Offshore Site and Layout .....	11
4.2	Floating Substructure Types .....	11
4.3	Anchor Type.....	12
4.4	Mooring System Configuration.....	12
4.5	Vessel and Equipment .....	12
4.5.1	Semi-Submersible Vessel .....	12
4.5.2	Heavy Lift Vessel.....	12
4.5.3	Anchor Handling Tug .....	12
4.5.4	ROV.....	13
4.5.5	Self-Propelled Modular Transporter .....	13
4.5.6	Onshore Crane .....	13
4.5.7	Offshore Access System .....	13
4.6	Environmental Conditions .....	13
4.6.1	Water Depth.....	13
4.6.2	Wind .....	13
4.6.3	Wave .....	14
4.6.4	Current .....	14
4.6.5	Tidal.....	14
5	Work Breakdown Structure and Method Statement .....	15
5.1	Anchor Installation .....	15
5.2	Mooring Line Pre-lay .....	17
5.3	Hook-up .....	19
5.4	Power Cable installation .....	23
5.5	Fabrication and Transportation.....	24
5.6	Launching Method.....	26
5.7	Potential Risk Assessment .....	29
6	Analysis Methodology and Results.....	30

6.1	Overview of Studies and Software .....	30
6.2	Environmental Load Calculation .....	30
6.2.1	Vessel Axis Convention.....	30
6.2.2	Wind Loads.....	31
6.2.3	Current Loads .....	31
6.2.4	Wave Loads .....	32
6.3	Towing Analysis .....	32
6.4	Suction Anchor Installation Analysis.....	33
6.5	Mooring Line Hook-Up Station Keeping Analysis .....	37
6.5.1	Floating Substructure Modelling.....	37
6.5.2	Mooring System Modelling .....	38
6.5.3	Force Allocation Calculation.....	39
6.5.4	Results for ActiveFloat Semi-submersible.....	39
6.5.5	Results for Windcrete Spar .....	41
6.6	Upending Analysis .....	43
6.6.1	Introduction .....	43
6.6.2	Methodology .....	44
6.6.3	HAWC2 Analysis for the Normal Sea State Conditions .....	46
6.6.4	Extreme Sea State Analysis .....	50
6.7	Conclusions.....	54
7	Weather Downtime Analysis and Cost Modelling.....	56
7.1	Guiding Principles and Assumptions .....	56
7.2	Weather Downtime Analysis .....	58
7.2.1	Simulation Model Description.....	58
7.2.2	Boundary Conditions.....	60
7.2.3	Weather Time Series Investigation .....	62
7.2.4	Results .....	64
7.3	Cost Modelling and Analysis.....	77
7.3.1	Approach .....	77
7.3.2	Project Scenarios.....	82
7.3.3	Key Assumptions .....	83
7.3.4	CAPEX Results From Marine Operations .....	85
7.3.5	Conclusion .....	89
8	Conclusion and Perspective .....	90
9	References.....	93

## 1 Nomenclature

Abbreviation	Description
AHT	Anchor Handling Tug Vessel
BOEM	Bureau of Ocean Energy Management
BP	Bollard Pull
CAPEX	Capital Expenditure
CSV	Construction Support Vessel
COG	Centre of Gravity
DAF	Dynamic Amplification Factor
DNV	Det Norske Veritas
DP	Dynamic Positioning
ECMWF	European Centre for Medium-Range Weather Forecasts
EPC	Engineer, Procure, Construct
FOWT	Floating Offshore Wind Turbine
GPS	Global Positioning System
HLV	Heavy Lift Vessel
HVAC	High Voltage Alternating Current
HVDC	High Voltage Direct Current
IAC	Inter-Array Cable
LCOE	Levelized Cost of Energy
LOA	Length Overall
MBL	Minimum Breaking Load
MPM	Most Probable Maximum
MWS	Marine Warranty Surveyor
NREL	National Renewable Energy Laboratory
O&G	Oil and Gas
OCV	Offshore Construction Vessel
O&M	Operations and Maintenance
OPEX	Operational Expenditure
OSS	Offshore Substation
PMC	Platform Mooring Connector
RNA	Rotor Nacelle Assembly
ROV	Remotely Operated Vehicle
SPA	Suction Pile Anchor

SPMT	Self-Propelled Modular Transporter
T&I	Transport and Installation
WAB	West of Barra
WBS	Work Breakdown Structure
WROV	Work-class Remotely Operated Vehicle
WTG	Wind Turbine Generator

## 2 Executive Summary

The purpose of this report is to investigate the time, cost and potential risks for T&I strategies of a floating offshore wind farm based on state-of-art offshore equipment and recommended methodologies. Many combinations of constructions, assembly methods and anchoring methods have to be considered as well as the involved T&I costs.

The impact on the time and costs of T&I mainly depends on the following factors:

- Availability of the hired equipment for transport and installation
- Number of items to be transported
- Dimension of the structure (anchors & substructure) to be transported
- Vessel lifting capacity
- Tug boats capacity
- Number of available vessels
- Delays due to bad weather conditions
- Costs of insurance
- etc.

In this study the T&I strategy for a commercial-scale reference floating wind farm of 80 units at 15 MW nameplate rating and two floating OSS is modelled with reference site conditions (Morro Bay, USA) for two different floater designs, i.e. Windcrete (spar) and ActiveFloat (semi-submersible). The operation steps and estimated available vessels are specified for the different substructure types. First, temporary marine operations are analysed using standard vessels with representative limiting factors such as lifting capacity and vessel motion to assess operational limits of the towing, anchor installation and hook-up campaigns. Based on these preliminary studies sequential weather downtime analyses are performed in a second step to estimate installation durations and associated cost.

**Table 2-1: Overview of T&I analyses.**

Study	Objective	Analysis	Tool	Outcome
<b>1 – Temporary marine operations (Chapter 6)</b>	Towing	Towing analysis	In-house Python	Required tug capacity and tug number; sailing speed
	Anchor installation	Simplified lifting analysis (through wave zone)	Ansys AQWA, OrcaFlex, Excel	Workability Hs-Tp combination
	Hook-up	Force allocation calculation	In-house Python	Tug capacity and heading control
<b>2 – Sequential weather downtime analysis (Chapter 7)</b>	Weather downtime, cost estimation	Work breakdown analysis, probabilistic cost model	Shoreline, Excel	Estimated project duration, operation costs

The workability of the selected vessels for different marine operations is estimated and summarised in Table 2-2. The actual operational limits for the execution phase are determined during the detailed project preparation phase. It has been noted that the marine warranty surveyor and the master of vessels may recommend additional working limits based on the actual circumstances. In such events, the most stringent limits prevail and shall not be exceeded. In addition, an analysis of the upending process of the Windcrete spar is carried out (not related to the ActiveFloat semi-submersible) to investigate limiting wave conditions during the operation. The results of

the upending analysis are not used to calibrate the sequential weather downtime analysis to ensure comparability between floating substructures concepts.

**Table 2-2: Summary of operational limits for temporary marine operations for the reference concepts.**

Item	ActiveFloat Semi-submersible	Windcrete Spar
<b>Anchor Installation</b>		
Significant Wave Height Hs	1.5 m for heading and following sea	1.5 m for heading and following sea
Peak Wave Period Tp	From 6 to 18 s	From 6 to 18 s
<b>Sailing to Offshore Site</b>		
Tug Boat Bollard Pull	2 tugs x 200 t	2 tugs x 120 t
Towing Speed	2.2 kn	2.1 kn
<b>Mooring Line Hook-up</b>		
Significant Wave Height Hs	Up to 3.0 m	Up to 3.0 m
Min. Required Tug Boat Bollard Pull	3 tugs x 142 t	3 tugs x 120 t

The sequential weather downtime analysis deploys assets (vessels and equipment) considering specific operational limits, and evaluates the work durations and waiting times for each asset in a site specific weather time series of each sub-campaign.

**Table 2-3: Summary of weather downtime analysis results at the reference site.**

Item	ActiveFloat Semi-submersible	Windcrete Spar
<b>Overall Campaign</b>		
Campaign Duration	920 d (P10) to 1430 d (P90)	985 d (P10) to 1477 d (P90)
Rel. Weather Down Time	43% (P10) to 63% (P90)	45% (P10) to 63% (P90)
<b>Anchor Installation</b>		
Campaign Duration	440 d (P10) to 943 d (P90)	559 d (P10) to 1209 d (P90)
Rel. Weather Down Time	60% (P10) to 81% (P90)	60% (P10) to 82% (P90)
<b>Mooring Line Pre-lay</b>		
Campaign Duration	437 d (P10) to 742 d (P90)	561 d (P10) to 1018 d (P90)
Rel. Weather Down Time	65% (P10) to 82% (P90)	63% (P10) to 79% (P90)
<b>Floating Foundation Hook-up</b>		
Campaign Duration	367 d (P10) to 684 d (P90)	503 d (P10) to 873 d (P90)
Rel. Weather Down Time	43% (P10) to 69% (P90)	50% (P10) to 71% (P90)
<b>Power Cable Installation</b>		
Campaign Duration	479 d (P10) to 1003 d (P90)	578 d (P10) to 1070 d (P90)
Rel. Weather Down Time	57% (P10) to 69% (P90)	58% (P10) to 78% (P90)



A probabilistic CAPEX analysis for the marine operations is conducted based on the results of the weather downtime analysis and the vessel requirements. Both floater concepts form one scenario. The results are shown in Table 2-4. The high and the low range describe the maximum relative deviation to the P50 value.

**Table 2-4: Summary of the probabilistic CAPEX assessment for both floater concepts.**

Scenario	P10	P50	P90	Low Range	High Range
<b>Scenario 1: ActiveFloat</b>	279.1 MEUR	313.4 MEUR	348.7 MEUR	-25.3 %	26.3 %
<b>Scenario 2: Windcrete</b>	365.9 MEUR	409.9 MEUR	453.6 MEUR	-24.4 %	26.3 %

### 3 Introduction

The COREWIND project investigates the influence of different T&I strategies and new requirements on the marine operations in the prospect of future floating offshore wind farms. The T&I of floating wind farms being a major cost driver motivates the assessment of new strategic opportunities and developments to reduce the T&I costs.

A comprehensive overview of the floating wind specific T&I requirements, as well as a review of state-of-the-art inspection and maintenance strategies and monitoring techniques, have already been published in Deliverable D4.1 of August 2020 [1]. Deliverable D2.2 of June 2022 [2] focussed on mooring installation assets and techniques to identify FOWT compatible and installation friendly procedures. An overview on mooring equipment with a track record in O&G and FOWT was given and innovative concepts and state of the art tools were discussed. For different combinations of mooring pattern and floater archetype the installation strategies were developed with breakdown of operational sequences as well as required types and amounts of assets for the installation.

This Deliverable D4.5 continues on the previous considerations, and summarised the activities undertaken to assess T&I strategies specific to floating wind. The operational work breakdown and associated time, cost and risk of a commercial-scale floating wind farm were evaluated for several T&I campaigns. COREWIND's reference wind farm consisting of 80 units at 15 MW rating per unit and two floating OSS was modelled using a combination of the reference floater designs – i.e. Windcrete (spar) and ActiveFloat (semi-submersible) – and the reference site conditions – i.e. Morro Bay, USA (COREWIND reference site C).

Chapter 4 provides relevant input data and boundary conditions to perform the floating wind specific T&I analysis. In chapter 5, the T&I procedures and the method statement/work breakdown structure are presented based on state-of-art offshore equipment. After defining the T&I methods the operational limits of temporary marine operations are assessed in chapter 6 to define input conditions for the weather downtime analysis. Chapter 7 describes the analysis of transportation and installation durations and costs using sequential weather downtime analyses. From the assessment of a pre-defined work breakdown the probability of down time due to sea state conditions is calculated. At the end of this report, conclusions and perspectives are presented in chapter 8.

## 4 Input Data and Baseline Conditions

This chapter summarises all the input data for the T&I analyses.

### 4.1 Offshore Site and Layout

The reference offshore site selected for this analysis is Morro Bay, which is located on the West Coast of the USA at California State. In COREWIND's design basis Deliverable D1.2 [3] a reference water depth of 870 m was defined. Depending on the actual location of the floating offshore wind turbine the water depths in this deepwater area can vary between 600 to 900 meters. Morro Bay was chosen for the installation strategy assessment because it allowed to consider both COREWIND's reference floating foundation concepts ActiveFloat and Windcrete and floating Offshore Substations (OSS). The West of Barra site is not suitable for the Windcrete spar, and the Gran Canaria site does not feature OSS due to its direct electrical link to shore. See also the reference scenarios for LCOE assessment in Deliverable 6.1 [4] from which scenario 9A was chosen in this study (80 floating wind turbines at 15 MW nameplate rating and two floating OSS).



Figure 4-1: Reference sites of the COREWIND project [Source: Ramboll, modified from Google Maps].

### 4.2 Floating Substructure Types

Two reference floating substructures types are selected for this analysis, one is a semi-submersible substructure (ActiveFloat), the other one is spar buoy type of substructure (Windcrete). The wind turbine chosen is the IEA 15 MW reference turbine from NREL as also defined in the design basis D1.2.



ActiveFloat



WindCrete

Figure 4-2: Illustration of COREWIND's reference floating wind concepts [Source: COBRA, UPC taken from D1.2].

### 4.3 Anchor Type

Suction pile anchors (SPA) have been selected particularly in a soft cohesive soil. Different from other types of anchors, suction embedded anchors have been introduced in deep water applications where it may prove less costly and require less use of a large derrick barges. In addition, noise considerations during installation benefit suction piles in relation to driven pile anchors which can be important for future application in the considered offshore area. Table 4-1 summarises the particulars of the anchor selected in this analysis, which is determined based on preliminary and conservative geotechnical design estimates.

Table 4-1: Anchor properties.

Item	Value	Unit
Mass	120.0	[t]
Diameter of SPA	5.0	[m]
Length of SPA	20.0	[m]

### 4.4 Mooring System Configuration

At the reference site a taut mooring system is implemented with lower and upper chain section (studless) and a fibre rope (polyester) in the mid water column. An optimised mooring system developed within WP2 of COREWIND is used in this analysis with a 3x1 mooring system for the ActiveFloat semi-submersible and a 4x1 mooring system for the Windcrete spar.

### 4.5 Vessel and Equipment

#### 4.5.1 [Semi-Submersible Vessel](#)

A semi-submersible barge could be deployed for launching of the substructure in the harbour basin. During a load-out procedure, the substructure will be transferred over a heavy-duty ramp onto the barge. This results into requirements on the quayside load-bearing capacities, ramp, and water depth at the quayside. The float-over procedure, submersing the barge until the floater is afloat, adds further requirements to the harbour basin dimensions and water depth, if not performed outside the port. Alternatively, assembly on the semi-submersible barge can help to overcome special requirements mentioned above and only load bearing capacities for the crane and the crane outreach need to be addressed in detail when defining the final setup. If the harbour or shore near the assembly area allows for grounding of the barge, hydrostatic requirements like deck strength ( $t/m^2$ ), and pump capacities for submersing and emerging are reduced.

#### 4.5.2 [Heavy Lift Vessel](#)

A Heavy Lift Vessel (HLV) is involved in the anchor and mooring legs pre-installation phase. Lifting the anchor and mooring legs from deck and lowering to the seabed is performed by crane and guided by a ROV system equipped onboard. The vessel shall have sufficient deck space for loading several piles on deck and have a lifting capacity enabling their installation using heave compensation.

#### 4.5.3 [Anchor Handling Tug](#)

Anchor Handling Tug Vessels (AHTVs) are the key vessels in the installation process. They are involved in mooring line deployment and hook-up activities. Tentatively, further offshore tug operations as manoeuvring and tow-out could be performed by AHTVs. The number of required AHTVs depends on the selected installation sequence. It shall be capable of loading high quantity of mooring components such as mooring chains, mooring lines, buoyancy modules and have a bollard pull capacity sufficient for towing activities.

#### 4.5.4 ROV

Subsea activities will require involvement by work class ROVs (WROVs). These are deployed from deck of a heavy lift vessel or AHT equipped with means to launch and retrieve an ROV. Suction pile anchor installation and mooring legs connection are such activities where ROV support is needed.

#### 4.5.5 Self-Propelled Modular Transporter

Transport of components with large masses at the yard and during load-out on flooring with sufficient load bearing capacities can be carried out with self-propelled modular transporters (SPMT).

#### 4.5.6 Onshore Crane

The marshalling port for RNA is assumed to be a flat construction area on the quayside. Crane operations will be required for precast segment handling and assembly operations. There are average requirements on the onshore crane regarding both hook height and crane capacity as well as requirements on the port parameters, especially the ground bearing capacity of the wharf and the required port space to store and handle the WTG components. For the 15 MW reference a large crane with sufficient lifting capacity (>1000 t), lifting height (>140 m) and outreach is required, especially if WTG is located in the center of the floating substructure.

#### 4.5.7 Offshore Access System

The offshore access system is an extendable gangway suspended in two hydraulic cylinders and motion stabilised in order to compensate the vessel motion relative to the offshore platform (motion compensated walk to work system/gangway).

### 4.6 Environmental Conditions

#### 4.6.1 Water Depth

According to the wind farm layout of scenario 9A at Morro Bay [4], the water depth of all turbine locations ranges between 419 m and 613 m. Assuming that the required cable and mooring line lengths over all turbines scales linearly with the arithmetic average of the water depths, an average water depth of 496.4 m was selected.

#### 4.6.2 Wind

Based on the wind rose in Figure 4-3 taken from D1.2 a maximum wind speed of 14 m/s has been considered for the T&I analyses. This selection is also based on general engineering judgement.

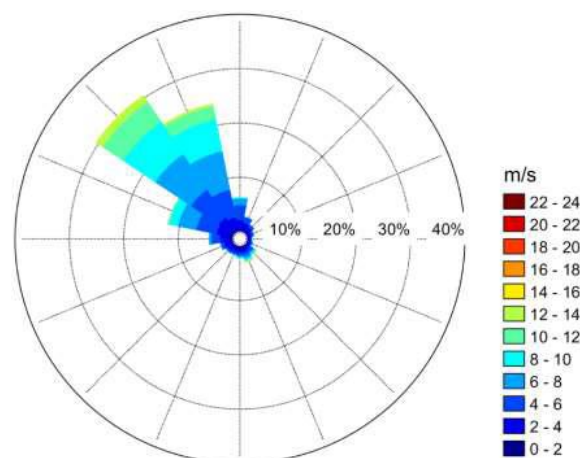


Figure 4-3: Wind speed rose [Source: COREWIND D1.2].

### 4.6.3 Wave

According to the wave scatter diagram in Figure 4-4 taken from D1.2 the maximum  $H_s$  considered in the T&I analyses is 3 m with a  $T_p$  range from 6 to 18 s. This selection is also based on general engineering judgement.

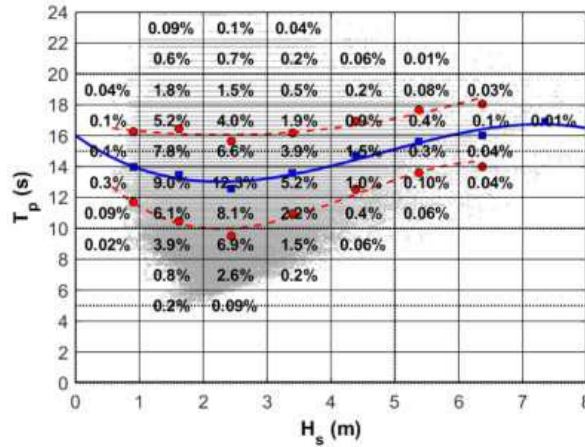


Figure 4-4: Scatter diagram  $H_s$ - $T_p$  (blue line: polynomial fit of average  $H_s$  probability, red line: polynomial fit including standard deviation) [Source: COREWIND D1.2].

### 4.6.4 Current

Due to lack of information about current, current speed of 1.0 m/s (2 kn) has been considered in the T&I analyses.

### 4.6.5 Tidal

Tidal effect with changes in water levels has not been taken into account in the T&I analyses.

## 5 Work Breakdown Structure and Method Statement

For the T&I strategies of the reference floating offshore wind turbines in this study three main operations are considered referred to as the loadout or launching, transportation and installation operations at the offshore site. The marine operations affect the cost and schedule of the overall project. Given a large number of possible operation concepts, the objective of this chapter is to provide the basic understanding of the chosen concepts of T&I for the Work Breakdown Structure (WBS). Selected marine operations are analysed in Chapter 6 to assess operational limits for the WBS. Both, the WBS and the operational limits serve as input for the sequential weather downtime analysis in Chapter 7.

The work breakdown of the sequence of T&I operations in this study consists of four main packages A to D for both substructure concepts:

- A. Anchor installation;**
- B. Mooring line pre-lay;**
- C. Floating foundation hook-up;**
- D. Power cable installation.**

Each of these packages is described in this Chapter. The work breakdown for anchor installation, mooring line pre-lay and power cable installation are identical for both foundations concepts ActiveFloat and Windcrete, except for differences in the number of mooring legs. The main difference is the hook-up package arising from additional working steps to be taken for Windcrete.

Further important steps for the T&I campaign are the packages E and F. These are assumed completed at the beginning of this study and as such not part of the work breakdown. However, general method statements are provided in this Chapter.

- E. Floater substructure fabrication and transportation;**
- F. Floater launching and assembly.**

For completeness, common procedures for these packages are also briefly addressed in this section.

### 5.1 Anchor Installation

The SPA and mooring legs with the mooring lines will be installed prior to the FOWT arriving at the offshore site to perform hook-up operations. The anchor installation is performed by a Heavy Lift Vessel (HLV). The suction pile and other required equipment will be loaded onboard the HLV before it transits to site. Sequentially, the vertically loaded anchors will be lifted and lowered to the seabed using the onboard crane. The SPAs will be installed by means of extracting water from the anchor using suction effect of the pile to create vertical holding capacity. Unlike the drag embedment anchors, proof loading is not needed in this study for the SPA because it is assumed that the lower chain section is mounted to the top of the pile for the semi-taut mooring system avoiding an inverse catenary.





**Figure 5-1: Example of Suction Anchor Piles with temporary lower chain segment positioning [Source: Island Offshore].**

A trial of the HLV's DP capabilities must be conducted prior to the operation. In addition, a lifting motion analysis should be performed to determine the workability and to define the weather window for the operations.

The choice of the installation vessel depends on the size and the number of anchors for the installation campaign. Exemplary monohull HLV are shown in Figure 5-2.



**Figure 5-2: Exemplary monohull heavy lift crane vessels; Left: Heerema Aegir [Source: Heerema], Middle: Deme Orion [Source: Deme], Right: Boskalis Boka Lift 2 [Source: Boskalis].**

The generic monohull HLV introduced by Ramboll in Deliverable D4.2 [5] with main specifications, motion RAOs and viscous damping is used in this study again. Main properties are given in Table 5-1.


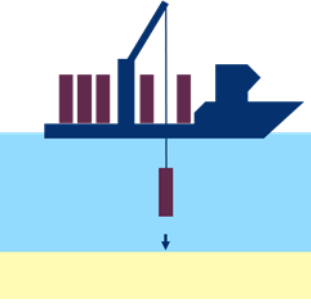
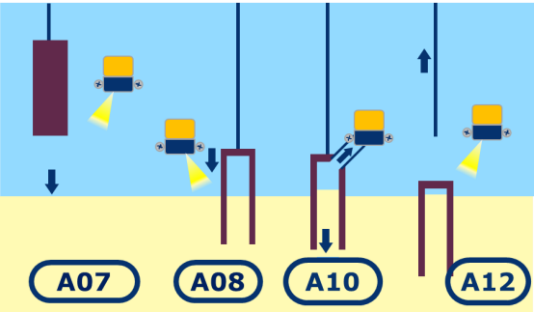
**Table 5-1: Main dimension of generic heavy lift vessel.**

Parameter	Unit	Generic HLV
Length	m	216.0
Breadth	m	49.0
Height (keel to working deck)	m	21.0
Operational draft	m	9.0
Lightship Weight (LSW)	t	40,900
Displacement at operational draft	t	71,900
Lifting capacity of main crane(s)	t	1x 4,000



The work breakdown of the anchor installation campaign, as modelled in the weather down time analysis, is described in Table 5-2 (figures from Source: Ramboll).

**Table 5-2: WBS for anchor installation.**

ID	Description	Illustration
A01	Mobilise HLV	
A02	Load suction pile anchor in base port	
A03	Transit to Morro Bay site	
A04	Position at site, launch ROV, locate anchor position	
A05	Connect anchor to rigging arrangement	
A06	Lift and overboard suction pile anchor	
A07	Position anchor at seabed, monitored by ROV	
A08	Self-penetration of suction pile anchor at seabed	
A09	Connect ROV to suction pile anchor discharge valve	
A10	Perform suction operation until target penetration is reached	
A11	Disconnect ROV and rigging from anchor	
A12	Survey anchor location	
A13	Relocate HLV to next anchor position	
A14	Return to base port	

**5.2 Mooring Line Pre-lay**

Mooring line pre-lay includes the installation of bottom chain and fibre rope section. Separating these operations from the anchor installation campaign is required to account for fibre rope storage limitations on the seabed. Usually, storage is limited to approximately one month and only for unstretched fibre rope. Installation will be performed by an Anchor Handling Tug Vessel (AHT). Bottom chain, fibre ropes, and other required equipment will be loaded onboard the AHT prior to the transit to site. At site the mooring lines are layed on the seabed according to the predefined pattern. The top end of the fibre rope is supplied with pick-up loops that will be held in position using small buoyancy elements and buoyed off until the FOWT arrives for mooring line hook-up. Connection of anchor and ground chain is performed by means of a heave compensated crane hook and

supported by ROV. Ramboll’s contribution in Deliverable D2.2 [2] provides additional relevant information for installation techniques, for example installation equipment specific to suction pile anchors and operational procedures. For reference, an exemplary anchor handling tug with motion compensated gangway is shown in Table 5-3 and Figure 5-3.

**Table 5-3: Exemplary Anchor Handling Tug Supply Vessel.**

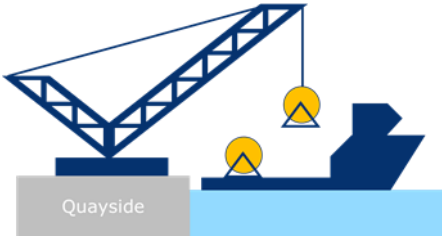
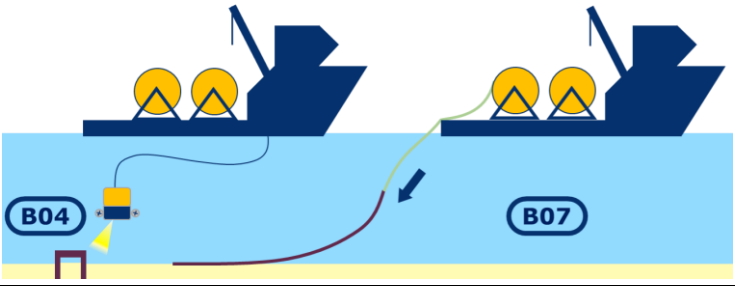
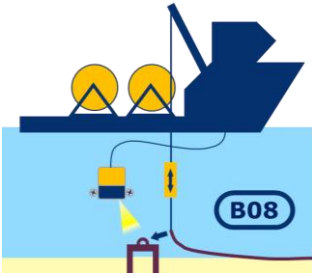
Item	Generic AHT
Length Overall	70.9 m
Beam	16.0 m
Max. Draught	5.7 m
Bollard pull capacity	120 t
DP classification	DP2



**Figure 5-3: Exemplary AHTS Smit Nicobar [Source: Boskalis], AHT Bylgia [Heerema], AHT Britoil 120 [Source: Britoil Offshore Services].**

The work breakdown of the mooring line pre-lay campaign is described in Table 5-4 (figures from Source: Ramboll).

Table 5-4: WBS for mooring line pre-lay.

ID	Description	Illustration
B01	Mobilise anchor handling support vessel	
B02	Mooring line load-off: ground chain in chain lockers and fibre rope in drums on deck	
B03	Transit to Morro Bay site	
B04	Launch ROV and locate anchor	
B05	Overboard bottom chain	
B06	Connect bottom chain to fibre rope thimble	
B07	Lay mooring line on seabed	
B08	Connect bottom chain with anchor mooring connector using heave compensation equipment	
B09	Survey mooring line position with ROV	
B10	Abandon mooring line on seabed	
B11	Relocate to next anchor position	
B12	Return to base port	

### 5.3 Hook-up

The hook-up campaign consists of different phases: For ActiveFloat, it mainly consists of transit and mooring line hook-up, whereas for Windcrete, erection of the floating foundation is considered as well. The top chain is assumed to be already fitted to the floating foundation prior to the hook-up campaign.

Towing of the FOWT is performed by multiple AHTs (at least one main tug and one assistance tug). The minimum required number of tugboats is based on the towing calculation under survival conditions (e.g. unrestricted weather condition in DNVGL-ST-N001). The minimum towline breaking load (MBL) is defined according to the DNV guideline (DNVGL-ST-N001). The MBL of the main and spare towlines, and the ultimate load capacity of the towline connections to the tow including each bridle leg, shall be related to the continuous static bollard pull (BP) of the actual tug to be used. Exemplary minimum towing assemblies for both floating foundations are illustrated in Figure 5-4. Before the floating substructure is towed out of the harbour, the weather condition has to be checked. Planning of the tow route will be done with proper seamanship and include contingencies such as safe havens as shelter area in case of bad weather.

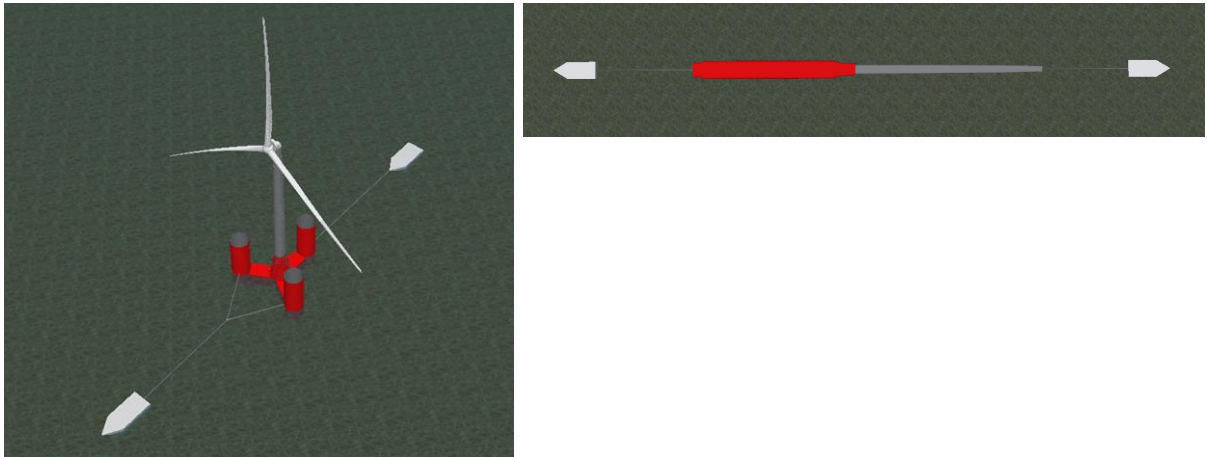


Figure 5-4 Minimum towing configurations for ActiveFloat (left) and Windcrete (right) [Source: Ramboll].

For reference, an exemplary ocean towing tug is shown in Table 5-5 and figures.

Table 5-5: Exemplary ocean towing tugboat.

Item	Generic Ocean Towing Tug
Length Overall	75.5 m
Beam	18.0 m
Depth main deck	8.0 m
Bollard pull capacity	206 t
Free running speed	17 kn



Figure 5-5: Exemplary AHTS Manta [Source: Boskalis], AHTS 200 [Source: Damen], AHTS Atlantic Merlin [Source: Atlantic Towing].

The erection of Windcrete requires a sheltered area with sufficient water depth and is performed by an ocean towing tug and a bulk carrier with a temporary pump installed for ballasting to operational draught with liquid

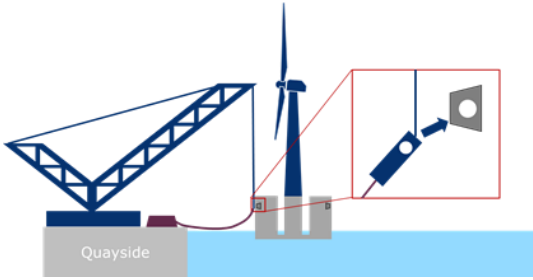
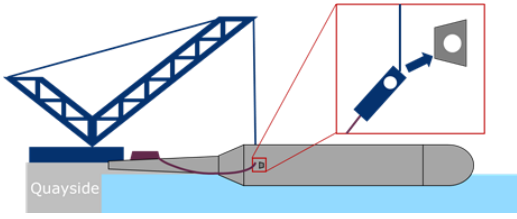
dense fluid ballast. Installation of the wind turbine is excluded from the weather downtime analysis to guarantee a fair comparison between the two concepts. After erection and turbine integration, towing to site is continued.

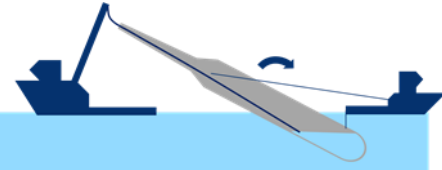
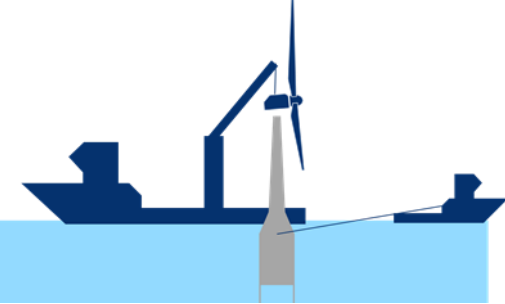
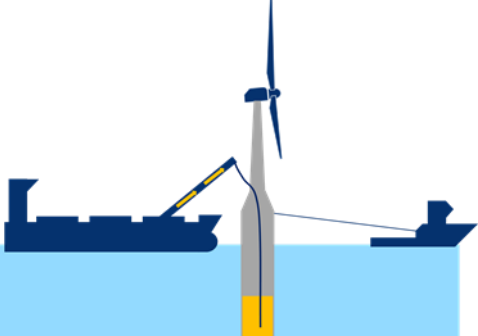
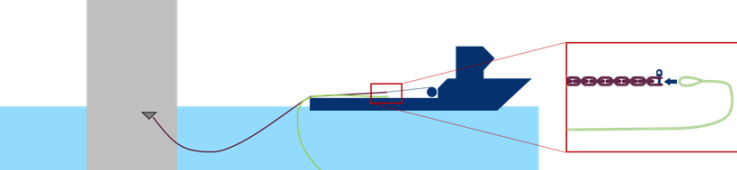
When arrived at the offshore installation site, the FOWT will be positioned in a corridor over the pre-installed mooring lines (lower chain section and fibre rope). The station keeping operation is planned with assistance of two or three (depending on their capacities) small offshore tugs/ AHTS with dynamic positioning. The tugs configuration including heading and bollard pull shall be calculated in relation to the predominate wind, wave and current pattern.

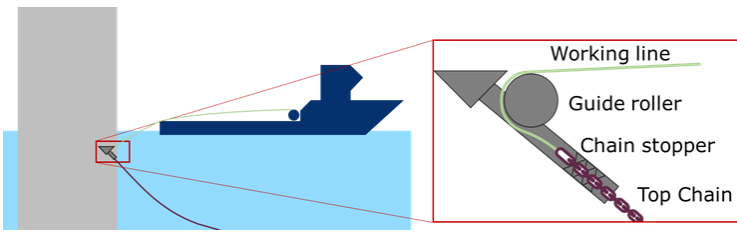
The mooring lines are individually hooked-up and connected one by one subsequently using an AHTS equipped with DP and WROV system, while the FOWT is held in position by tugs. After recovery of fibre rope top end and retrieval of top chain from the floating foundation, connection of both parts is performed on deck of the AHTS. For mooring leg(s) 3 for ActiveFloat (and 4 for Windcrete), preinstalled in-line tensioners at the floating foundation are used for tensioning.

The work breakdown of the floating substructure hook-up campaign is described Table 5-6 (figures from Source: Ramboll).

**Table 5-6: WBS for floating substructure hook-up.**

ID	Description		Illustration
C01	Mobilise offshore tugs, AHTS (with mobile dredging pump and bulk carrier for Windcrete)		
C02	Connect top chains to FOWT mooring padeyes, secure top chain for transport		<p><b>ActiveFloat:</b></p>  <p><b>Windcrete:</b></p> 
C03	Connect FOWT to offshore tugs		
	<b>ActiveFloat:</b>	<b>Windcrete:</b>	
C04	Sail out of port/transit to site	Sail out of port/transit to erection site (sheltered area)	

ID	Description		Illustration
C05	Ballast to operational draught	Uprighting of spar	<p><b>Windcrete:</b></p> 
C06	Position semi-sub at site	Ballast for wind turbine integration (not considered in this study)	
C07	-	Turbine integration (not considered in this study)	<p><b>Windcrete:</b></p> 
C08	-	Ballast to operational draught (bulk carrier with liquid dense fluid ballast)	<p><b>Windcrete:</b></p> 
C09	-	Tow to site	
C10	-	Position spar at site	
C11	Launch ROV, locate fibre rope top section near anchor position, recover mooring line		
C12	Recover top chain end from FOWT		
C13	Connect top chain and fibre rope on AHTS deck		
C14	Release mooring line		
C15	Relocate to next mooring line		

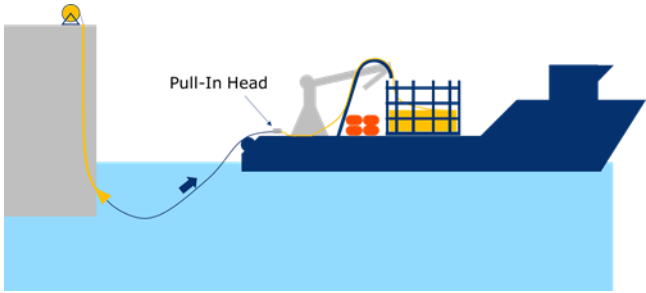
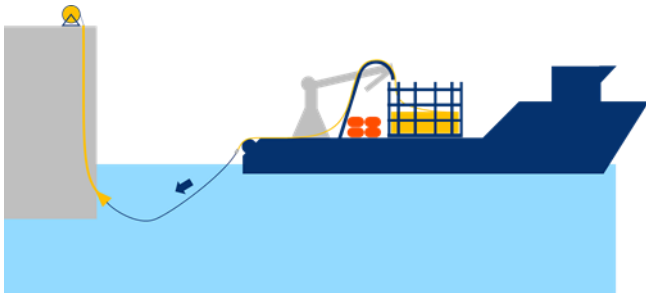
ID	Description	Illustration
C16	In-line tensioning: For mooring line 3 (and 4 for Windcrete) pull in working line from floating substructure onto AHTS, pull on working line (mooring line tensioning).	
C17	Return to base port	

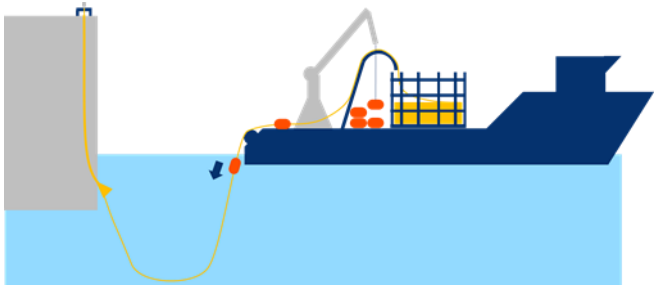
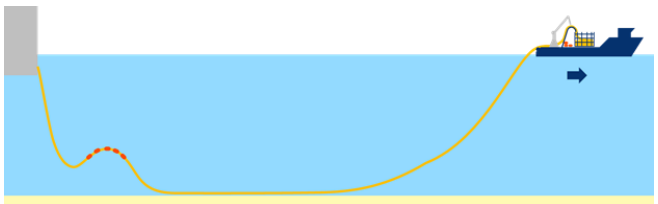
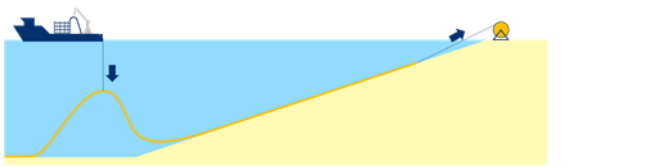
#### 5.4 Power Cable installation

Power cable installation is performed with a generic Cable Laying Vessel (CLV) and temporary or on board winches at the floating foundations and the onshore connection points. Pre fabricated cables, buoyancy elements, and other required equipment is loaded at the base port onto the CLV. At site, working lines from the floating foundation are retrieved by the CLV to connect the power cables and perform the pull-in. After connection to the platform, buoyancy elements are connected to the dynamic cable and the cable laying proceeds until the next connection point (floating asset or onshore). The second end is connected similarly.

The work breakdown of the power cable installation campaign (inter-array and export cable) is described in Table 5-7 for both the FOWT and floating OSS (figures from Source: Ramboll).

Table 5-7: WBS for power cable installation.

ID	Description	Illustration
D01	Load power cable on CLV at base port	
D02	Transit to Morro Bay site	
D03	Pull-out initiation wire from floater and transfer it to CLV and connect to cable pull in head	
D04	Pull in cable with (temporary) winch on board of FOWT/OSS, lock cable on FOWT/OSS	

ID	Description		Illustration
D05	Install cable ancillaries		
D06	Lay cable		
	<b>Pull in to other FOWT/OSS (inter-array):</b>	<b>Shore landing (export cable):</b>	
D07	Installation of cable ancillaries	Float cable end	
D08	Pay-out initiation wire from floater and transfer it to CLV and connect to cable pull in head	Cut cable to length	
D09	Pull in cable with winch on board of FOWT/OSS, lock cable on FOWT/OSS	Seal cable	
D10		Pay-out initiation wire from onshore connection point and connect to cable pull in head	
D11		Cable pull in with initiation wire from onshore winch	

## 5.5 Fabrication and Transportation

The fabrication strategy for the floating substructure is not modelled in this study. **The base case considers a delivery of the assembled floating substructure at quayside.**

General considerations for the transportation using a semi-submersible heavy transport vessel are described in the following paragraph. In case of a long journey (e.g. from Asia to the USA) of the fabricated floating substructure, it's required to investigate the transportation from a structural point of view focusing on the fatigue behaviour of the structures onboard. Prior to each such long voyage a detailed motion response analysis



is to be conducted. The maximum design acceleration at cargo (here floater foundation) CoG due to ship motion under design environmental conditions should be computed, the accelerations are limited by the foundation structural design, that cannot be exceeded. Each heavy transport vessel is equipped with a weather monitoring and analysing data program, which provide the vessel master the weather forecast information and tools to optimise the voyage planning. Design accelerations are not to be exceeded, vessel heading, speed and route are to be adjusted to avoid exceeding the limits. Seafastening and grillage supports shall be designed to be able to withstand the determined acceleration. In case the large floater overhangs the transport vessel, wave slamming load will occur when the structure makes the first contact with the water surface. It's recommended to carry out the analysis for the worst case. Stability and strength are also the main aspects of transportation. A sufficient ballasting plan shall be designed for load-out/ discharge and transportation. Vessel stability must be such that stability requirements are passed. Draft does not exceed the vessel summer load line draft. And the global bending moment and shear force shall be within the allowable limits.

For reference, an exemplary semi-submersible HTV is shown in Table 5-8:

**Table 5-8 : Example of semi-submersible heavy transport vessel.**

Item	Generic HTV
Length Overall	216.7m
Beam	63.0m
Depth main deck	13.0m
Submersible draft	26.0m



**Figure 5-6: Exemplary semi-submersible heavy transport vessel White Marlin [Source: Boskalis], semi-submersible HTV Seaway Swan [Source: Seaway 7], semi-submersible HTV Xin Guang Hua [Source: Cosco Heavy Transportation].**

In addition, prior to towing the floater from the float-over location to the offshore site, a stability assessment for the floater itself which meets (or exceeds) the requirements of an appropriate classification society (e.g. DNV) shall be conducted to prove the floater will remain adequately stable during each installation stage. A certificated commercial hydro-stability software (e.g. GHS) shall be used for this analysis.

A ballast plan shall be prepared for the following T&I steps:

- Launch floater to the port basin
- Towing floater to installation site
- Final operating draft

For each step above, intact stability shall be checked against the selected requirements. Moreover, damage stability (for compartment damage) shall be checked for all the critical steps as well.

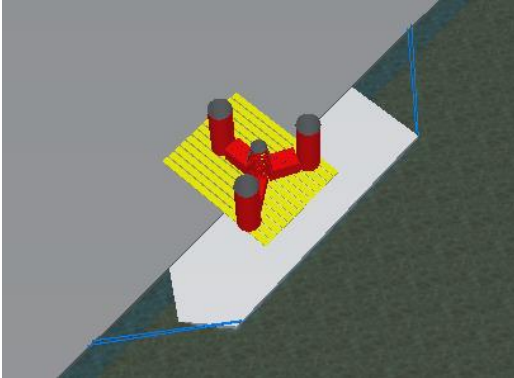
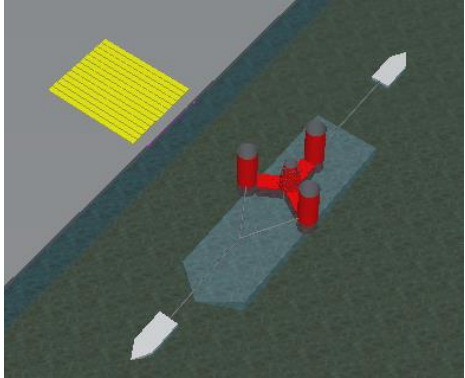
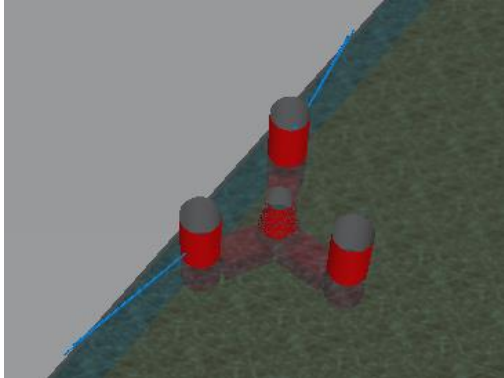
## 5.6 Launching Method

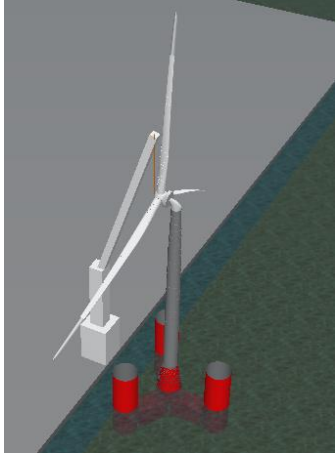
The wind turbine and tower integration is conducted after the floating substructure is fully assembled. The substructure is launched from quayside to the port basin prior to towing to the offshore site. A commonly used method for this operation is loading the floating substructure onto a semi-submersible barge and then floating it off (by submerging the barge) into the port basin. Sufficient water depth for the float-off operation is necessary.

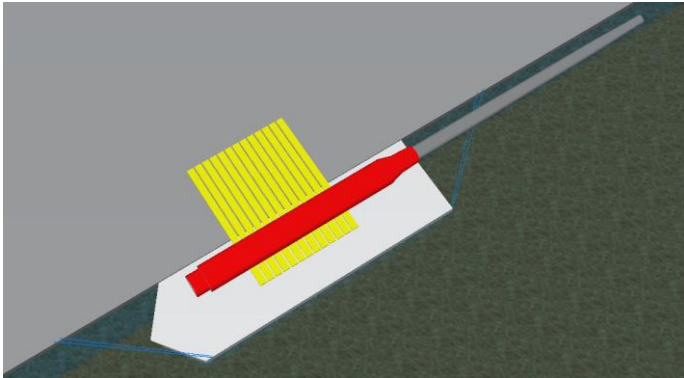
**The sequential weather downtime analysis assumes that all equipment and materials are stored at the base port and are ready for tow-out neglecting fabrication, mobilisation, pre-commissioning, supply chain, launching etc. The WTG integration is not modelled in detail meaning that tower and RNA installation as well as ballasting are performed for ActiveFloat at the base port, and for Windcrete at a sheltered offshore area close to base port.**

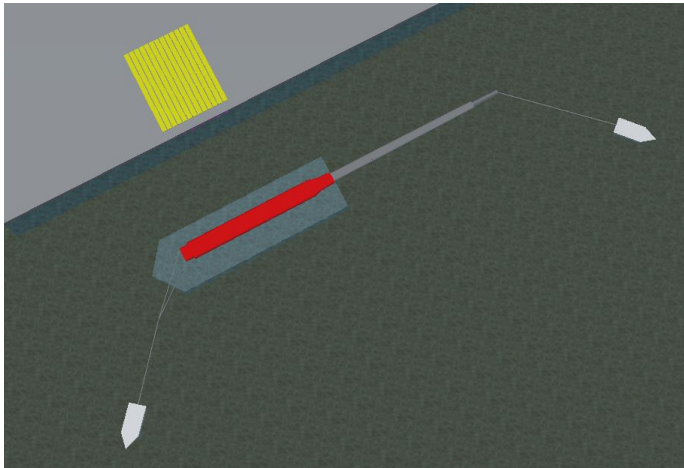

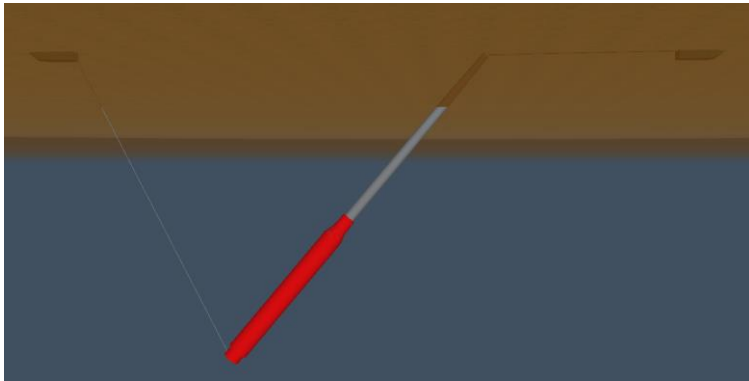
The below method statement (Table 5-9) presents an activity-based sequence (figures from Source: Ramboll).

**Table 5-9: Method Statement**

ID	Description and Illustration for Launching of ActiveFloat
F01	Floating substructure prepared at assembly site.
F02	<p>Launch the floating substructure from the quayside:</p> <ul style="list-style-type: none"> <li>- Semi-submersible barge moored alongside the assembly yard quay</li> <li>- Load floating substructure from quay to a semi-submersible barge using SPMTs</li> <li>- Float-off the floating substructure from barge guided by port tugs</li> <li>- Berthing the substructure to the quayside</li> </ul> <div style="display: flex; justify-content: space-around; align-items: flex-start;">   </div> <div style="display: flex; justify-content: space-around; align-items: flex-start; margin-top: 10px;">  </div>

ID	Description and Illustration for Launching of ActiveFloat
<b>F03</b>	<p>Installation of tower and RNA of the wind turbine using a quayside crane.</p> 

ID	Description and Illustration for Launching of Windcrete
<b>F01</b>	Floating substructure prepared at assembly site.
<b>F02</b>	<p>Launch the Floating substructure from the quayside:</p> <ul style="list-style-type: none"> <li>- Semi-submersible barge moored alongside the assembly yard quay</li> <li>- Load floating substructure from quay to a semi-submersible barge using SPMTs</li> <li>- Float-off the floating substructure from barge guided by port tugs</li> </ul> 

ID	Description and Illustration for Launching of Windcrete
	
<b>F03</b>	<p>Towing the spar buoy to the assembly location.</p> 
<b>F04</b>	<p>Upending the spar to the upright position in a sheltered area with sufficient water depth.</p> 
<b>F05</b>	<p>Ballast the Windcrete spar to a sufficient draft. Installation of RNA on top of foundation (with integrated concrete tower) by means of a crane vessel in the sheltered area.</p>

ID	Description and Illustration for Launching of Windcrete
	

## 5.7 Potential Risk Assessment

Prior to the T&I operation, risk assessment sessions are organised addressing all involved parties to identify all risks (e.g. technical, safety, financial) related to the operational procedures and to propose mitigations to reduce risks to an acceptable level. The risks should be continuously reviewed throughout the project's development.

Exemplary risks foreseen in the T&I operation and the associated mitigation measures are listed in Table 5-10.

**Table 5-10: Risks in T&I operation and associated mitigation measures**

Risk	Mitigation Measures
Tug breakdown/ towline failure	<ul style="list-style-type: none"> <li>- Ensure sufficient redundancy of tugs</li> <li>- Testing equipment before use</li> <li>- Availability of certification of towing rigging</li> <li>- Ensure sufficient spare rigging is available</li> <li>- Ensure emergency towing line is part of the design</li> </ul>
ROV breakdown	<ul style="list-style-type: none"> <li>- Ensure spare parts are available</li> <li>- Ensure experienced technicians are available onboard in case repair work is needed</li> <li>- Mobilise a vessel with 2 ROVs for critical operations</li> <li>- Optional, for harbour operations only: Diver team to replace ROV (but higher HSE risk)</li> </ul>
Reduced towing speed	<ul style="list-style-type: none"> <li>- Ensure sufficient strength of towing points</li> <li>- Perform towing calculation under survival condition</li> <li>- Ensure sufficient tugs are available</li> </ul>
Miscommunication	<ul style="list-style-type: none"> <li>- Kick-off meeting with all parties involved</li> <li>- Organise tool-box meetings prior to each T&amp;I procedure</li> <li>- Develop a procedure for simultaneous operations</li> </ul>
Inaccurate weather forecast	<ul style="list-style-type: none"> <li>- Multiple weather sources to be provided</li> <li>- Weather forecast update at least 3 times per day</li> </ul>

## 6 Analysis Methodology and Results

### 6.1 Overview of Studies and Software

Table 6-1 provides an overview of the T&I analyses performed. The results of the studies are used to develop installation strategies for the reference floating offshore wind farm. In the first loop temporary marine operations are simulated with a focus on towing operations, anchor installation and mooring line hook-up. The results are used to define input conditions for the sequential weather downtime analysis in Chapter 7. The studies aim to assess time and associated cost of installation strategies with respect to the given reference scenario and assumptions.

Table 6-1: Overview of T&I analyses.

Study	Objective	Analysis	Tool	Outcome
<b>1 – Temporary marine operations (Chapter 6)</b>	Towing	Towing analysis	In-house Python	Required tug capacity and tug number; sailing speed
	Anchor installation	Simplified lifting analysis (through wave zone)	Ansys AQWA, OrcaFlex, Excel	Workability Hs-Tp combination
	Hook-up	Force allocation calculation	In-house Python	Tug capacity and heading control
<b>2 – Sequential weather downtime analysis (Chapter 7)</b>	Weather downtime, cost estimation	Work breakdown analysis, probabilistic cost model	Shoreline, Excel	Estimated project duration, operation costs

In addition, an analysis of the upending process of the Windcrete spar is carried out (not related to the ActiveFloat semi-submersible) to investigate limiting wave conditions during the operation using focused wave groups. A combined multi-fidelity approach is applied with a radiation-diffraction (HAWC2) and a CFD model (OpenFOAM). The results of the upending analysis are not used to calibrate the sequential weather downtime analysis to ensure comparability between floating substructures concepts (see also Section 7.1).

### 6.2 Environmental Load Calculation

#### 6.2.1 Vessel Axis Convention

Colinear environmental loads are assumed for the following T&I analyses, because it's a conservative approach. Figure 6-1 shows the convention used for the directions of environmental conditions:

- 0 degree is from aft to forward: following sea
- 90 degrees is from starboard to portside: beam sea
- 180 degrees is from forward to aft: head sea

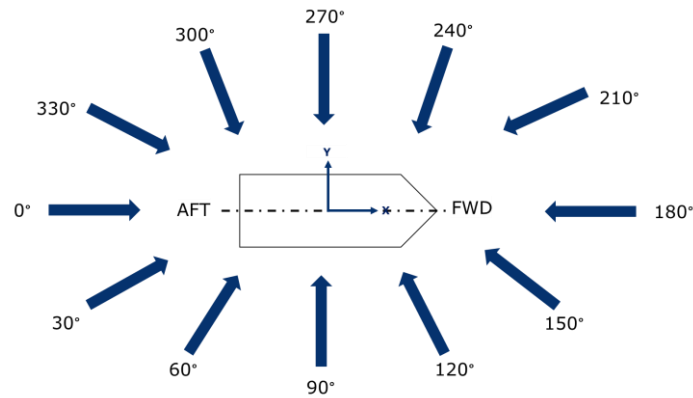


Figure 6-1: Environmental direction convention [Source: Ramboll].

### 6.2.2 Wind Loads

The wind drag force on the floating substructure is calculated based on the following formula:

$$F_{wind} = 0.5 \rho_{air} C_w A_w v_{wind}^2$$

with the coefficients defined in Table 6-2 below.

Table 6-2: Coefficients for calculation of wind loads.

Symbol	Description	Unit
$F_{wind}$	Wind drag force	[kN]
$\rho_{air}$	Density of air, here is 0.001225	[t/m <sup>3</sup> ]
$C_w$	Wind drag coefficient	[-]
$A_w$	Projected wind area	[m <sup>2</sup> ]
$v_{wind}$	Wind speed	[m/s]

### 6.2.3 Current Loads

The current force is calculated using the following equation:

$$F_{current} = 0.5 \rho_{sea} C_d A_c v_{current}^2$$

with the coefficients defined in Table 6-3 below.

Table 6-3: Coefficients for calculation of current loads.

Symbol	Description	Unit
$F_{current}$	Current force	[kN]
$\rho_{sea}$	Density of sea water, here is 1.025	[t/m <sup>3</sup> ]
$C_d$	Drag coefficient	[-]
$A_c$	Submerged area of the hull	[m <sup>2</sup> ]
$v_{current}$	Current speed	[m/s]

### 6.2.4 Wave Loads

The mean wave drift force is calculated in OrcaFlex based on the 3D diffraction analysis. If there's no diffraction model, the wave drift force can be approximated by the following equation (DNVGL-ST-N001).

$$F_{wd} = \frac{1}{8} \rho_{sea} g R^2 L H_s^2$$

with the coefficients defined in Table 6-4 below.

**Table 6-4: Coefficients for calculation of wave loads.**

Symbol	Description	Unit
$F_{wd}$	Wave drift force	[kN]
$\rho_{sea}$	Density of sea water, here is 1.025	[t/m <sup>3</sup> ]
$g$	Acceleration of gravity, 9.81	[m/s <sup>2</sup> ]
$R$	Typical reflection coefficient	[-]
$L$	Characteristic length perpendicular to the wave direction	[m]
$H_s$	Significant wave height	[m]

### 6.3 Towing Analysis

The towing calculations are performed using an in-house developed Python tool. For the towing calculation, two weather conditions are checked:

- **Survival condition:** This is the most severe condition. Minimum required bollard pull is calculated based on the colinear environmental loads of wind, current and wave. DNV unrestricted weather condition (DNVGL-ST-N001) has been considered as survival condition in this analysis, since it's a conservative approach. The number of tug boats with available bollard pull capacity is to be selected to compensate the total load.
- **Sailing condition:** The standard average sailing condition has been considered here. Sailing speed is calculated based on the performance curve defined in the guidelines.

The environmental conditions considered in this towing analysis and the calculated sailing speed are summarised in the following table:

**Table 6-5: Summary results of the towing analysis.**

Item	ActiveFloat		Windcrete	
	Survival Case	Sailing Case	Survival Case	Sailing Case
Towing draft [m]	27.8		160.0	
Wind Speed [m/s]	20.0	10.0	20.0	10.0
Current Speed [m/s]	0.5	0.0	0.5	0.0
Wave Height [m]	5.0	2.0	5.0	2.0
Min. Required BP [t]	164	-	105	-
Tug BP Capacity [t]	200	200	120	120
Tug Efficiency	75%	75%	75%	75%



Item	ActiveFloat		Windcrete	
	Survival Case	Sailing Case	Survival Case	Sailing Case
Number of Tugs	2	2	2	2
Calculated Sailing Speed [kn]	-	2.2	-	2.1

The tug efficiency is taken into account, which is determined by the dimension of the tug boats and the environmental conditions. The following equation in DNV standard (DNVGL-ST-N001) can be used:

$$T_{eff} = 80 - (18 - 0.0417 \text{ LOA} \sqrt{BP - 20}) (H_s - 1)\%$$

with:

LOA = tug length overall in metres (using 45 m for LOA > 45)

BP = Static continuous bollard pull in tonnes (with BP > 20 tonnes, and using 100 when BP > 100 tonnes)

$H_s$  = Significant wave height (with 1 m <  $H_s$  < 5m)

In addition, according to DNV standard (DNVGL-ST-N001) the MBL of the main and spare tows, and the ultimate load capacity (ULC) of the towline connections to the tow including each bridle leg, shall be related to the continuous static bollard pull of the actual tug to be used as following:

- MBL=2 x BP
- ULC = 1.25 x required towline MBL for the actual tug (for MBL < 160t)
- ULC = required towline MBL for the actual tug + 40 (for MBL > 160t)
- The documented MBL of shackles forming part of the towline shall be at least 130% of the required MBL of the towline to be used.

The results are summarised in the following table:

**Table 6-6: Towing equipment capacity.**

Item	ActiveFloat	Windcrete
Maximum bollard pull [t]	164	105
MBL tow line [t]	164/2*2=164	105/2*2=105
ULC pennant [t]	164+40=204	1.25*105=131
MBL shackles [t]	1.3*164=213	1.3*105=137

#### 6.4 Suction Anchor Installation Analysis

The installation analysis for the suction pile anchors is performed using a simplified method according to section 4 in DNV-RP-N103. This method provides a simplified and conservative estimation of forces acting on objects lifted through the wave zone. The method is applied for full-directional environmental conditions and has the following assumptions:

- The horizontal dimension of the lifted object (in the wave propagation direction) is relatively small compared to the wave length.
- The vertical motion of the object follows the crane tip motion.

- The load case is dominated by the vertical relative motion between object and water – other modes of motions such as pitch and roll can be disregarded.
- No resonance effect occurs (crane tip oscillation period or wave period is close to the resonance period of the hoisting system).

The following load cases are checked in this analysis:

- **SPA Installation Phase 1:** Lifted object in air just above the wave zone
- **SPA Installation Phase 2:** Lifted object half submerged
- **SPA Installation Phase 3:** Lifted object fully submerged

The criteria to be checked are listed below, see also Table 6-7:

- Total load (static + dynamic load) against crane capacity
- Vessel motion (roll and pitch) against limits
- Dynamic amplification factor (DAF) against limits
- No snap loads in lines

An example heavy lift vessel has been modelled in OrcaFlex, the hydrodynamic database is imported from OrcaWave. OrcaWave carries out the radiation diffraction analysis in potential theory to obtain the hydrodynamic coefficients (added mass, hydrostatic stiffness, radiation damping etc.) and global motion RAOs for a specified loading condition. For this analysis, an additional viscous roll damping, which is 3% of the critical roll damping is taken into account.

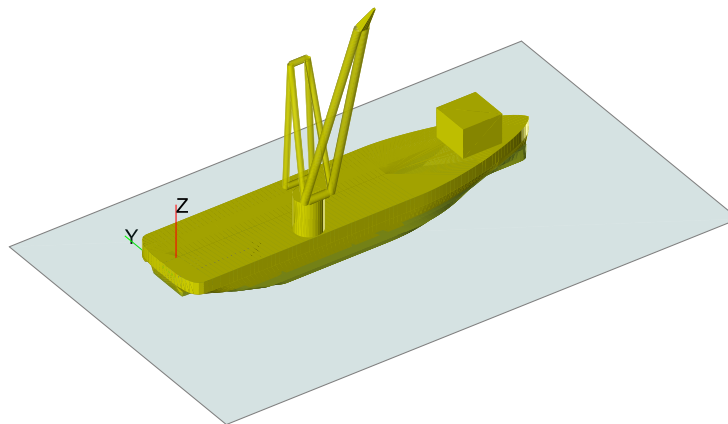


Figure 6-2: Illustration of the generic HLV [Source: Ramboll].

The vessel motions and the crane tip accelerations are calculated in frequency domain and 3 h MPM single seed extreme values are extracted. Since wind and current loads are static load, they are not taken into account in this calculation.

The limits to be checked for this example heavy lift vessel are summarised in the following table:

Table 6-7: Limits of an exemplary heavy lift vessel.

Item	Criteria	Unit
Crane capacity	1200	[t]
DAF	1.25	[-]

Item	Criteria	Unit
Vessel Roll Motion	1.5	[deg]
Vessel Pitch Motion	1.0	[deg]

The resulting operational limits of the SPA installation are shown in Table 6-8 until Table 6-10. In these table the maximum allowable significant wave height for different Tp range and wave direction are presented based on the criteria above (Table 6-7). The colour code indicates that the highest workability is in green and lowest workability is in red.

**Table 6-8: Workability limits during suction pile anchor installation – in air**

Direction [deg]	Workability - In-Air Case						
	Tp [sec]						
	6	8	10	12	14	16	18
0	1.5	2.5	2.5	1.5	1.5	1.5	1.0
30	1.5	2.5	2.0	1.5	1.0	1.0	1.0
60	1.5	2.0	1.0	0.0	0.0	0.0	0.0
90	1.5	2.0	0.0	0.0	0.0	0.0	0.0
120	1.5	2.0	1.0	0.0	0.0	0.0	0.0
150	1.5	2.5	2.0	1.5	1.5	1.5	1.0
180	1.5	2.5	2.5	1.5	1.5	1.5	1.0
210	1.5	2.5	2.0	1.5	1.5	1.5	1.0
240	1.5	2.0	1.0	0.0	0.0	0.0	0.0
270	1.5	2.5	0.0	0.0	0.0	0.0	0.0
300	1.5	2.0	1.0	0.0	0.0	0.0	0.0
330	1.5	2.5	2.0	1.5	1.0	1.0	1.5

**Table 6-9: Workability limits during suction pile anchor installation – half submerged**

Direction [deg]	Workability - Half Submerged Case						
	Tp [sec]						
	6	8	10	12	14	16	18
0	2.5	2.5	2.5	1.5	1.5	1.5	1.5
30	2.5	2.5	2.0	1.5	1.0	1.0	1.5
60	2.5	2.0	1.0	0.0	0.0	0.0	0.0
90	2.5	2.5	0.0	0.0	0.0	0.0	0.0
120	2.5	2.0	1.0	0.0	0.0	0.0	0.0
150	2.5	2.5	2.0	1.5	1.5	1.5	1.5
180	2.5	2.5	2.5	1.5	1.5	1.5	1.5
210	2.5	2.5	2.0	1.5	1.5	1.5	1.5
240	2.5	2.0	1.0	0.0	0.0	0.0	0.0
270	2.5	2.5	0.0	0.0	0.0	0.0	0.0
300	2.5	2.0	1.0	0.0	0.0	0.0	0.0
330	2.5	2.5	2.0	1.5	1.0	1.0	1.5

**Table 6-10: Workability limits during suction pile anchor installation – fully submerged**

Direction [deg]	Workability - Fully Submerged Case						
	Tp [sec]						
	6	8	10	12	14	16	18
0	2.5	2.5	2.5	1.5	1.5	1.5	1.5
30	2.5	2.5	2.0	1.5	1.0	1.0	1.5
60	2.5	2.0	1.0	0.0	0.0	0.0	0.0
90	2.5	2.5	0.0	0.0	0.0	0.0	0.0
120	2.5	2.0	1.0	0.0	0.0	0.0	0.0
150	2.5	2.5	2.0	1.5	1.5	1.5	1.5
180	2.5	2.5	2.5	1.5	1.5	1.5	1.5
210	2.5	2.5	2.0	1.5	1.5	1.5	1.5
240	2.5	2.0	1.0	0.0	0.0	0.0	0.0
270	2.5	2.5	0.0	0.0	0.0	0.0	0.0
300	2.5	2.0	1.0	0.0	0.0	0.0	0.0
330	2.5	2.5	2.0	1.5	1.0	1.0	1.5

Based on the results above (Table 6-8 until Table 6-10) it can be concluded that the (near) heading sea and (near) following sea with longer period are more favourable than beam sea, as the vessel roll motion becomes a hard limit for such heavy lift vessel. In addition, higher snap loads, which occur in splash zone drives the workability as well for anchor installation.

## 6.5 Mooring Line Hook-Up Station Keeping Analysis

### 6.5.1 Floating Substructure Modelling

The software used to model the two reference floating substructures as defined in Section 4.2 is OrcaFlex based on inputs from COREWIND’s deliverables D1.2 [3] and D1.3 [6]. Each column and pontoon are modelled with 6D buoy elements with different diameter, length and drag coefficients. Tower sections are modelled with line elements. The RNA components are modelled with the wind turbine element.

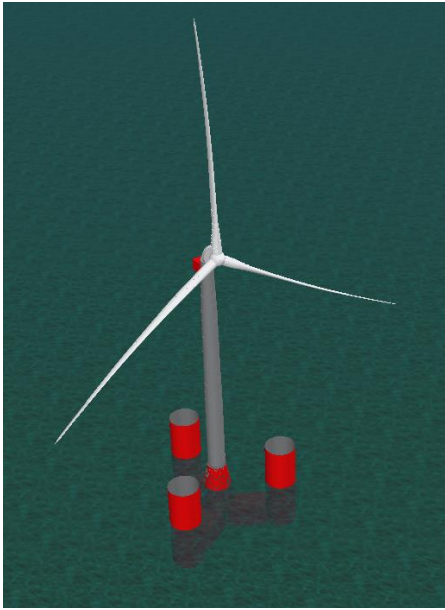


Figure 6-3: Illustration of the OrcaFlex model of the ActiveFloat semi-submersible equipped with the IEA 15 MW reference wind turbine [Source: Ramboll].



Figure 6-4: Illustration of the OrcaFlex model of the Windcrete spar equipped with the IEA 15 MW reference wind turbine [Source: Ramboll].

### 6.5.2 [Mooring System Modelling](#)

Line objects in OrcaFlex are used to represent the mooring lines consisting of several segments and defined with different line types with unit weight, diameter, axial stiffness, MBL, drag coefficients etc. The mooring system is based in inputs from COREWIND's WP2 and optimisation works done for deliverable D2.2 [2]. See Section 4.4 for more details.

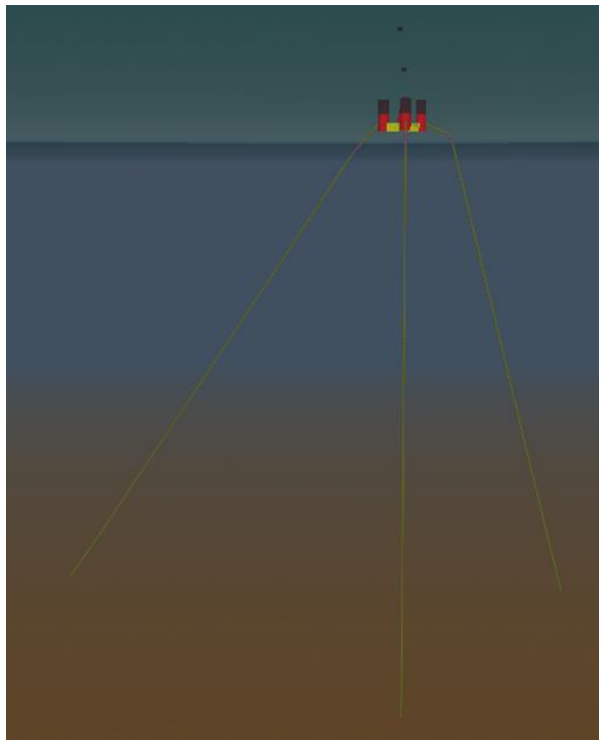


Figure 6-5: Illustration of the reference mooring system of the ActiveFloat semi-submersible [Source: Ramboll].

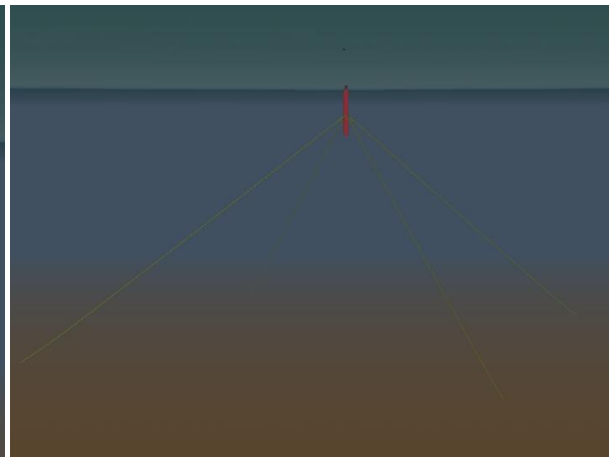


Figure 6-6: Illustration of the reference mooring system of the Windcrete spar [Source: Ramboll].

### 6.5.3 Force Allocation Calculation

The mooring leg is used to reference a group of mooring lines. In this analysis three 4.6.24.6.24.6.34.6.34.6.44.6.4. Subsequently, it is determined if the resulting horizontal loads can be counteracted by the bollard pull of the selected tug boats. A force allocation calculation is performed for each environmental direction to determine the minimum required tug bollard pull and the required heading control of each tug. The resultant force and moment acting at COG are all zero. It's assumed in this analysis that the installation winch capacity on the floater is not limited, so that the mooring force on the connected mooring legs can be negligible.

The environmental direction for wind, current and wave are considered as colinear in this analysis. However, in the real offshore operation, the probability of occurrence for colinear environmental conditions is quite low. The purpose of this analysis is to verify the capacity of the tug boat to be selected using a conservative approach.

### 6.5.4 Results for ActiveFloat Semi-submersible

Figure 6-7 illustrates the tug bollard pull of an exemplary force allocation case for all tugs with  $H_s = 3$  m,  $T_p = 6$  s and incident waves, wind and current from 120 deg direction.

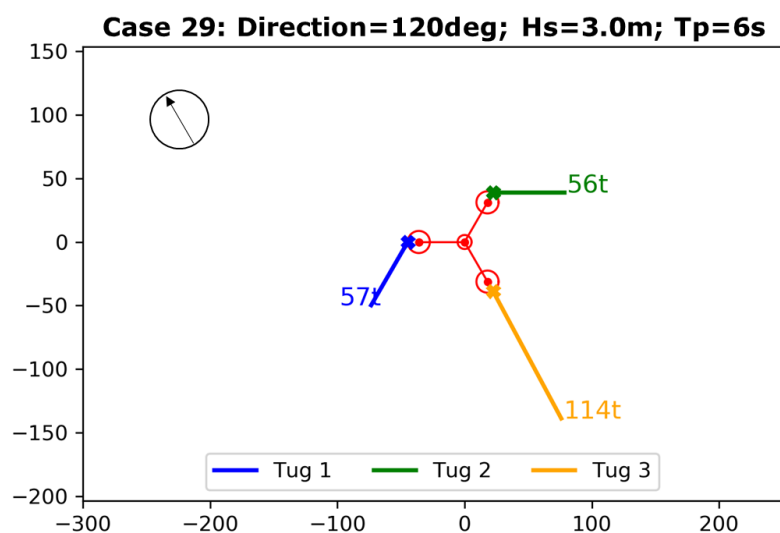


Figure 6-7: Exemplary tug configuration for station keeping during mooring line hook-up ActiveFloat (wave direction shown in top left corner) [Source: Ramboll].

The required bollard pull of all considered cases is included in Table 6-11.

Table 6-11: Results of the force allocation for each tug for Hs = 3.0 m and ActiveFloat.

Load Case [-]	Heading [deg]	Wave period Tp [s]	BP Tug 1 [t]	BP Tug 2 [t]	BP Tug 3 [t]
1	0	6	109	55	55
2	0	8	104	52	52
3	0	10	99	49	49
4	0	12	95	48	48
5	0	14	93	46	46
6	0	16	91	46	46
7	0	18	91	45	45
8	30	6	98	18	71
9	30	8	97	19	71
10	30	10	92	18	67
11	30	12	88	16	65
12	30	14	86	16	63
13	30	16	85	16	62
14	30	18	84	16	62
15	60	6	86	0	90
16	60	8	80	0	84
17	60	10	76	0	80
18	60	12	73	0	77
19	60	14	71	0	76
20	60	16	70	0	75
21	60	18	69	0	73
22	90	6	72	23	103
23	90	8	71	23	102
24	90	10	68	22	97
25	90	12	65	21	93
26	90	14	64	20	91
27	90	16	63	20	89



Load Case [-]	Heading [deg]	Wave period Tp [s]	BP Tug 1 [t]	BP Tug 2 [t]	BP Tug 3 [t]
28	90	18	62	19	89
29	120	6	57	56	114
30	120	8	54	53	108
31	120	10	52	51	103
32	120	12	50	49	99
33	120	14	49	47	97
34	120	16	48	47	95
35	120	18	48	46	94
36	150	6	25	71	100
37	150	8	25	70	99
38	150	10	24	66	95
39	150	12	23	64	90
40	150	14	22	62	88
41	150	16	22	61	87
42	150	18	22	61	86
43	180	6	0	85	85
44	180	8	0	79	79
45	180	10	0	75	75
46	180	12	0	72	72
47	180	14	0	70	70
48	180	16	0	69	69
49	180	18	0	68	68
<b>Maximum BP</b>			<b>109</b>	<b>85</b>	<b>114</b>
<b>Maximum BP with 80% tug efficiency</b>			<b>136</b>	<b>106</b>	<b>142</b>

Based on the results above (Table 6-11), it can be concluded that the required minimum bollard pull for installation of ActiveFloat is 142 ton (incl. efficiency). Hence, the three proposed tug boats with bollard pull capacity of 200 ton (as used for the towing analysis in Section 6.3) are sufficient to keep the floating offshore wind turbine in position under design weather conditions during mooring line hook-up operations.

### 6.5.5 Results for Windcrete Spar

Figure 6-8 illustrates the tug bollard pull of an exemplary force allocation case for all tugs with  $H_s = 3$  m,  $T_p = 6$  s and incident waves, wind and current from 120 deg direction.

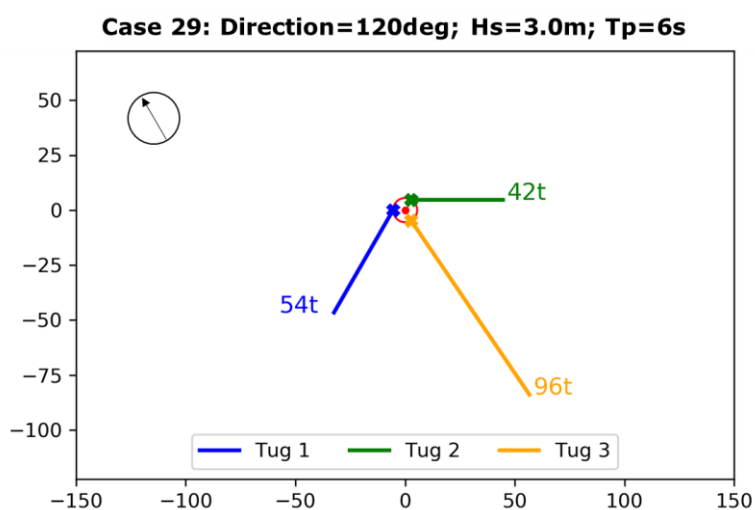


Figure 6-8: Exemplary tug configuration for station keeping during mooring line hook-up Windcrete (wave direction shown in top left corner) [Source: Ramboll].

The required bollard pull of all considered cases is included in Table 6-12.

Table 6-12: Results of the force allocation for each tug for Hs = 3.0 m and Windcrete.

Load Case [-]	Heading [deg]	Wave period Tp [s]	BP Tug 1 [t]	BP Tug 2 [t]	BP Tug 3 [t]
1	0	6	92	46	45
2	0	8	90	46	44
3	0	10	88	44	43
4	0	12	87	44	43
5	0	14	87	44	43
6	0	16	87	44	43
7	0	18	87	44	43
8	30	6	92	23	54
9	30	8	91	22	53
10	30	10	90	22	52
11	30	12	89	22	51
12	30	14	88	22	51
13	30	16	88	22	51
14	30	18	88	22	51
15	60	6	82	0	62
16	60	8	80	0	60
17	60	10	79	0	59
18	60	12	78	0	59
19	60	14	78	0	59
20	60	16	78	0	58
21	60	18	78	0	58
22	90	6	68	15	88
23	90	8	67	15	86
24	90	10	66	15	85
25	90	12	66	14	84
26	90	14	65	14	83
27	90	16	65	14	83
28	90	18	65	14	83

Load Case [-]	Heading [deg]	Wave period $T_p$ [s]	BP Tug 1 [t]	BP Tug 2 [t]	BP Tug 3 [t]
29	120	6	54	42	96
30	120	8	53	41	94
31	120	10	52	40	93
32	120	12	52	39	91
33	120	14	52	39	91
34	120	16	51	39	91
35	120	18	51	39	91
36	150	6	27	56	91
37	150	8	26	54	89
38	150	10	26	53	88
39	150	12	26	53	87
40	150	14	26	53	87
41	150	16	26	52	86
42	150	18	26	52	86
43	180	6	0	69	69
44	180	8	0	67	68
45	180	10	0	66	67
46	180	12	0	65	66
47	180	14	0	65	66
48	180	16	0	65	65
49	180	18	0	65	65
<b>Maximum BP</b>			<b>92</b>	<b>69</b>	<b>96</b>
<b>Maximum BP with 80% tug efficiency</b>			<b>116</b>	<b>86</b>	<b>120</b>

Based on the results above, it can be concluded that the required minimum bollard pull for installation of Windcrete is 120 ton (incl. efficiency). Hence, the three proposed tug boats with bollard pull capacity of 120 ton (as used for the towing analysis in Section 6.3) are sufficient to keep the floating offshore wind turbine in position under design weather conditions during mooring line hook-up operations.

## 6.6 Upending Analysis

### 6.6.1 Introduction

“Upending” in the context of a spar type floating foundation refers to the process of installing the platform in an upright position in the water during the T&I phase. Different fabrication and assembly methodologies are feasible for a concrete spar. For example, it can be constructed vertically inshore using slip forming, or fabricated in segments onshore before being transported to the mating location. Ballasting and rigging are used during the upending of the platform, which is gradually raised and turned into vertical orientation. By using cranes, winches, and other heavy machinery, specialised marine contractors can carry out this task.

The length of the Windcrete spar including concrete tower of 285 meters, and its structural mass (without assembly) of around 40,000 tons (see COREWIND deliverable D1.3 [6]) make the installation and turbine integration a challenging operation. Depending on site and project specific parameters such as the metocean conditions, vessel operational limits for the installation sequence, durations required, number of units to be installed, distance to port, etc. installation of a floating offshore wind farm can be challenging. Hence, a detailed knowledge of critical wave-structure interaction during the installation process is beneficial to de-risk the T&I campaign. In this report a detailed hydrodynamic analysis for the upending process is carried out to investigate limiting wave conditions during the upending of the spar. A combined multi-fidelity approach is applied. The radiation-diffraction driven HAWC2 model [2] is used for the broader parameter range of orientations and wave

heights. For the detailed wave-structure interaction, an OpenFOAM CFD model is applied. With focused wave groups an efficient representation of a wave group with a large crest height is obtained.

### 6.6.2 Methodology

In this chapter the upending process is transformed into a numerical problem along with the wave characteristics, the applied software and the test matrix.

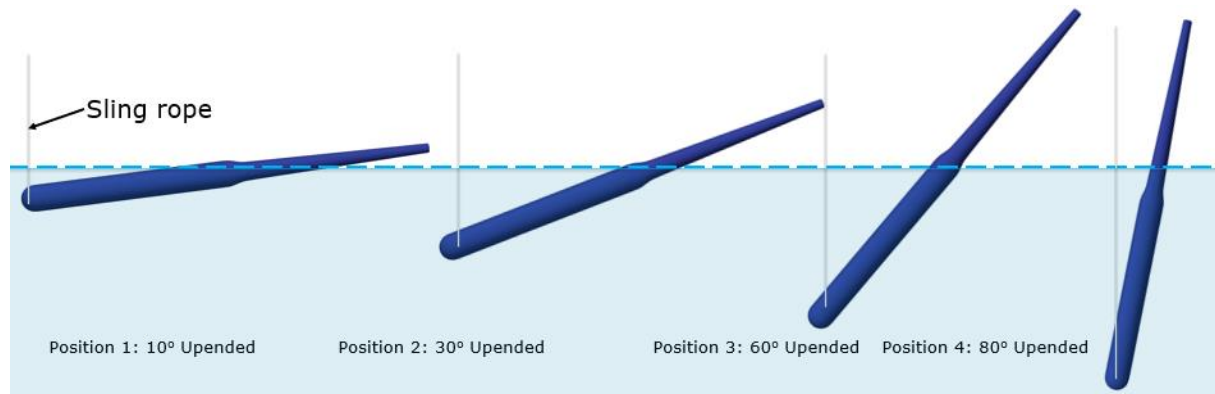


Figure 6-9: The upending process and the chosen four positions [Source: DTU].

The upending process entails gradually tilting the Windcrete spar from a horizontal to a vertical position in water. Certain operational limits and durations apply for this procedure. From the entire process, four orientations are chosen for the detailed analysis. These are shown in Figure 7-3. Position 1 corresponds to an angle of 10 degrees between spar centre axis to the mean sea level based on input from COREWIND partner UPC. Positions 2, 3, and 4 are upended by 30, 60, and 80 degrees to cover a wider spread of positions, respectively. The results of each position's wave interaction analysis are discussed in the next section. At the bottom hemisphere's end, a sling rope is attached with a specification chosen from an exemplary supplier for wire rope and rigging for offshore construction. A specific pretension is needed in the lines so that the sling also compensates for a portion of the foundation mass during the upending process.

#### 6.6.2.1 Wave Conditions

Extreme wave events are modelled as a focusing wave group, following the NewWave theory [3]. The NewWave theory expresses the wave kinematics analytically in space and time of an extreme wave event for a given sea state. The phase-focused wave group combines multiple regular waves of different height, period and phase which form an extreme wave crest. This is advantageous for high fidelity models resulting in shorter simulation times, since the event is confined to a short time duration. Although possibly being applied for ULS analyses, in reality, the ocean environment is more complex and other environmental conditions may be governing for the design of offshore structures and mooring systems.

Three wave groups of different wave steepness are considered with peak wave period ( $T_p$ ) of 6 s at a water depth of 200 m (representing most probable conditions at the COREWIND reference site B at Gran Canaria): Wave 1 ( $H/L = 3\%$ ), Wave 2 ( $H/L = 7\%$ ) and Wave 3 ( $H/L = 11\%$ ), where  $H$  represents wave height and  $L$  represents wave length. The wave groups are shown in the Figure 6-10 and the wave propagation direction is parallel with the upending axis of the spar. The focusing time is set to 150 s for the total duration of simulation 300 s.

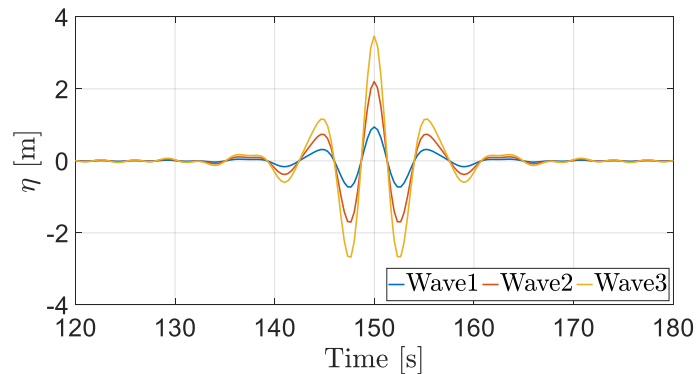


Figure 6-10: Focusing waves are generated using NewWave Theory [Source: DTU].

### 6.6.2.2 HAWC2 Methodology

DTU Wind and Energy systems developed and distributes the HAWC2 model for aero-elastic calculation of the wind turbine response [7] [8]. The model has been applied in numerous studies and industrial applications, also for offshore and floating wind turbines. HAWC2 utilises the output files generated by the radiation-diffraction solver WAMIT for the hydrodynamic analysis. The HAWC2 model is setup via the following steps:

- Each floater orientation is meshed in the CAD software RHINO and analysed in the radiation diffraction solver WAMIT for a range of wave frequencies;
- The focussed waves (Wave 1, Wave 2, Wave 3) kinematics are calculated using NewWave theory;
- The previous outputs are called in HAWC2 and the simulation is examined in the HAWC2-WAMIT solver.

### 6.6.2.3 OpenFOAM Methodology

OpenFOAM (Open Field Operation and Manipulation) is a free, open-source computational fluid dynamics (CFD) software platform. It provides a suite of tools for modelling, solving, and post-processing of various types of fluid flows. The waves2Foam [8] [9] package converts wave data into the OpenFOAM format and allows users to analyse the interaction between waves and structures including wave loads, hydrodynamic coefficients and floating body motion. The current study utilises this solver in conjunction with a mesh morphing approach for evaluating the upending analysis. The methodology adopted for (in each position) CFD investigation is:

- Parametric study on focusing wave generation
- Mesh generation for the floater and domain
- Hydrostatic analysis – To evaluate the accuracy of mass properties and buoyancy
- Wave structure interaction – calculation of motion response during the wave group passage

### 6.6.2.4 Test Matrix

Each of the four upending positions is examined for its interaction to three focusing waves resulting in a total of 12 test cases. The peak wave periods of 9 s and 12 s are chosen for the investigation of extreme wave conditions, and various H/L values (3% to 11%) are analysed to identify the limiting wave height for upending that can be sustained before the sling rope starts to slack. Table 7-1 illustrates the test matrix used. Position 1 is selected for the CFD study, and it is investigated for Wave 3 from peak wave period 6 s. These results are compared with HAWC2 later in the next section, and the detailed flow characteristics around the spar are described.

**Table 6-13: Test matrix for upending analysis.**

Test Case	Wave Period $T_p$ [s]	Wave type	Upending Position
Case 1-3	6	Wave 1,2,3	Position 1
Case 4-6	6	Wave 1,2,3	Position 2
Case 7-9	6	Wave 1,2,3	Position 3
Case 10-12	6	Wave 1,2,3	Position 4
Case 13	9	Limiting Wave	Position 1
Case 14	12	Limiting Wave	Position 1

### 6.6.3 HAWC2 Analysis for the Normal Sea State Conditions

The results of the HAWC2 investigation presented in this section focus on the behaviour for the four different upending positions of the spar under normal sea state conditions (Case 1-12 at  $T_p = 6$  s). The key outputs of the investigation include the spar's motions of surge, pitch, and heave, as well as the force acting in the sling line. No mooring system is attached to the spar to restrict the motion but restoring moment is provided by the sling rope. The behaviour of the spar's upending bending moment is also included in the analysis to show how it changes with different upending positions. The results are presented to demonstrate the implications for the installation process in challenging sea states.

#### 6.6.3.1 Decay Investigation

The eigen, or natural, period of each of the four upending position is determined through numerical simulations where an initial push is applied in a specific direction and then released, allowing the natural period of the platform to be measured. The sling rope is attached during the decay test. The results of the investigation Table 6-14) show that as the waterplane area decreases from position 1 to position 4, the natural periods in both surge and heave increase. The heave and pitch frequency at position 1 and 2 are 13 s and 18 s respectively, whereas surge is above 100 s.

**Table 6-14: Eigen period observation for different upending position.**

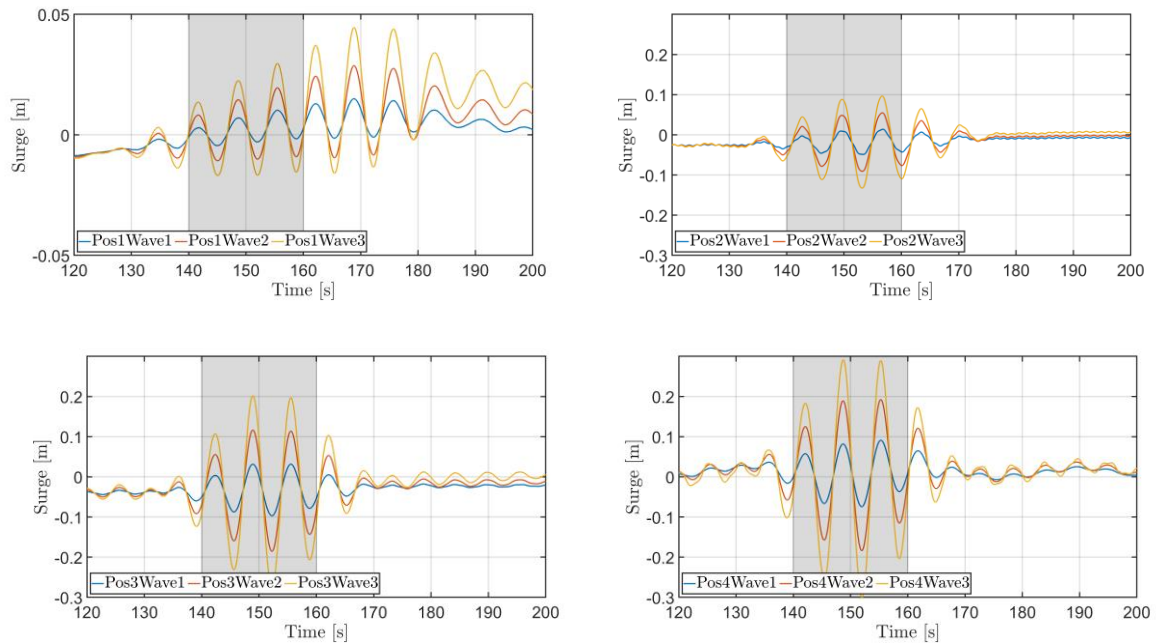
Upending Position	Eigen period [s]		
	Surge	Heave	Pitch
Position 1	125	13	13
Position 2	166	18	18
Position 3	200 – 250s*	25	25
Position 4	250 – 300s*	30.5	30.5

*\*Values are estimated as the sling rope starts to slack at high inclinations of the spar*

The heave and pitch periods of the spar are observed to be similar due to the influence of the sling rope connection. The sling rope restricts the motion of the spar, such that heave and pitch are practically locked together due to the small excursion of the sling attachment point. For positions 3 and 4, the surge natural period

surpasses 200 seconds. Overall, the key takeaway from this analysis is that the heave and pitch eigen period of the spar starts at 13 seconds and reaches 30 seconds as it approaches its final position (according to D1.2 the heave natural period is 33 s and the pitch natural period is 41 s).

### 6.6.3.2 Surge Motion



**Figure 6-11: Surge motion in focusing waves for the four different positions [Source: DTU].**

The spar platform's upending positions are analysed under three different wave steepness conditions using the focused waves and four different positions, and the results are presented in Figure 6-11. The investigation reveals that the amplitude of the oscillations of the spar increases as the upending position progresses from position 1 to position 4, although the overall amplitudes remain within 40 cm with respect to the COG, which is relatively small compared to the size of the structure. The shadowed grey window refers to the zone of the focusing wave interaction at the point of flotation (midpoint of water plane area) over the floating structure (see also Figure 6-10 with main waves captured between 140 to 160 s). Position 1 experiences more oscillations compared to the other positions, likely due to natural periods in heave and pitch being close to the wave excitation period. There is also a slight observation of second-order behaviour, manifested through the low-frequency drift motion in position 1, which continues after the main wave group passage. This motion is much less pronounced for position 2-4. A more detailed investigation of position 1 is presented in Section 6.6.4.2, which includes a Computational Fluid Dynamics (CFD) analysis.

### 6.6.3.3 Heave and Pitch Motion

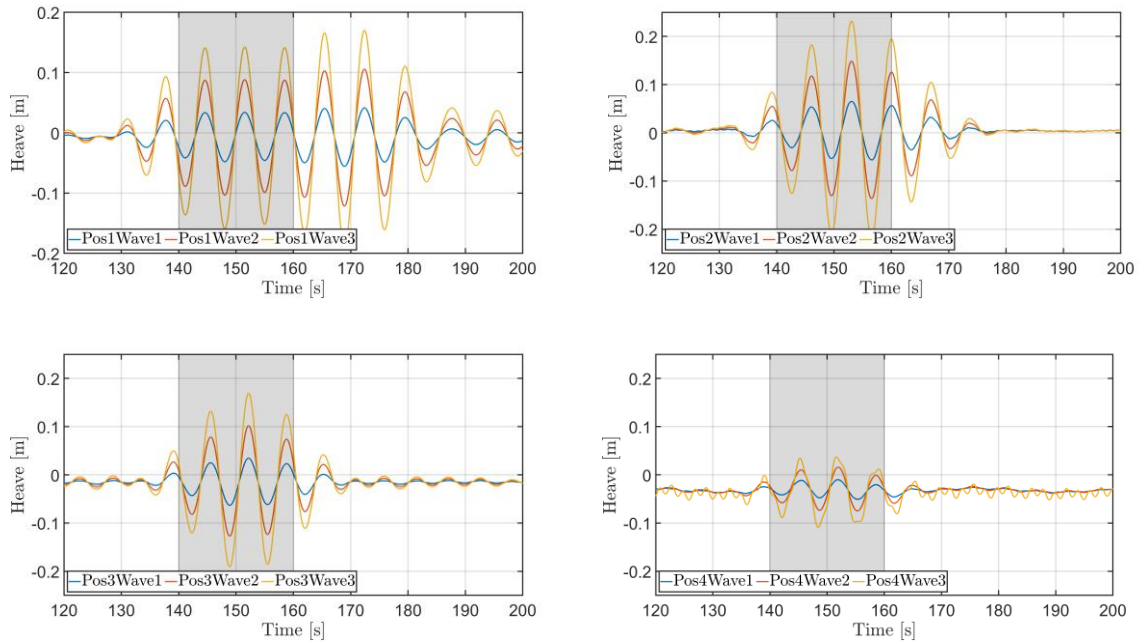


Figure 6-12: Heave motion in focusing waves for four different positions [Source: DTU].

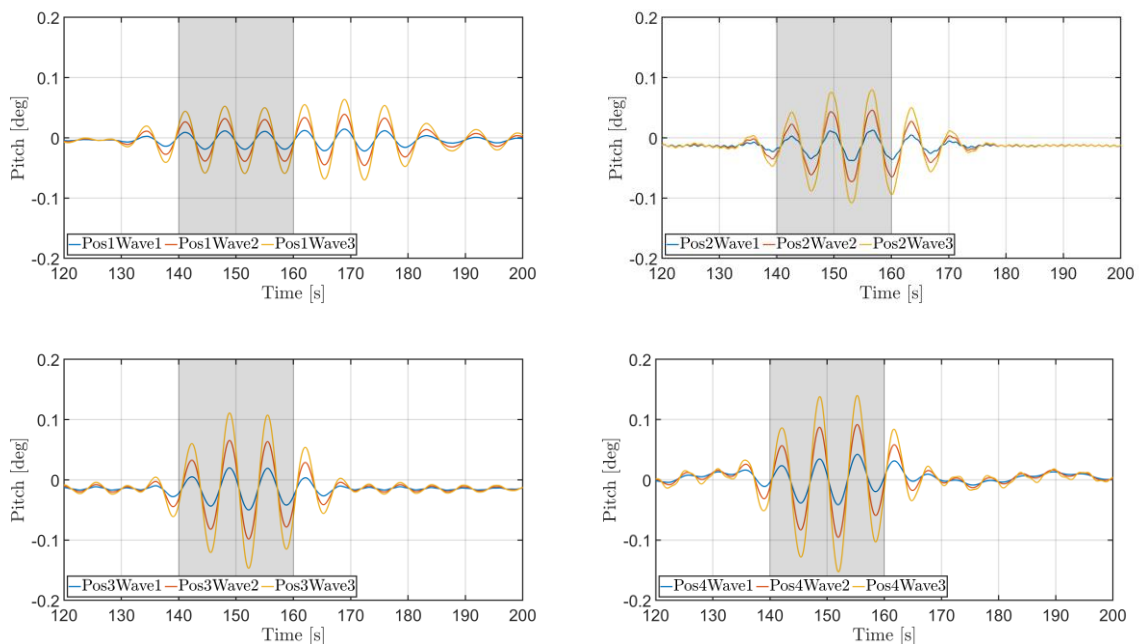


Figure 6-13: Pitch motion in focusing waves for four different positions [Source: DTU].

The heave and pitch motions exhibit a comparable trend to the surge motion. As the spar moves from position 1 to position 4 in its upended state, the amplitude of the heave decreases. The heave oscillation reaches a maximum amplitude of 30 cm, but drops to less than 10 cm at position 4. Due to its natural period, position 1 exhibits more oscillations compared to other positions. The pitch motion follows a similar pattern. In the pitch, the amplitude increases from 0.1 degrees to a maximum of 0.25 degrees at position 4 (measured at the COG of the rigid structure). The rigidity of the sling rope attached to the spar is accountable for the minimum amount of rotational motion. As for the surge case, substantial motion after the passage of the wave group is visible in



position 1. Additional to the second-order effects of drift loads, the heave and pitch in position 1 after the focused wave has passed the structure can also be linked to the long spatial extent close to the mean water level for the spar in this position. The waves that make up the focused wave group at the point of flotation will also be present along the spar away from the focus point and thus create heave and pitch forcing in a wider time window.

#### 6.6.3.4 Sling Rope Tension

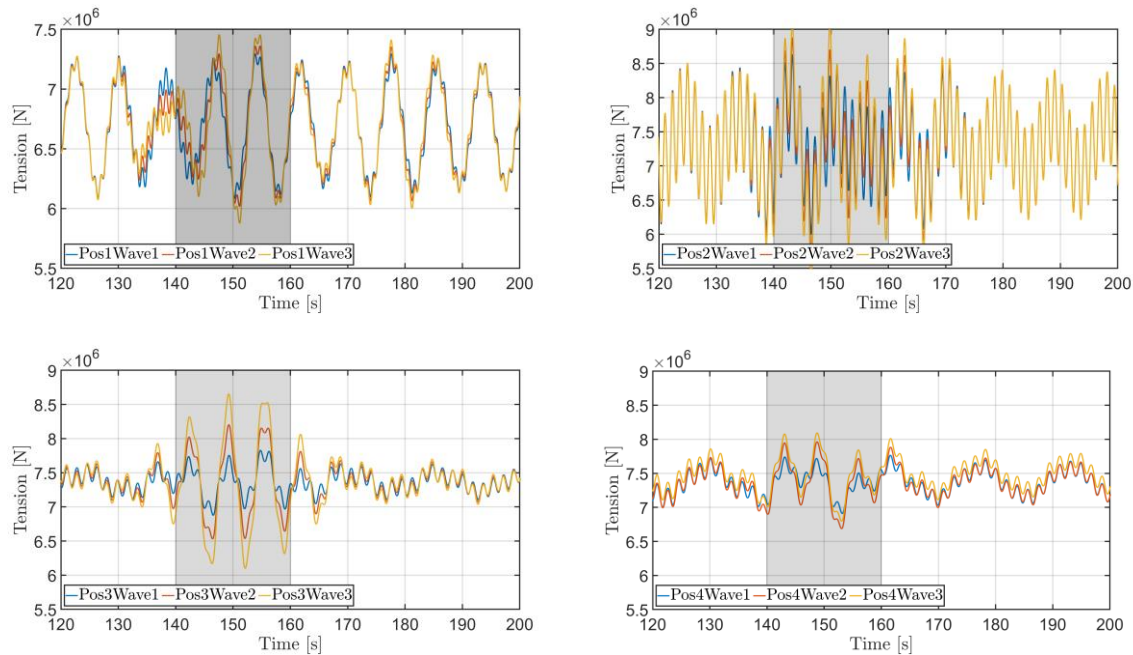


Figure 6-14: Sling Tension in focusing waves for four different positions [Source: DTU].

To achieve a realistic sling configuration, the modelled sling is made out of a pair of two identical sling ropes, both positioned at the hemispherical junction of the cylinder at the bottom of the spar. Each sling has a diameter of 318 mm chosen from an exemplary supplier for wire rope and rigging for offshore construction, a Minimum Breaking Load (MBL) of 55,000 kN and a working load of 11,300 kN (including contingency for safety). These slings are subjected to a certain level of pretension to set the spar's position in hydrostatics. The level of pretension varies from one position to another. During the interaction of the waves with the upending spar, the influence of the waves on the sling tensions is negligible in positions 1 and 2 (negligible variation of tension per wave), and slightly more pronounced in positions 3 and 4. Wave 3 has an increment in the sling tension amplitude of  $0.5 \times 10^7$  N compared to Wave 2, and  $1 \times 10^7$  N compared to Wave 1. Sling vibration is observed in all the cases, especially for position 2. This indicates that the damping (hydrodynamic and in the sling) is important. A detailed analysis of the source of vibration is planned as future work. This information is presented here not as a definitive solution regarding the slings, but to provide an understanding of the forces expected during upending and its variation.

### 6.6.3.5 Quasi-Static Heave Contribution to Bending Moment

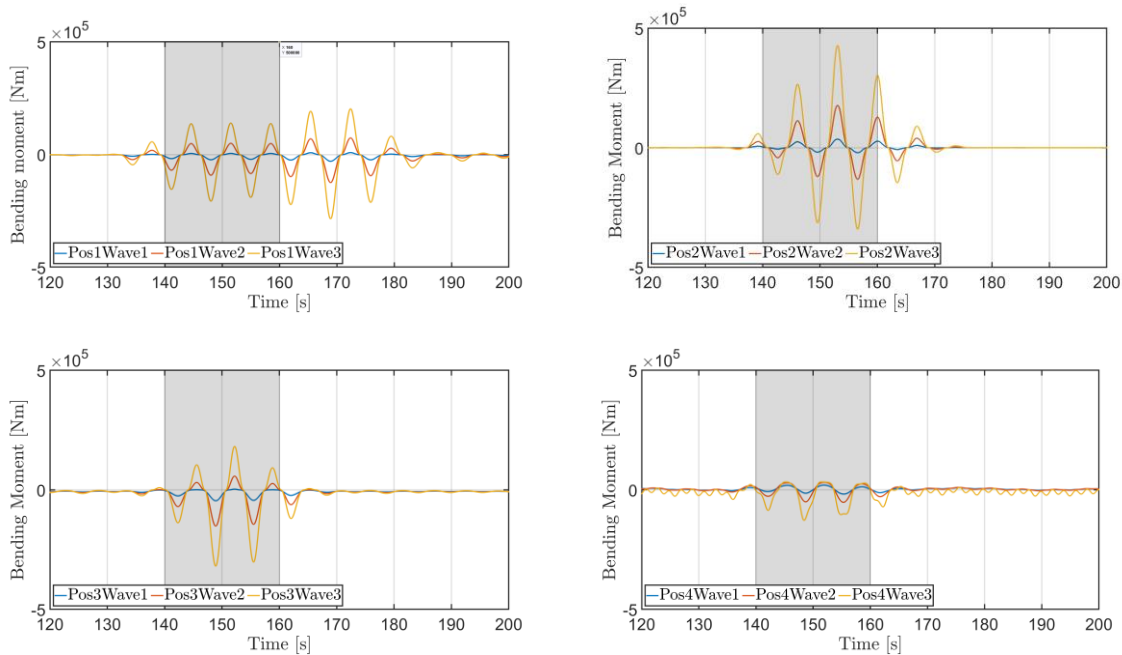


Figure 6-15: Wave induced bending moment in focusing waves for four different positions [Source: DTU].

The wave-induced bending moment at different upending positions is estimated using the following procedure: First, the crossing of the spar centre line with the mean water level at equilibrium is determined and the static moment from the freely hanging end of the spar is calculated in the intersection point. Second, the wave-induced heave motion causes the body to move above and below mean sea level, adding and subtracting extra dynamic bending moment to the total bending moment. This heave-induced bending moment is calculated for all four upending positions and three different wave steepness and is shown in the Figure 6-15. The wave induced bending moment is directly proportional to the amplitudes of heave motion. As a result, positions 1 and 2 show a higher bending moment compared to the other positions. The additional bending moment is seen to range from 200 to 800 kNm, due to the interaction of the waves. This wave-induced dynamic contribution must be added to the static bending moment from the unsupported length outside of the free surface.

### 6.6.4 Extreme Sea State Analysis

For the extreme sea state analysis the peak wave periods of 9 s and 12 s are investigated (Case 13 and 14). When the waves become too steep, the floater's motions can increase, causing the mooring lines to become slack and potentially increasing the risk of damage or loss of control. This is particularly dangerous for upending operation in exposed locations, such as open oceans or in areas with severe weather conditions. To mitigate this risk, it is important to understand the risk involved in the installation process.

#### 6.6.4.1 Radiation-Diffraction Results

In the current investigation using HAWC2 with the radiation-diffraction results from WAMIT, two additional peak wave periods (9 s and 12 s) are tested for position 1 in addition to the results of peak wave period 6 s for different wave steepness. This position is of high importance, since the spar stays longer in this posture during towing and also in the early phase of upending. An exemplary time series of sling tension is shown in Figure 6-16, for Tp 9 s and H/L 8%. Abrupt vibrations are seen after the wave group passage, each related to occurrence of slack in the line.

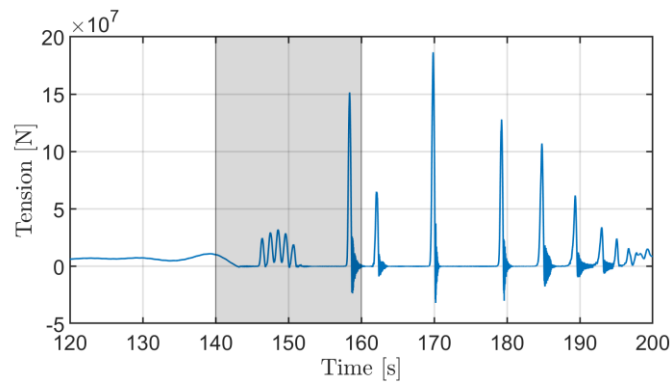


Figure 6-16: Typical slacking behaviour observed for  $T_p$  of 9 s and H/L of 8% for position 1 [Source: DTU].

The results show that the sling ropes fall slack at 8% and 6% wave steepness for peak wave periods of 9 and 12 s, respectively (see Table 6-15 below) The slack events exert a massive impact on the offshore crane and sling, increasing line tension and exciting the sling natural frequency. Consequently, it is advised against doing upending operations in the red coloured weather windows.

Table 6-15: Indication of slack line events (red cells) for different combinations of wave period and wave steepness.

$T_p$ , H/L	3%	4%	5%	6%	8%	10%	11%
6 s	Green	Green	Green	Green	Green	Green	Green
9 s	Green	Green	Green	Green	Red	Red	Red
12 s	Green	Green	Green	Red	Red	Red	Red

#### 6.6.4.2 CFD Analysis for Extreme Sea State

In this section the results of the CFD investigation are presented. To validate the previous results, position 1 is modelled in OpenFOAM. The wave generation inside the CFD domain is generated with the waves2Foam toolbox and the NewWave theory for focused wave groups. At first, two-dimensional parametric studies for the wave generation are conducted considering the effect of numerical dissipation in the CFD domain. The spar position 1 is meshed using the SnappyHexMesh tool inside OpenFOAM, and the hydrostatic equilibrium is assessed to verify mass and buoyancy properties. The focused wave is then generated inside the domain after being verified in the previous parametric study. Since the focused wave in the CFD domain is not identical to a linear wave originally modelled in HAWC2 due to CFD accounting for nonlinear effects, the wave measured in CFD is used as a revised input (wave elevation time series) for the comparative simulation in HAWC2. Most notably, the waves are subject to nonlinear wave propagation in the CFD setup, which is not part of the HAWC2 model approach.

The resulting spar motions are presented in Figure 6-17, for HAWC2 and CFD. The heave motion is quite similar between the two models. This is in line with the general tendency for heave motion to be relatively linear in its response to wave motion. For the pitch, the responses show a similar phase and amplitude variation between HAWC2 and CFD, but the CFD amplitude is larger. This may relate to a difference in hydrodynamic damping between the two setups, which in the case of HAWC2 needs to be supplied as an external damping value. Accurate damping is one of the driving reasons for carrying out model tests for floating structures. CFD has the potential to be used as an alternative method to determine the damping characteristics.

The largest deviation is seen for surge, which in both solvers is characterized by a low-frequency motion. One reason for the difference is the linear model used in HAWC2, which ignores drift loads. The CFD setup is fully

nonlinear with respect to the wave motion and wave-structure interaction and therefore can capture the drift loads much better. It is possible to include second-order drift loads into the HAWC2-WAMIT setup. This is a relevant next extension of the study. Experience show, however, that a good reproduction of the second-order response requires reliable forcing and damping. Usually, the latter can be calibrated to achieve a certain measured or CFD modelled response level. Hence, the difference in surge motion in Figure 6-17 illustrates the potential use of CFD to calibrate engineering models.

The simulation in the CFD solver took four days on 200 processors to cover 200 seconds of simulation whereas the HAWC2 results are obtained within minutes.

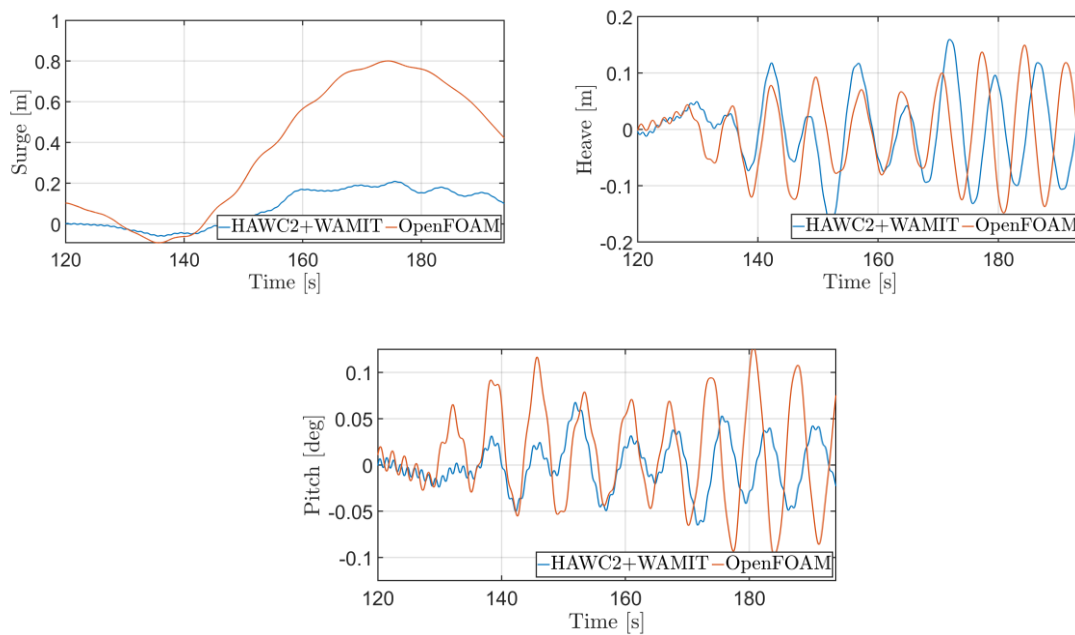


Figure 6-17: HAWC2 and OpenFOAM comparison between position 1 wave interaction with sling rope [Source: DTU].

Based on previous observations, position 1 has been deemed particularly critical due to its prolonged exposure in a single position during towing and the initial phase of upending. To gain a deeper understanding of this position, visualisations from the CFD analysis are provided in Figure 6-18 and Figure 6-19.

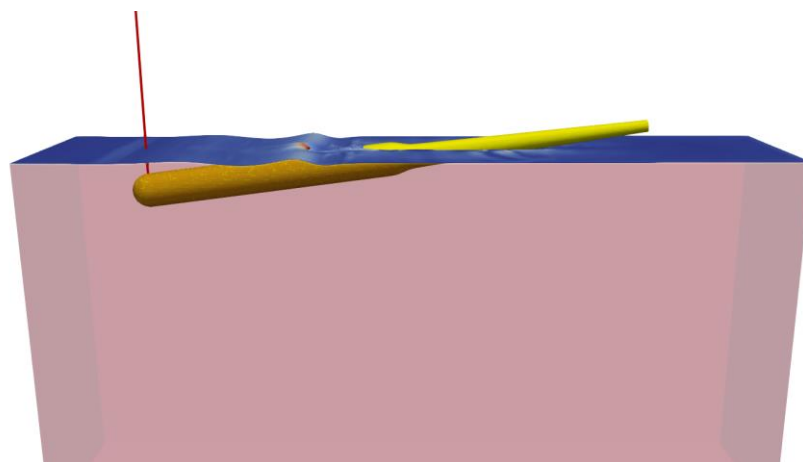
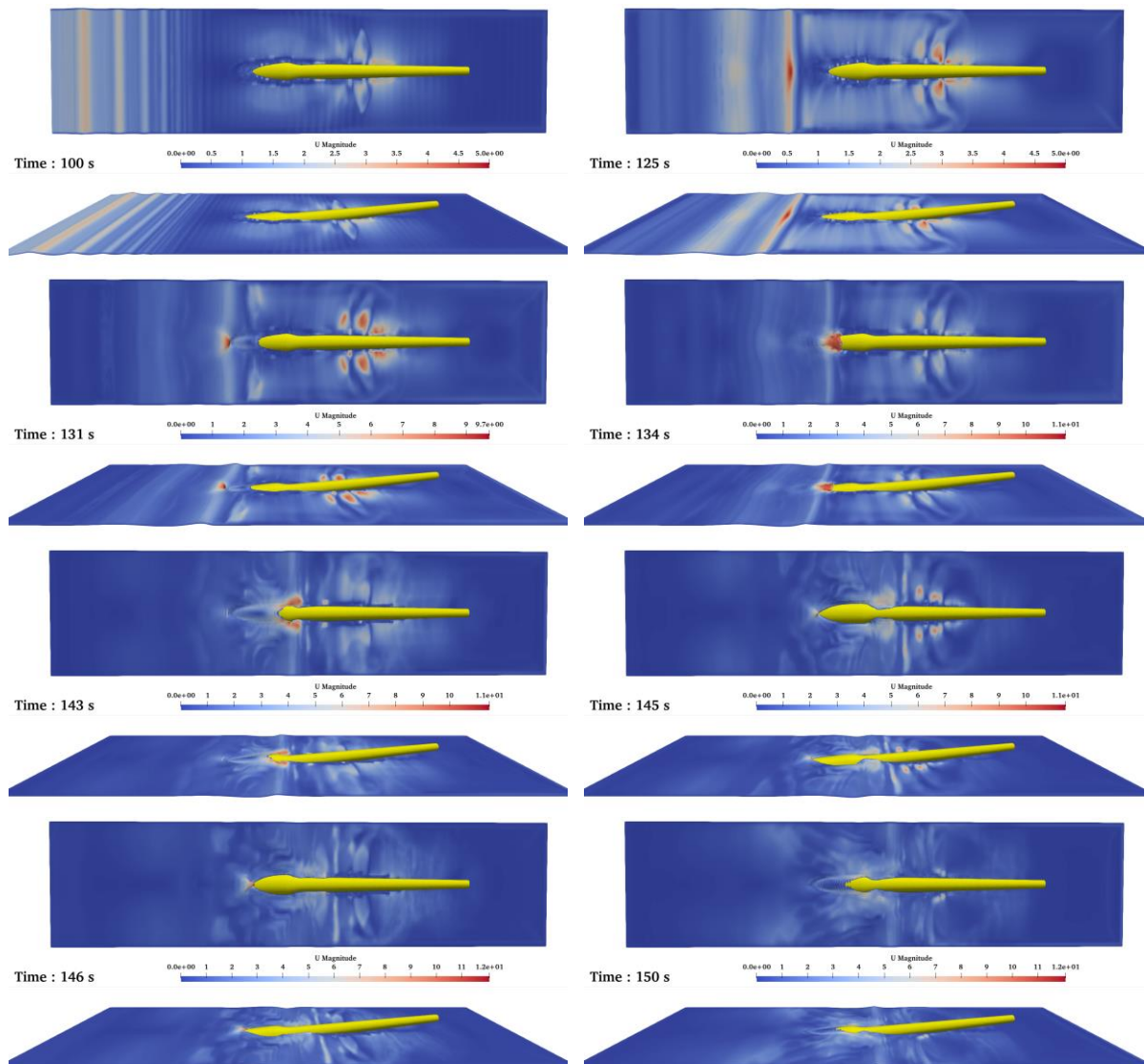


Figure 6-18: Typical CFD domain of investigation for focusing wave interaction at position 1 during upending [Source: DTU].

First, Figure 6-18 presents a side view of the spar. The incident focused wave group with wave propagation direction from left to right is visible. It can be seen that the wave crest breaks locally above the floater, due to the decreased local depth in this region and changing wave kinematics (slope induced wave breaking).

More details are provided in Figure 6-19. The inclination slope causes the focusing wave to break and create a local high-pressure zone, with a good amount of run-up along the spar. This run-up appears to generate a wave amplitude increase in the vicinity of the spar. Additionally, as depicted in Figure 6-19, there is a substantial wave run-up and a minimal impact of the spar on the free surface during wave run-down. Finally, the figure shows an interesting diffraction pattern downstream of the intersection zone with the mean water level. Here the suppression of the incident wave front at the spar leads to forward bending of the wave crests, visible at e.g.  $t = 125$  s. The detailed wave-structure interaction at the underside of the spar, where it protrudes through the water is also captured by the numerical results. The velocity legend has been chosen to help to illustrate the increase in velocity of the free surface variation.



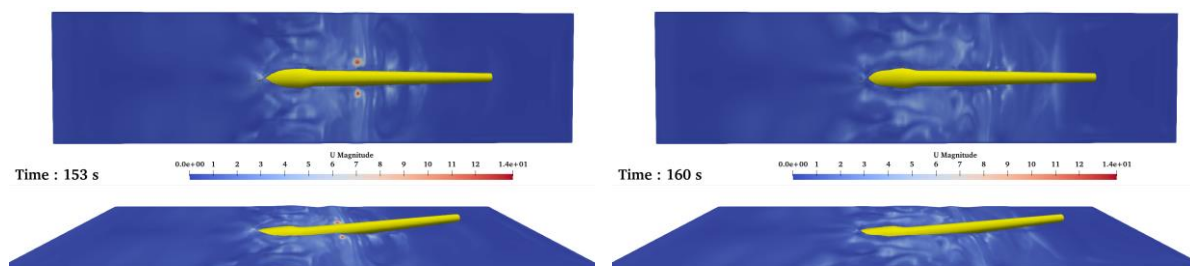


Figure 6-19: Time snapshots (top and side view) of wave breaking and wave run-up along the spar in position 1 during upending [Source: DTU].

## 6.7 Conclusions

For the installation of a FOWT, the anchor pre-installation, towing and mooring line hook-up are the main critical marine operations that influence the workability based on the operational weather conditions.

In this study, suction pile anchors are assumed, which will be installed before the floating foundation is hooked-up. A heavy lift vessel or construction vessel with a crane onboard is selected for the installation. The workability is mainly driven by the vessel type and the snap load from passing the splash zone. Typically, the heading and following sea is more favourable than beam sea due to less vessel roll motion. The further the wave period is from the vessel eigen period, the less excited the vessel roll motion is. Towing of the floating foundation from the assembly yard to the offshore installation site is performed using at least two tug boats. The minimum required tug bollard pull capacity is determined by the total environmental load to be resisted. Once the floating foundation arrives at the site, it is hold in position by means of two or three tug boats. The required weather window can be defined based on the tug boat bollard pull capacity, that can be extracted by force allocation calculation.

In this analysis, a standard vessel or equipment type are assumed. For different vessels or equipment the delivered results can differ, but a large difference is generally not expected. Hence, the calculated operational limits can be observed as a good reference for the floater installation. In addition, the environmental direction for wind, current and wave are considered as co-linear because it is a conservative approach. In the real operation, the probability of co-linear environmental condition is expected to be low.

The following table summarises the operational limits calculated for the selected temporary marine operations. This outcome is used to refine the input conditions of the sequential weather downtime analysis in Chapter 7.

**Table 6-16: Summary of operational limits for temporary marine operations for the reference concepts.**

Item	ActiveFloat Semi-submersible	Windcrete Spar
<b>Anchor Installation</b>		
Significant Wave Height Hs	1.5 m for heading and following sea	1.5 m for heading and following sea
Peak Wave Period Tp	From 6 to 18 s	From 6 to 18 s
<b>Sailing to Offshore Site</b>		
Tug Boat Bollard Pull	2 tugs x 200 t	2 tugs x 120 t
Towing Speed	2.2 kn	2.1 kn
<b>Mooring Line Hook-up</b>		
Significant Wave Height Hs	Up to 3.0 m	Up to 3.0 m
Min. Required Tug Boat Bollard Pull	3 tugs x 142 t	3 tugs x 120 t

The upending of a spar platform was numerically evaluated using HAWC2 and OpenFOAM to gain physical insights. The results showed that the initial position of 10 deg upending angle is the most critical position compared to other positions. In this position, the wave group forcing spans over a longer time duration due to the large size of the water-plane crossing of the floater. The weather windows with respect to slack loads in the sling during the installation were also presented and showed restrictions for wave periods of 9 and 12 s. It is important to note that the results are sensitive to various factors such as the sling rope connection points, sling properties, and ballast weight.

A CFD analysis for the initial position 1 at 10 deg was made to complement the radiation-diffraction analysis. A relatively good agreement was seen for heave, while damping effects are the likely cause of the observed motion amplitudes in pitch. For surge, where the response takes place at the natural surge frequency, stronger deviations were seen. This relates to the incomplete description of second-order wave forcing in the HAWC2 setup and differences in damping. These differences illustrate the potential of CFD calculations as a mean to calibrate faster engineering models. The wave breaking, wave run-up, and wave-structure interaction of the spar over the free surface during wave interaction was examined through visual simulation output. Further investigation through experimental comparison and the consideration of second-order drift loads in HAWC2 will gain a better understanding of the installation strategy.



## 7 Weather Downtime Analysis and Cost Modelling

The weather downtime analysis is performed with the commercial tool Shoreline. In preparation of the analyses, several input data according to Chapter 4 are selected and further required modelling estimates for the T&I campaigns are made. Modelling inputs and estimates feed into a work breakdown structure (WBS) in Chapter 5 for each FOWT concept which serves as main input to setup and calculate the Shoreline runs. Following the general approach of Table 6-1 the pre-calculated operational limits of temporary marine operations summarised in Table 6-16 are used to refine the input conditions of the weather downtime analysis. After the weather downtime analysis is performed, output data are post processed and applied as inputs for the cost modelling.

### 7.1 Guiding Principles and Assumptions

In this section, main assumptions and definitions are outlined to set a starting point for the weather downtime and cost analysis.

**Base port:** Los Angeles port is defined as base port for installation operations, with storage space, harbour basin dimensions, harbour entry dimensions, and air clearance assumed to be sufficient. Another option was San Francisco harbour, but the air clearance below the Golden Gate Bridge is assumed to be too restrictive. No detailed port assessment has been conducted.

**Port activities:** Port activities are reduced to loading and departure and installation activities are omitted.

**Supply chain:** Supply chains and requirements for storage of equipment at the port is not addressed. The investigation and modelling starts with the floating structures stored at the quayside and ready for tow to site. As such, fabrication, mobilisation, and pre-commissioning is not part of the developed procedures. All assets, equipment, foundations, mooring lines, and anchors are assumed present at port when needed for loading.

**WTG integration:** For ActiveFloat quayside integration is assumed, as such it is omitted for the study and assumed to be completed prior to tow-out. WTG integration for Windcrete is mandatory to be performed in deep water areas. To ensure comparability between floating substructures concepts, the WTG integration is omitted also for Windcrete and a blocker is integrated in the WBS for Windcrete.

**Sheltered area:** Upending of Windcrete is performed in a sheltered area south of Santa Cruz Island. No detailed site investigation has been conducted or whether temporary mooring lines could be deployed.

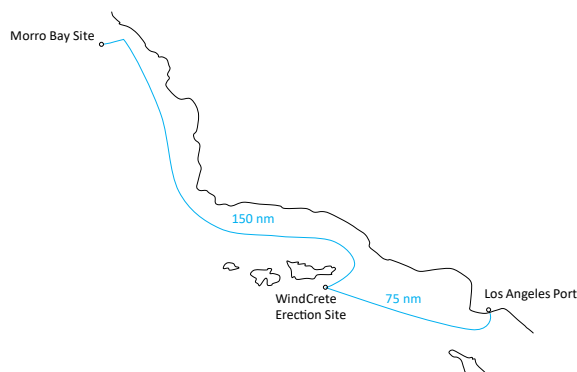


Figure 7-1: Windcrete – Route from Los Angeles port to Morro Bay site in blue and location of sheltered area for erection south of Santa Cruz Island [Source: Ramboll].



Figure 7-2: ActiveFloat – Route from Los Angeles port to Morro Bay site in blue [Source: Ramboll].

**Weather timeseries:** For the port and all other relevant locations in this study the Morro Bay site weather timeseries are applied. The time series for the site were generated via the Shoreline software from the included



ERA5 database. To account for the sheltered environment in other locations, the operational limits regarding significant wave height, peak period, wind speed, and current speed are amplified as shown in Table 7-1. For the port, limits regarding significant wave height, peak period and current speed have been discarded, as significantly more benign conditions would apply compared to the offshore site.

**Table 7-1: Increased operational limits for different locations of the study.**

Location	Wind Speed	Current Speed	Significant Wave Height	Peak Wave Period
Site (Morro Bay)	100%	100%	100%	100%
Los Angeles port	120%	Inf	Inf	Inf
Off Los Angeles port (ballasting of semi-submersible)	160%	160%	165%	115%
Off Santa Cruz Island (sheltered area for uprighting of spar)	130%	160%	170%	115%
Landfall Morro Bay	160%	140%	125%	100%

**Power cables general:** Cost reduction is possible by accommodating minimum required cross sectional area of the cables for minimum material costs. Another option is having one or a limited set of cross sections to benefit from scaling effects in the production of e.g. cables, tethers, and buoyancy elements. As on one hand production and installation costs rise at low material costs, on the other hand material costs rise with lower production and installation costs. Two different cross sections were chosen as a compromise.

**Inter array cables:** The power cables between turbines and the floating offshore substation (OSS) are considered preconfigured dynamic cables without joints, defined as cable type CW005 in D3.2 [10]. No distinction between static and dynamic sections is made here. As such, during cable lay, only works for buoyancy elements, clump weights and pull-in head preparation are considered.

**Export Cable:** The power cables for OSS to onshore grid connection is achieved by four preconfigured 220 kV HVDC cables of standard IEC equipment type (two per OSS for redundancy reasons). HVDC connection from the floating OSS to the onshore station is assumed considering the distance of about 100 km to shore, but no detailed assessment pro/contra HVAC or HVDC is made. Connection joints between dynamic and static cable sections are preconfigured. Pull-in at the landfall is assumed to be performed by an onshore winch of sufficient winching capacity. No additional floating assets are required. No trenching or horizontal drilling is assumed at the onshore substation in the work breakdown as infrastructure is ready for installation at campaign start.

**Work duration and shifts:** In this study, 24/7 working time was assumed. Factors like reduction of daily working times by legal purposes (marine mammal protection, breeding, etc.) are not considered in this study. Personnel transfer and restrictions of max. vessel operation durations are omitted.

## 7.2 Weather Downtime Analysis

In this section, the results of the sequential weather downtime analyses are summarised.

### 7.2.1 Simulation Model Description

The time-based weather downtime analyses are performed using the Design module of the commercial tool Shoreline [11], which is a browser application and as such available for various computing architectures. In the following, the main working principles, required inputs and generated outcomes of the applied methods are introduced.

#### 7.2.1.1 Required Modelling Inputs

The inputs can mainly be grouped in locations, weather time series, work breakdowns, assets and restrictions.

**Locations:** Geographic coordinates of relevant locations like harbours, waypoints, sites (WTG locations) and onshore connection points can be input manually or uploaded. Transits between these points are simulated directly according to distance and asset (vessel) velocity.

**Weather time series:** For a simulation, at least one set of meteorological weather time series is required. These time series of processed data can either be uploaded (significant wave height, wave peak period, wind speed, and current speed) via a data sheet/input matrix, or imported from public online database like ERA5 (meteorological reanalysis product by ECMWF as part of Copernicus Climate Change Services).

**Marine Work Breakdown Structure:** The logical structure/sequence of the marine works is defined in a work breakdown structure (WBS). It defines the order of tasks/activities (dependencies of single tasks or campaigns), and the associated net duration (duration calculated without influence of weather data), required weather windows, assets and operational limits such as significant wave height, peak wave period, wind speed, etc. The WBS is the main input and starting point describing the different T&I campaigns for each simulations.

**Assets<sup>1</sup>:** All physical assets considered for the transport and installation of an offshore wind farm. This can include WTG, foundation, mooring components (i.e. anchors, mooring lines), vessels and other machinery such as cranes. Different vessel types can be defined with individual operational limits (Hs, Tp, current and wind speed). The work breakdown structure can supersede/override the asset properties for certain tasks.

**Condition based restrictions:** In some cases (not considered in this study), works can only be allowed during daytime, on week days (work shifts) or at high tide.

#### 7.2.1.2 Simulation Scheme

Shoreline deploys the inputs from Section 7.2.1.1 and performs a time series analysis of the work breakdown for the defined assets. According to the asset's operational limits, the prevailing weather conditions and the duration of each work step in the sequence of operations, the weather down times and duration of all works are simulated.

---

<sup>1</sup> Modelling limitation of applied software version: Shoreline cannot estimate the amount of technically possible equipment, such as anchors or mooring lines, being installed per journey. To track efficiently across the total amount of installed WTG units, Shoreline restricts the installation to full sets of anchors or mooring lines per WTG unit. This means that not all possible amount of equipment can be installed per journey based on geometrically available vessel deck space which is contrary to common planning by installation contractors. As a result of this limitation a full number of assets per journey is required as modelling input (e.g. three mooring legs for ActiveFloat and four for Windcrete).

**Weather time series:** Weather time series can either be fed directly into the simulation or it can be used as basis to create new sets of weather time series according to the Markov algorithm<sup>2</sup> (not applied in this study), if the time series is too short for statistically reliable simulations. In both cases, a weather time series covering several years (around 20-40 years) is considered. The chronological order of the time series is not changed but both ends (i.e. start point and end point) are tied together to form a continuous time series that is used for the simulation of the installation processes.

Multiple runs of the installation operations are simulated with each run using the same time series but with progressing starting year. For example, the first simulation run starts on 1 January 2022, the second on 1 January 2023, the third on 1 January 2024, etc. This allows to calculate statistical properties such as percentiles for the duration of the installation operations. The more runs simulated, the more reliable the statistical properties. However, the number of individual runs is limited to the total length of the weather time series in years.

**Weather down times:** If the asset's operational limits are higher in magnitude than the values of the simulated time stamp for at least the duration of the task's corresponding weather window, the working steps are started. The evaluation is performed at the beginning of each working step and waiting times for the next appropriate weather window to perform the operation are defined as weather down times.

**Completed installation time series:** Each individual simulation run starts at a predefined start date (e.g. 1 February 2022, 1 February 2023, etc.). The simulation is executed until all WTGs are installed and all vessels have returned to port, or a maximum duration of the campaign, such as ten years, has been reached. Depending on the individual weather time series with individual starting year, the number of turbines to be installed and the number of vessels deployed for the installation, the duration of each run can vary. For each simulation run, the resulting weather down times for each vessel and each task as well as time series indicating the number of installed assets (turbines, foundations, moorings) are reported.

**Workability:** The workability describes the ability to perform a work task during each month, for example. 100% workability constitutes that the task can be performed without any delays from weather down time. In case of 50% workability the task can only be performed during half the time whereas the other half is spent waiting on better weather. With the simulated weather down times from each individual simulation for each work task, the workabilities can be calculated as a quantitative measure (in percentage per month) to evaluate and compare each asset and campaign.

**Probability level:** For each installation time series, the percentile over all installation time series is evaluated. Resulting from this probability distribution, the probability levels are defined as PX with X ranging from 0 to 100. In this study, P10, P30, P50, P70 and P90 values are shown. Workabilities, weather down time days and other processed quantities can be evaluated according to the associated installation time series probability level. For example, in Table 7-2 exemplary workability scores are displayed for one month with the P10 value meaning that 10% of the simulated results for this month have a workability of 74% and higher, and vice versa for P90 that 90% of the simulated results have a workability of 33% and higher.

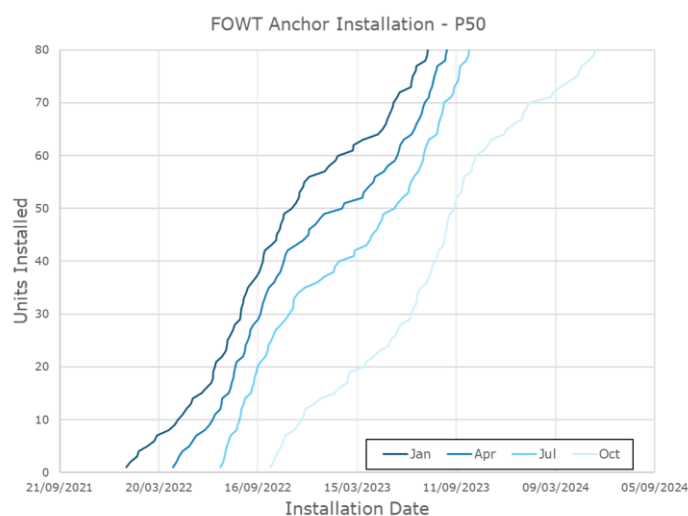
---

<sup>2</sup> With the Markov algorithm, available time series are reassembled to create a larger variety of weather time series or to enhance very short time series. Weather samples of a defined length are assembled so that the beginning of one time sample fits the end of the previous. Sampling is taken from the same calendar months from other years in the time series, if available. Otherwise another fitting sample is chosen.

**Table 7-2: Monthly workability for an exemplary installation campaign.**

Installation Campaign	Month
Workability: P10	74%
Workability: P30	62%
Workability: P50	51%
Workability: P70	42%
Workability: P90	33%

**PX installation time series:** According to the probability levels, installation time series can be plotted as S-curves (see Figure 7-3). If more than one installation time series is available for one probability level, the mean value over all respective installation time series for this probability level PX is used.



**Figure 7-3: Exemplary S-curve plot for an anchor installation campaign @P50 [Source Ramboll].**

### 7.2.1.3 Generated Outputs

Shoreline can generate various plots in the browser interface or create different outputs in spreadsheet format for external post-processing. The main outputs for the performed investigations in this study are the completion dates for each asset, campaign and probability level. Further, the weather downtime ratio output per vessel, campaign, probability and month is used to calculate the workability per campaign.

### 7.2.2 Boundary Conditions

The applied input conditions of the weather down time simulation model are described in this section.

**Weather time series:** A baseline historic weather time series of the Morro Bay site was already provided by the COREWIND partner IHCantabria (referenced as IHData) using hourly wave data from reanalysis for the assessment of floating wind specific O&M strategies in deliverable D4.2 [5]. Additionally, three public weather data sources are investigated in this study to evaluate the sensitivity of the resulting weather down times. The data are referenced as follows with more details given in Section 7.2.3:

- DOE: US Department of Energy’s Water Power Technology Office's US Wave dataset with 32 year wave hindcast (1979 – 2010) for the West Coast of the United States at 3-hour temporal resolution and down to 200 m spatial resolution [12]. This data was generated using WaveWatch III and SWAN models and can be accessed through NREL’s Marine Energy Atlas [13]. Wind data are derived from NCEP Climate Forecast System Reanalysis (CFSR) dataset [14], a coupled reanalysis of the atmospheric, oceanic, sea-ice, and land data, and can also be accessed through Marine Cadastre by BOEM [15].

- WIS: Wave Information Study by the U.S. Army Corps of Engineers [16] with hindcast nearshore wave datasets (1980 – 2020) providing hourly wave information.
- ERA5: Fifth generation ECMWF reanalysis for the global climate and weather with hourly data from 1979 to present [17], [18], [19].

A comparison of two wave reanalysis datasets based on ERA5 and operational waves modelled through CFSR wind forcing (WaveWatch III) against satellite altimeter measurements is presented by Stefanakos [20].

**Work breakdown structure:** As outlined in the above Sections 5.1 to 5.4 and 7.2.1, two work breakdown structures were developed, one for each floating foundation type ActiveFloat and Windcrete.

**Locations:** The input locations are set as introduced in Section 7.1.

**Table 7-3: Shoreline input locations.**

Functional Area	Location
Site	COREWIND reference site C at Morro Bay
Base port	Port of Los Angeles
Sheltered area for uprighting of Windcrete spar	Off Santa Cruz Island
Ballasting of ActiveFloat semi-submersible	Off Port of Los Angeles
Landfall	Landfall at Morro Bay

**Assets:** Assets used in this study are listed in Table 7-4. A brief description of the assets can be found in Section 4.5.

**Table 7-4: List of implemented assets in the weather downtime analysis.**

Assets:	Abbreviation
Anchor Handling Supply Vessel	AHTS
Heavy Lift Vessel / Offshore Construction Vessel	HLV / OCV
Remote Operated Vehicle	ROV
Offshore Tugs	-
Cable Laying Vessel	CLV
Lines Boat	-
Crew Transfer Vessel (not used)	CTV
Service operations Vessel (not used)	SOV

**Restrictions regarding working times:** As stated in Section 7.1, 24/7 working times are assumed in this study. As such, no restrictions like daytime working hours or other legal and environmental requirements are taken into account.

### 7.2.3 Weather Time Series Investigation

During first investigations, a preliminary work breakdown structure was developed with more conservative estimates of operational limits for vessels and certain marine operations. However, it was challenging to obtain reliable and realistic results for transport and installation operations at the reference site during the initial phase of the weather down time analysis. Only a small number of WTGs were installed within the maximum time frame of ten years (default abortion criterion) making the T&I campaign operationally and financially not feasible. It was found that the deployed baseline weather time series, as referenced in Section 4.6.3, are critical to selected operational limits in the preliminary work breakdown resulting in high weather down time and waiting times.

To overcome this issue, safety factors are reduced and working activities are broken down into smaller steps after revisiting, refining and optimising the preliminary work breakdown to achieve an optimised work breakdown. The implemented combination of shorter work step durations and increased operational limits, such as a higher limit of the significant wave height for a certain operation, succeeds in increasing the number of installed WTG units until the abortion criterion is met. However, accomplishing the installation of the complete reference floating wind farm with 80 units is still not possible considering a reasonable time frame.

An investigation of available weather time series for Morro Bay is performed and the baseline weather time series (referenced as IHData) is compared to other public metocean databases introduced in Section 7.2.2 (referenced as ERA5, DOE and WIS). The four considered weather time series show seasonal variations and differences in significant wave height or peak wave period per month averaged over all years of available data, as shown in Figure 7-4 and Figure 7-5. Data from ERA5 tend to be lower in magnitude (more benign) than observed for IHData or DOE (harsher), while WIS data varies between other sources. The quality of the different weather time series is not evaluated in this study. A reason for the deviations is seen in varying spatial and temporal resolution of the underlying analysis models.

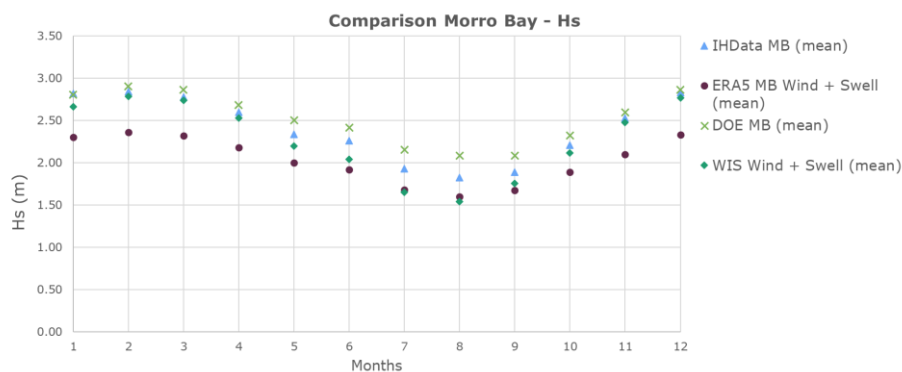


Figure 7-4: Comparison of seasonal variation of significant wave height (Hs) at Morro Bay for weather time series IHData, ERA5, DOE and WIS [Source Ramboll].

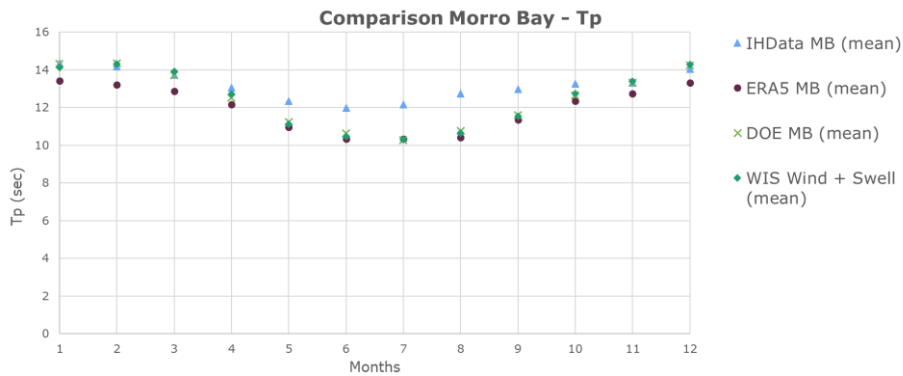


Figure 7-5: Comparison of seasonal variation of peak wave period (Tp) at Morro Bay for weather time series IHData, ERA5, DOE and WIS [Source Ramboll].

Furthermore, wave scatter diagrams are created from the metocean data sources as shown in Figure 7-6 to Figure 7-9. A clear offset can be seen for the highest probabilities between ERA5 and WIS on the one hand with relatively low significant wave height of  $1\text{ m} < H_s < 2\text{ m}$  at a broad band of peak wave period  $8\text{ s} < T_p < 14\text{ s}$ , and on the other hand IHData and DOE with higher values of  $2\text{ m} < H_s < 3\text{ m}$  at a small band of  $12\text{ s} < T_p < 14\text{ s}$ .

Tp	Hs	0.0	1.0	2.0	3.0	4.0	5.0	6.0	7.0	Sum
		1.0	2.0	3.0	4.0	5.0	6.0	7.0	8.0	
0.0	2.0									0.0%
2.0	4.0									0.0%
4.0	6.0			0.16%						0.2%
6.0	8.0		0.80%	2.55%	0.17%					3.5%
8.0	10.0		3.92%	6.91%	1.45%					12.4%
10.0	12.0		6.11%	8.09%	2.20%	0.44%				17.0%
12.0	14.0	0.32%	8.96%	12.28%	5.16%	0.98%				27.8%
14.0	16.0	0.14%	7.79%	6.63%	3.94%	1.53%	0.31%			20.4%
16.0	18.0	0.12%	5.24%	3.95%	1.92%	0.94%	0.36%	0.10%		12.6%
18.0	20.0		1.75%	1.50%	0.52%	0.21%				4.1%
20.0	22.0		0.65%	0.65%	0.23%					1.6%
22.0	24.0			0.12%						0.3%
Sum		0.7%	35.4%	42.8%	15.6%	4.2%	0.9%	0.2%	0.0%	100.0%

Figure 7-6: IHData Hs/Tp Scatter Diagram [Source Ramboll].

Tp	Hs	0.0	1.0	2.0	3.0	4.0	5.0	6.0	7.0	Sum
		1.0	2.0	3.0	4.0	5.0	6.0	7.0	8.0	
0.0	2.0									0.0%
2.0	4.0									0.0%
4.0	6.0				1.32%					1.4%
6.0	8.0			5.38%	2.94%	0.12%				8.5%
8.0	10.0		0.11%	10.98%	6.06%	0.76%				18.0%
10.0	12.0		0.24%	11.84%	5.94%	1.10%	0.23%			19.4%
12.0	14.0	0.28%	13.98%	10.87%	2.11%	0.20%				27.5%
14.0	16.0	0.10%	8.62%	5.90%	2.41%	0.42%				17.5%
16.0	18.0		3.17%	1.97%	0.78%	0.20%				6.2%
18.0	20.0		0.69%	0.53%	0.12%					1.4%
20.0	22.0									0.2%
22.0	24.0									0.0%
Sum		0.8%	56.1%	34.4%	7.4%	1.1%	0.2%	0.0%	0.0%	100.0%

Figure 7-7: ERA5 Hs/Tp Scatter Diagram [Source Ramboll].

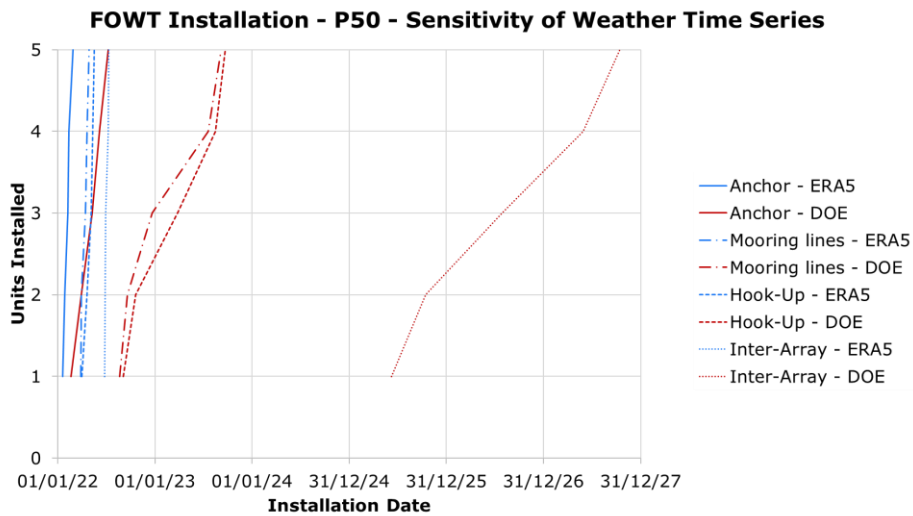
Tp	Hs	0.0	1.0	2.0	3.0	4.0	5.0	6.0	7.0	Sum
		1.0	2.0	3.0	4.0	5.0	6.0	7.0	8.0	
0.0	2.0									0.0%
2.0	4.0									0.0%
4.0	6.0			0.15%						0.2%
6.0	8.0		1.19%	4.69%	0.35%					6.2%
8.0	10.0		4.46%	7.10%	2.06%	0.14%				13.8%
10.0	12.0		7.61%	10.09%	2.61%	0.44%				20.8%
12.0	14.0	6.95%	14.10%	4.84%	0.73%	0.11%				26.8%
14.0	16.0	3.20%	5.79%	3.74%	1.06%					13.9%
16.0	18.0	3.51%	5.93%	3.69%	1.64%	0.51%				15.4%
18.0	20.0	0.48%	0.93%	0.44%	0.22%					2.2%
20.0	22.0	0.13%	0.34%	0.17%						0.7%
22.0	24.0									0.1%
Sum		0.1%	27.7%	49.1%	17.9%	4.3%	0.8%	0.2%	0.0%	100.0%

Figure 7-8: DOE Hs/Tp Scatter Diagram [Source Ramboll].

Tp	Hs	0.0	1.0	2.0	3.0	4.0	5.0	6.0	7.0	Sum
		1.0	2.0	3.0	4.0	5.0	6.0	7.0	8.0	
0.0	2.0									0.0%
2.0	4.0									0.0%
4.0	6.0				0.37%					0.4%
6.0	8.0			3.63%	1.68%					5.4%
8.0	10.0		0.41%	11.26%	5.92%	1.26%	0.13%			19.0%
10.0	12.0		0.42%	10.24%	6.55%	2.15%	0.67%	0.12%		20.2%
12.0	14.0	0.56%	8.67%	8.56%	3.45%	0.81%	0.22%			22.3%
14.0	16.0	0.46%	6.57%	6.83%	4.40%	1.74%	0.36%			20.4%
16.0	18.0	0.16%	3.08%	2.37%	1.62%	0.79%	0.34%	0.12%		8.5%
18.0	20.0		0.79%	0.85%	0.53%	0.23%	0.11%			2.6%
20.0	22.0		0.21%	0.38%	0.17%					0.9%
22.0	24.0				0.10%					0.2%
Sum		2.2%	44.9%	33.2%	13.7%	4.5%	1.2%	0.3%	0.1%	99.9%

Figure 7-9: WIS Hs/Tp Scatter Diagrams [Source Ramboll].

With the main characteristics of the weather time series and resulting differences identified, a sensitivity study is performed to assess the influence of the selected weather data on the weather down time and durations of the T&I campaign. Instead of the full 80 units of the reference floating wind farm a simulation is set up to install only five floating WTGs and one floating OSS using the same four campaigns anchor installation, mooring line pre-lay, floating foundation hook-up and power cable installation. For this comparison, the ERA5 weather time series, as the most benign available data (see Figure 7-4), and DOE weather time series, as the harshest one, are chosen to capture the overall modelling space. In Figure 7-10 the resulting S-curves using these time series are shown.



**Figure 7-10: Comparison of sensitivity case installation durations of 5 WTGs using the ERA5 and DOE weather time series [Source Ramboll].**

It can be seen, that the estimated campaign duration is highly dependent on the input weather time series. Conclusions about the quality of the respective weather time series cannot directly be drawn from this finding. Using the ERA5 weather time series the slope of the S-curves is much steeper than for the DOE data resulting in faster installation campaigns. For example, using DOE data only the anchor installation campaign is finished while at a similar time the full installation campaign is accomplished using ERA5 weather time series. Selected tasks in the work breakdown are highly impacted by the harsher weather conditions using the DOE data as operational limits or weather windows are less available. Clearly, the performed sensitivity analysis illustrates the importance of thorough weather data and environmental site assessment for a floating wind project to enable reliable T&I strategy development. Based on the above assessment the ERA5 dataset is used in the following analyses as it allows a full simulation of the installation campaign of the reference floating wind farm consisting of 80 WTG units. Using other weather data sets would result in unfinished works considering the full wind farm installation campaign and a reasonable time limit.

### 7.2.4 Results

A summary of the results of the weather downtime analysis for the four campaigns and two floating concepts is shown in Table 7-5.

**Table 7-5: Summary of weather downtime analysis results at the reference site.**

Item	ActiveFloat Semi-submersible	Windcrete Spar
<b>Overall Campaign</b>		
Campaign Duration	920 d (P10) to 1430 d (P90)	985 d (P10) to 1477 d (P90)
Rel. Weather Down Time	43% (P10) to 63% (P90)	45% (P10) to 63% (P90)
<b>Anchor Installation</b>		
Campaign Duration	440 d (P10) to 943 d (P90)	559 d (P10) to 1209 d (P90)
Rel. Weather Down Time	60% (P10) to 81% (P90)	60% (P10) to 82% (P90)
<b>Mooring Line Pre-lay</b>		
Campaign Duration	437 d (P10) to 742 d (P90)	561 d (P10) to 1018 d (P90)



Item	ActiveFloat Semi-submersible	Windcrete Spar
Rel. Weather Down Time	65% (P10) to 82% (P90)	63% (P10) to 79% (P90)
<b>Floating Foundation Hook-up</b>		
Campaign Duration	367 d (P10) to 684 d (P90)	503 d (P10) to 873 d (P90)
Rel. Weather Down Time	43% (P10) to 69% (P90)	50% (P10) to 71% (P90)
<b>Power Cable Installation</b>		
Campaign Duration	479 d (P10) to 1003 d (P90)	578 d (P10) to 1070 d (P90)
Rel. Weather Down Time	57% (P10) to 69% (P90)	58% (P10) to 78% (P90)

#### 7.2.4.1 [Starting Date Boundary Conditions](#)

In the weather downtime analysis, the first three installation packages mentioned in Sections 5.1 to 5.4 (anchor installation, mooring line pre-lay, floating foundation hook-up) are interdependent, meaning that the mooring line campaign kicks off as soon as enough anchors are installed for one mooring installation journey considering suitable weather conditions. The same mechanism works for the floating foundation hook-up campaign that waits until the first mooring line installation journey is completed. Slightly delayed, the power cable installation campaign kicks off after 25% of the WTG units are installed at site to avoid longer waiting times during the installation campaign aiming for cost reduction in day rates.

#### 7.2.4.2 [Investigated Campaign Starting Points](#)

Seasonal changes in weather conditions can impact campaign durations according to their starting dates. To account for this effect, different simulations are performed to identify seasonal weather down times also for packages with a shorter campaign duration than one year. The defined starting dates are.

- 1 January 2022
- 1 April 2022
- 1 July 2022
- 1 October 2022

#### 7.2.4.3 [Discussion of Results](#)

As described in the work breakdown in Sections 5.1 to 5.4, the procedures for anchor and mooring installation are identical for both floating foundations ActiveFloat and Windcrete. The difference in these campaigns originates from the different number of mooring legs (ActiveFloat: three, Windcrete: four), and accordingly different campaign durations and number of journeys. This leads to slightly different weather down times and workabilities for these packages between both concepts. Promoting technologies by comparing concepts against each other is not intended in this study.

For the cable installation campaigns, the only difference between both concepts is the respective start date because it depends on the completion of all preceding packages.

#### **A – Anchor Installation Campaign**

The monthly workability for the anchor installation campaign is shown in Table 7-6 for ActiveFloat and in Table 7-7 for Windcrete. In both cases, seasonal effects result in very low workabilities from January to March and higher workabilities between July and October. To the author's experience, the workabilities observed in this study for the whole campaign are relatively low, compared to other sites in western Europe or Asia. This finding

is driven by the weather conditions at the site with relatively large Hs and Tp values around the year leading to higher waiting times (see also the discussion in Section 7.2.3).

March is considered the worst month with workabilities between 2% (P90) and 32% (P10) for ActiveFloat and 3% to 29% for Windcrete. August on the other hand has the most benign weather conditions (see Figure 7-4) with scores between 33% (P90) and 74% (P10) for ActiveFloat and 33% to 75% for Windcrete.

**Table 7-6: Monthly workability for anchor installation of ActiveFloat.**

Anchor Installation	JAN	FEB	MAR	APR	MAY	JUN	JUL	AUG	SEP	OCT	NOV	DEC
Workability: P10	33%	36%	32%	41%	44%	44%	63%	74%	64%	61%	45%	41%
Workability: P30	25%	25%	22%	32%	31%	34%	54%	62%	55%	48%	37%	24%
Workability: P50	19%	14%	14%	24%	21%	29%	43%	51%	48%	38%	31%	19%
Workability: P70	10%	7%	8%	17%	16%	22%	40%	42%	43%	31%	18%	15%
Workability: P90	8%	1%	2%	11%	7%	15%	22%	33%	37%	23%	9%	9%

**Table 7-7: Monthly workability for anchor installation of Windcrete.**

Towing	JAN	FEB	MAR	APR	MAY	JUN	JUL	AUG	SEP	OCT	NOV	DEC
Workability: P10	32%	34%	29%	42%	41%	43%	60%	75%	64%	55%	45%	35%
Workability: P30	24%	25%	19%	33%	30%	34%	48%	59%	58%	48%	38%	25%
Workability: P50	19%	20%	12%	26%	23%	29%	42%	49%	50%	38%	31%	22%
Workability: P70	16%	11%	7%	21%	17%	24%	37%	44%	44%	34%	21%	17%
Workability: P90	10%	2%	3%	15%	9%	17%	28%	33%	39%	26%	7%	9%

In Table 7-8 and Table 7-9, the weather down time days for the whole anchor installation campaign are shown for the different campaign starting points and probability levels. The seasonal variation is also present in the amount of weather down time days and shows the influence of larger net durations between concepts (duration calculated without influence of weather data). For ActiveFloat, starting in July leads to the lowest number of weather down time days whereas January is the worst starting point. Due to the longer installation campaign durations for Windcrete, the preferred campaign starting point would shift to July and April whereas October becomes the worst in terms of weather down time days. While the procedures itself for both foundations are identical per mooring leg, the amount of weather down time days relative to the expected anchor installation time lies on a relatively high level of 60% to 76% for both foundations.

**Table 7-8: Weather down time days for anchor installation of ActiveFloat.**

Installation Start Date	01-Jan	01-Apr	01-Jul	01-Oct
WDT Days @P10	355	289	255	307
WDT Days @P30	379	320	273	392
WDT Days @P50	400	345	294	430
WDT Days @P70	449	397	364	482
WDT Days @P90	508	465	468	518

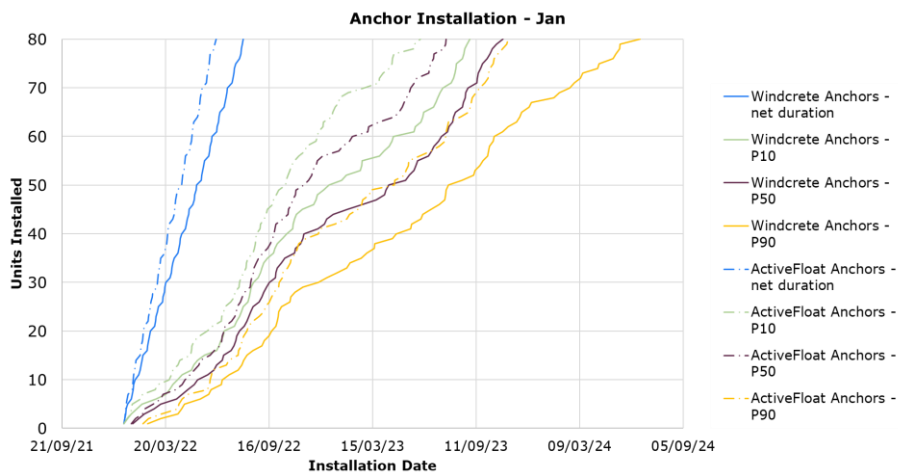
**Table 7-9: Weather down time days for anchor installation of Windcrete.**

Installation Start Date	01-Jan	01-Apr	01-Jul	01-Oct
WDT Days @P10	394	344	326	430
WDT Days @P30	411	370	385	458
WDT Days @P50	452	431	450	493
WDT Days @P70	578	536	540	557
WDT Days @P90	690	624	602	689

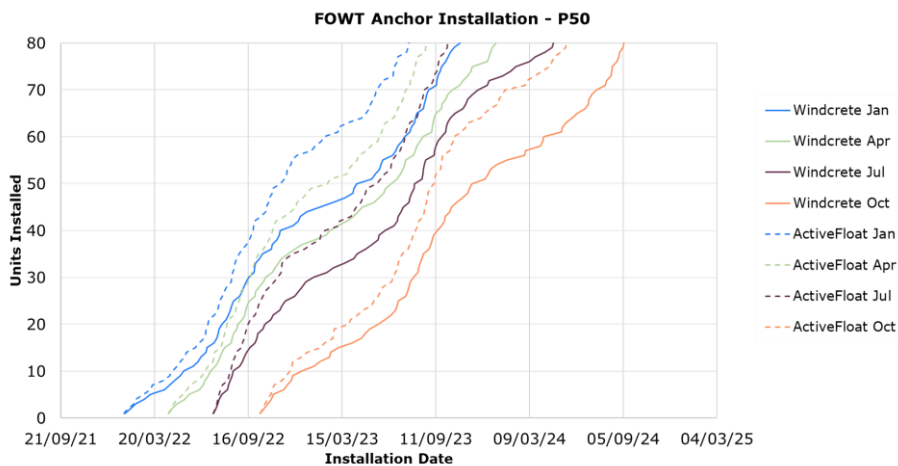
Figure 7-11 illustrates the weather down times relative to the net durations showing units installed versus time for ActiveFloat and Windcrete. Seasonal effects significantly delay campaign progress in the winter months. The seasonal effect and its impact on the campaign duration relative to the start date can be seen in the S-curves in Figure 7-12. For Windcrete, the seasonal downtimes seem to be more pronounced stretching campaign durations significantly.

Anchor installation for the two floating OSS was also investigated. As the installation procedures are equal to the above shown campaigns, the monthly workability results are similar to those shown in Table 7-6 and Table 7-7 with the relative weather downtime days in the range of 50% to 97%. This deviation is mainly driven by the low

number of samples (two OSS versus 80 floating foundations). Resulting from this, a similar amount of weather down time days relative to the net duration is expected for the OSS.



**Figure 7-11: Comparison of anchor installation campaigns for ActiveFloat and Windcrete with campaign start date in January for different probability levels [Source: Ramboll].**



**Figure 7-12: Comparison of anchor installation campaigns for ActiveFloat and Windcrete with different start dates at P50 [Source: Ramboll].**

### B – Mooring Line Pre-lay

The monthly workability for the mooring line pre-lay campaign is shown in Table 7-10 and Table 7-11. Significant seasonal effects are observed with higher workabilities between July and October, and low workabilities from December to February ( $\leq 21\%$  even at P10). August is the month with the best workability scores between 24% (P90) and 60% (P10). For ActiveFloat, February is considered the worst month with workabilities between 0% and 16% and for Windcrete, March is worst between 2% and 18%.

**Table 7-10: Monthly workability for mooring line pre-lay of ActiveFloat.**

Mooring Line Installation	JAN	FEB	MAR	APR	MAY	JUN	JUL	AUG	SEP	OCT	NOV	DEC
Workability: P10	16%	16%	18%	28%	36%	35%	48%	60%	57%	50%	28%	21%
Workability: P30	11%	10%	11%	18%	25%	23%	39%	51%	44%	34%	21%	13%
Workability: P50	8%	7%	8%	11%	18%	18%	34%	44%	37%	26%	15%	9%
Workability: P70	5%	4%	4%	8%	12%	15%	30%	36%	33%	22%	10%	7%
Workability: P90	2%	0%	2%	3%	4%	12%	18%	24%	28%	15%	5%	4%

**Table 7-11: Monthly workability for mooring line pre-lay of Windcrete.**

Mooring Line Installation	JAN	FEB	MAR	APR	MAY	JUN	JUL	AUG	SEP	OCT	NOV	DEC
Workability: P10	19%	19%	18%	28%	35%	30%	49%	59%	53%	42%	26%	21%
Workability: P30	11%	12%	12%	21%	23%	24%	41%	51%	45%	31%	20%	15%
Workability: P50	9%	9%	8%	13%	19%	19%	34%	42%	40%	27%	15%	12%
Workability: P70	6%	6%	5%	9%	13%	15%	31%	36%	35%	22%	11%	8%
Workability: P90	4%	2%	2%	5%	8%	13%	22%	25%	29%	17%	6%	4%

The total weather down time days for the mooring line pre-lay campaign (Table 7-12 and Table 7-13) indicate, that April is the best start month for the installation campaign for ActiveFloat. For Windcrete, starting in January leads to the least downtime days, but to the cost of increased weather down time days in the preceding anchor installation campaign. The relative weather down time remains relatively large for both foundations at Morro Bay with 65% to 81% (ActiveFloat) and 63% to 79% (Windcrete) of the expected mooring line installation time. The lower workability of this package compared to the anchor installation campaign mainly results from narrower weather envelopes for mooring line pre-lay and subsea works, where the Tp limit is the critical and driving factor.

**Table 7-12: Weather down time days for mooring line pre-lay of ActiveFloat.**

Installation Start Date	01-Jan	01-Apr	01-Jul	01-Oct
WDT Days @P10	311	274	283	385
WDT Days @P30	331	289	392	429
WDT Days @P50	362	364	480	444
WDT Days @P70	532	547	532	490
WDT Days @P90	635	585	588	632

**Table 7-13: Weather down time days for mooring line pre-lay of Windcrete.**

Installation Start Date	01-Jan	01-Apr	01-Jul	01-Oct
WDT Days @P10	348	364	436	412
WDT Days @P30	378	483	499	454
WDT Days @P50	527	532	529	502
WDT Days @P70	642	584	576	677
WDT Days @P90	686	654	764	757

Seasonal effects and weather down time trends can be identified in Figure 7-13. A delay between the start of the net duration graph at the earliest possible start date and the P10 graph for the most benign case of more than two months can be seen. This is due to waiting times caused from very harsh weather conditions. The impact of the start date of the campaign is illustrated in Figure 7-14. Especially in winter months the waiting times prolong campaigns resulting in significant increase in campaign durations, for example, comparing campaigns for ActiveFloat starting in April and July.

With regards to the mooring line installation for the floating OSS, the monthly workability is similar to the above shown campaigns (Table 7-10 and Table 7-11) as the installation procedures are equal. The relative weather downtime days are in the range of 36% to 87%. Like for the anchor installation package, this deviation is mainly driven by the low number of samples. Again a similar amount of weather down time days relative to the net duration is expected for the OSS.

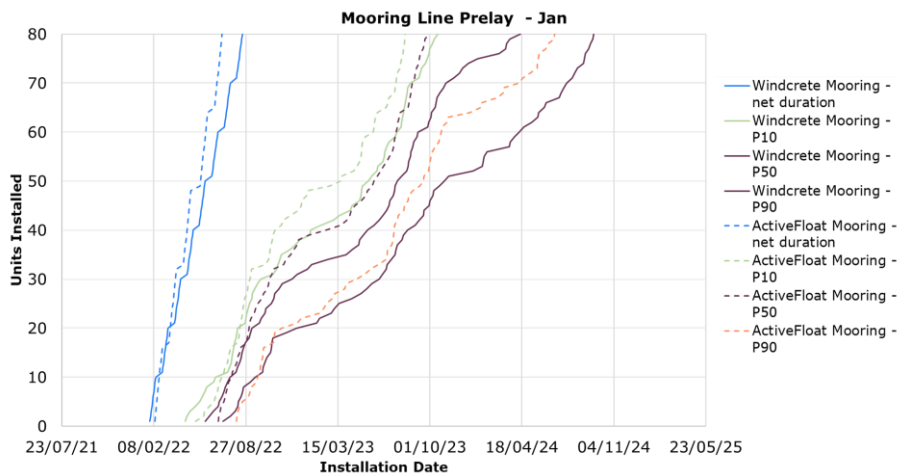


Figure 7-13: Comparison of mooring line pre-lay campaigns for ActiveFloat and Windcrete with campaign start date in January for different probability levels [Source: Ramboll].

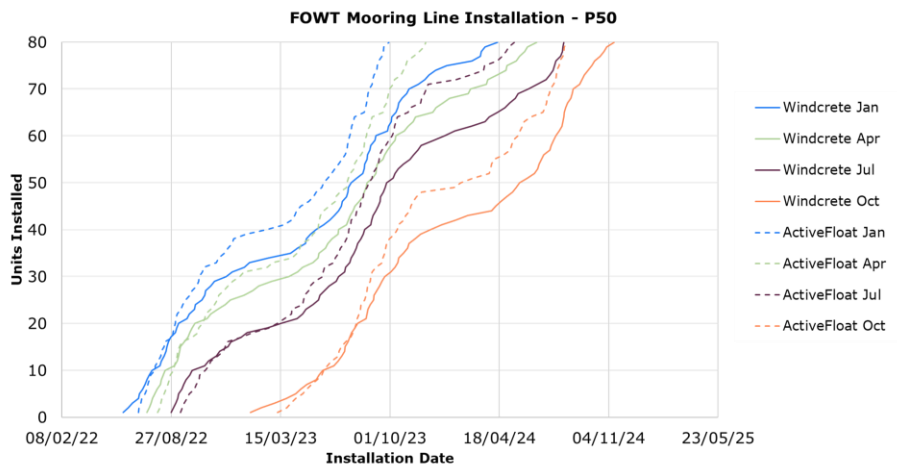


Figure 7-14: Comparison of mooring line pre-lay campaigns for ActiveFloat and Windcrete with different start dates at P50 [Source: Ramboll].

### C – Floating Foundation Hook-Up

The monthly workability for the floating foundation hook-up campaigns is shown in Table 7-14 and Table 7-15. Seasonal effects between summer and winter months can be observed. For both concepts, July and August are the months with the best workabilities ranging between 75% and 100% (ActiveFloat) and 59% and 89% (Windcrete). February is considered the worst month with workabilities between 0% and 53% (ActiveFloat) and 4% and 37% (Windcrete). It is found that the floating foundation technology impacts the workability of the hook up campaign: The additional erection process for Windcrete with its stricter weather envelope and additional transit distances leads to increased package duration and weather down time. The hook-up campaign would benefit from split campaigns because, especially, in summer months good conditions are found for Windcrete.

**Table 7-14: Monthly workability for floating foundation hook-up of ActiveFloat.**

Hook-Up	JAN	FEB	MAR	APR	MAY	JUN	JUL	AUG	SEP	OCT	NOV	DEC
Workability: P10	62%	53%	60%	59%	74%	83%	100%	100%	98%	81%	60%	61%
Workability: P30	41%	37%	37%	43%	63%	71%	96%	98%	91%	68%	44%	35%
Workability: P50	29%	30%	26%	32%	50%	60%	92%	94%	85%	59%	36%	22%
Workability: P70	19%	14%	17%	25%	38%	46%	87%	90%	78%	50%	26%	16%
Workability: P90	10%	0%	4%	17%	29%	36%	75%	82%	68%	38%	10%	9%

**Table 7-15: Monthly workability for floating foundation hook-up of Windcrete.**

Hook-Up	JAN	FEB	MAR	APR	MAY	JUN	JUL	AUG	SEP	OCT	NOV	DEC
Workability: P10	40%	37%	41%	51%	58%	61%	86%	89%	79%	63%	43%	40%
Workability: P30	30%	27%	28%	39%	48%	50%	78%	84%	74%	54%	35%	27%
Workability: P50	21%	19%	22%	31%	41%	44%	71%	77%	69%	48%	29%	19%
Workability: P70	17%	12%	14%	25%	33%	40%	65%	69%	65%	44%	23%	14%
Workability: P90	8%	4%	5%	18%	21%	33%	52%	59%	60%	37%	14%	7%

Table 7-16 and Table 7-17 show a broader range of minimum weather down time days for different start dates between ActiveFloat and Windcrete. This is due to the influence of the different campaign duration itself and the relative amount of winter months in the overall campaign, as can be seen in the S-curves in Figure 7-15 and Figure 7-16. The best start dates are July for ActiveFloat and October for Windcrete. Both cases show harsh conditions for floating foundation hook-up, as the number of weather down time days is still relatively high with 47% to 72% (ActiveFloat) and 58% to 77% (Windcrete) of the estimated full foundation hook-up time. The hook-up campaign is less restrictive than the preceding campaigns because the seasonal changes in weather conditions allow for higher workabilities in summer months.

**Table 7-16: Weather down time days for floating foundation hook-up of ActiveFloat.**

Commissioning Start Date	01-Jan	01-Apr	01-Jul	01-Oct
WDT Days @P10	161	178	158	160
WDT Days @P30	191	227	235	187
WDT Days @P50	205	277	269	197
WDT Days @P70	371	381	289	281
WDT Days @P90	471	385	324	381

**Table 7-17: Weather down time days for floating foundation hook-up of Windcrete.**

Commissioning Start Date	01-Jan	01-Apr	01-Jul	01-Oct
WDT Days @P10	273	364	357	252
WDT Days @P30	387	419	386	291
WDT Days @P50	420	433	396	353
WDT Days @P70	492	478	422	500
WDT Days @P90	541	558	592	551

The investigation for the OSS shows that, again, the monthly workabilities of the OSS is similar to the results for Windcrete. The more mooring lines are to be installed, the larger required weather windows become. As the eight mooring lines for the OSS would result in large weather windows and as such long waiting times, the installation was structured in two steps: four mooring lines for a storm safe state and a second step with the other four mooring lines. Reaching a storm safe state then has a weather window of the same properties like for Windcrete. The second step has only a slightly longer resulting weather window. However, again the number of samples for statistical evaluation is very low and the relative weather downtime days compared to the net duration shows a broad range from 0% to 81%. Due to the higher complexity of the hook-up procedure, slightly higher relative weather down time days than for Windcrete are expected.

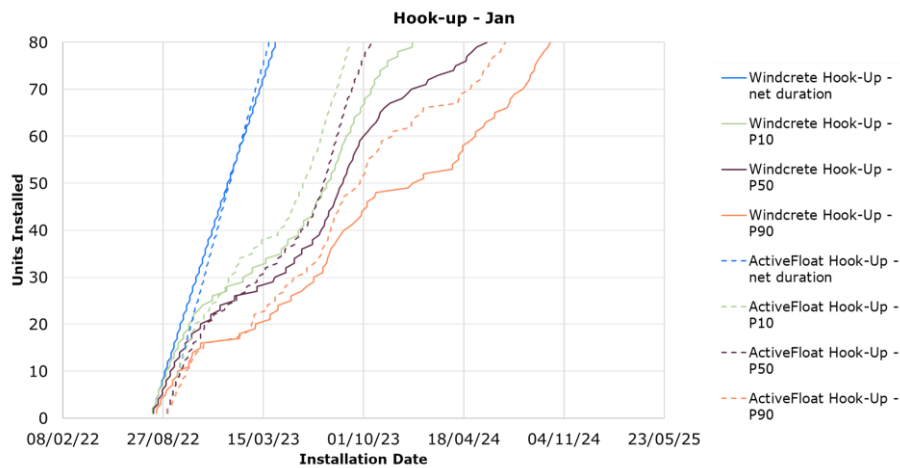


Figure 7-15: Comparison of hook-up campaigns for ActiveFloat and Windcrete with campaign start date in January for different probability levels [Source: Ramboll].

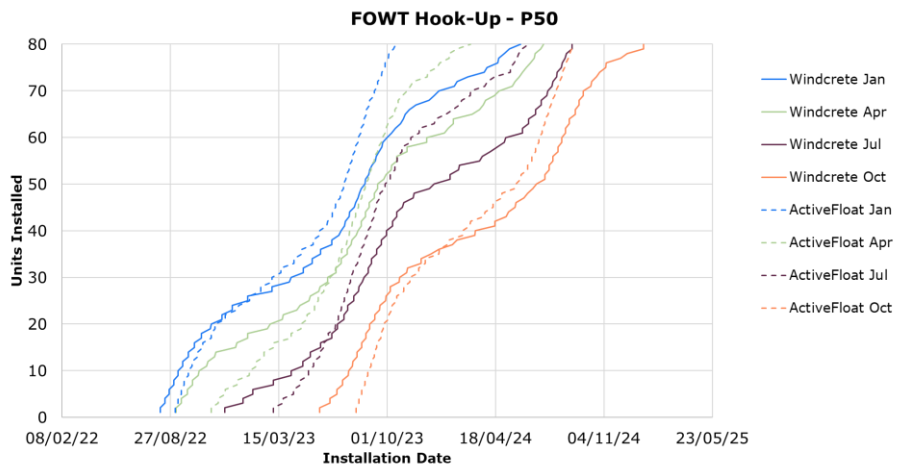


Figure 7-16: Comparison of hook-up campaigns for ActiveFloat and Windcrete with different start dates at P50 [Source: Ramboll].

#### D – Power Cable Installation

For both floating foundations, the cable installation campaigns (inter-array as well as export cable) are identical in terms of number of assets and net durations. Differences between both campaigns result from different start dates related to the completion of the preceding packages (anchor installation, mooring line pre-lay, floating foundation hook-up). In Figure 7-17 for the inter-array cables, the graphs for the net duration show different overall durations between ActiveFloat and Windcrete even though the work breakdown is identical. The steepness of these graphs follows the steepness of the net duration graphs in Figure 7-15. Generally, waiting times occur because the cable installation needs to wait for floating foundations to be installed in the previous campaign. For Windcrete, waiting times during summer months with more benign weather can be identified in Figure 7-18, especially during the first summer season (see P10 curve). At later stages, the impact of preceding campaigns vanishes because the weather envelope – i.e. the operational limits – for cable laying is much more restrictive than for hook-up. Cable pull-in and associated activities with low allowable Hs and Tp limits are the main drivers for large waiting times.

The monthly workability for the inter-array cable installation campaign is shown in Table 7-18 and Table 7-19. Very strong seasonal effects with medium high workabilities in summer months and very low workabilities in winter months result from the narrow weather envelope for cable pull-in activities. August is the month with the best scores ranging between 14% and 47% (ActiveFloat) and 12% and 47% (Windcrete), February and March are considered the worst months with workabilities between 0% and 19%.

**Table 7-18: Monthly workability for inter-array cable installation of ActiveFloat.**

Power Cable installation	JAN	FEB	MAR	APR	MAY	JUN	JUL	AUG	SEP	OCT	NOV	DEC
Workability: P10	14%	15%	19%	24%	20%	25%	36%	47%	43%	35%	21%	19%
Workability: P30	8%	9%	9%	14%	13%	18%	30%	37%	33%	24%	16%	12%
Workability: P50	6%	4%	5%	7%	10%	14%	26%	29%	28%	17%	13%	8%
Workability: P70	3%	2%	2%	4%	7%	9%	20%	22%	24%	13%	9%	5%
Workability: P90	1%	0%	1%	2%	2%	6%	12%	14%	15%	6%	2%	2%

**Table 7-19: Monthly workability for inter-array cable installation of Windcrete.**

WTG Commissioning	JAN	FEB	MAR	APR	MAY	JUN	JUL	AUG	SEP	OCT	NOV	DEC
Workability: P10	18%	19%	18%	26%	22%	26%	39%	47%	42%	40%	24%	27%
Workability: P30	11%	9%	9%	16%	14%	18%	31%	35%	34%	25%	15%	13%
Workability: P50	7%	5%	4%	10%	10%	13%	27%	29%	28%	18%	11%	9%
Workability: P70	4%	3%	1%	5%	6%	10%	21%	22%	22%	12%	8%	6%
Workability: P90	2%	0%	0%	3%	3%	7%	15%	12%	17%	7%	1%	3%

For start dates in July and April the inter-array cable laying campaigns come with the smallest number of weather down time days as can be seen in Table 7-20 and Table 7-21. The relative weather down time compared to the estimated campaign duration is comparably large with 60% to 82% of the full cable installation duration. The S-curves in Figure 7-17 and Figure 7-18 also indicate the seasonal differences with significant waiting times. Especially for ActiveFloat in Figure 7-17, the increase of installation campaign duration due to weather can be identified for P10 and P90, with very long delays for installation of the last inter array cables due to weather constraints.

**Table 7-20: Weather down time days for inter-array cable installation of ActiveFloat.**

Commissioning Start Date	01-Jan	01-Apr	01-Jul	01-Oct
WDT Days @P10	422	311	270	390
WDT Days @P30	430	322	311	461
WDT Days @P50	451	371	399	481
WDT Days @P70	593	510	515	597
WDT Days @P90	694	584	593	779

**Table 7-21: Weather down time days for inter-array cable installation of Windcrete.**

Commissioning Start Date	01-Jan	01-Apr	01-Jul	01-Oct
WDT Days @P10	433	384	335	470
WDT Days @P30	468	398	438	487
WDT Days @P50	476	449	497	521
WDT Days @P70	611	586	545	632
WDT Days @P90	685	627	678	790

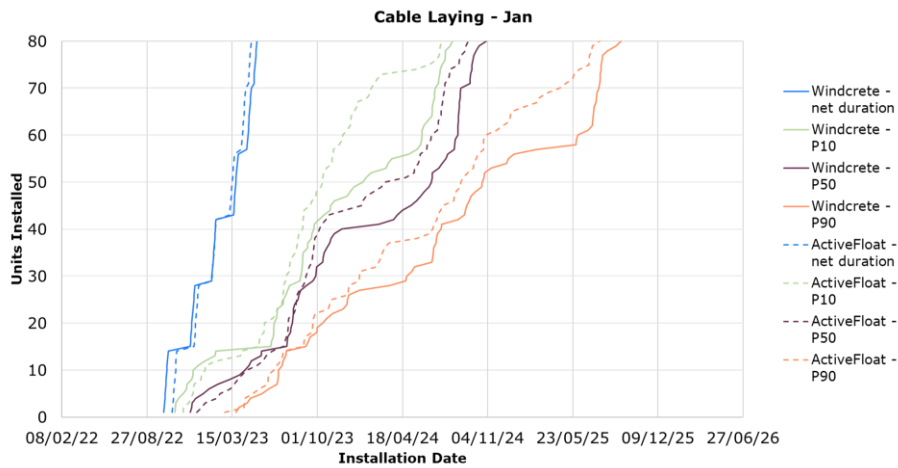
Export cable installation is also investigated. The weather envelopes for single tasks are similar to the inter-array cable campaign. Table 7-22 shows good workabilities in almost every month for P10 to P70. This is due to only minor impact of cable pull-in operations, as export cable laying operations with higher allowable Hs and Tp are dominating. This is in contrast to the inter-array cable installation as, relatively, more pull-in works are required.



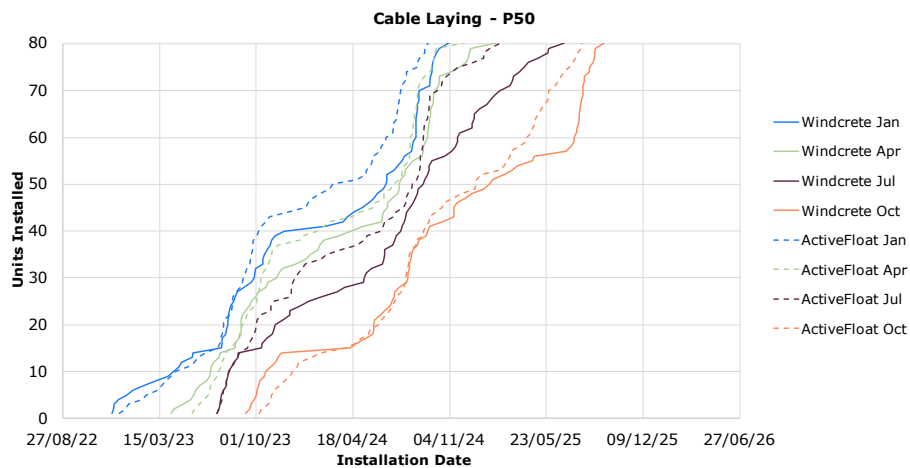
However, cable pull-in and associated activities may follow the workabilities shown in Table 7-18 and Table 7-19. This suggests performing installation in summer months is more favourable also for the export cables.

**Table 7-22: Monthly workability for export cable installation.**

WTG Commissioning	JAN	FEB	MAR	APR	MAY	JUN	JUL	AUG	SEP	OCT	NOV	DEC
Workability: P10	100%	100%	100%	100%	100%	100%	100%	100%	100%	100%	100%	100%
Workability: P50	92%	87%	91%	100%	95%	93%	96%	99%	94%	84%	75%	73%
Workability: P70	67%	61%	67%	76%	81%	88%	91%	84%	74%	61%	59%	
Workability: P90	12%	4%	6%	7%	13%	36%	14%	51%	40%	27%	12%	1%



**Figure 7-17: Comparison of cable lay campaigns (inter-array) for ActiveFloat and Windcrete with campaign start date in January for different probability levels [Source: Ramboll].**



**Figure 7-18: Comparison of cable lay campaigns (inter-array) for ActiveFloat and Windcrete with different start dates at P50 [Source: Ramboll].**

### A to D – Overall Installation Campaign

In the above shown results, the installation campaign is analysed with a specific start date of the total campaign. However, each campaign package has dependencies with the preceding packages. For the presented study, the ideal start date could either be chosen according to the best overall campaign durations – i.e. overall best workability and lowest weather down time days – or according to the findings in the cost analysis (Section 0).

In Figure 7-19 and Figure 7-20 S-curves for campaign start in January are shown for different probability levels. For each curve, the first 80 units are the corresponding floating foundations for anchor installation, mooring line pre-lay and hook-up. The additional two units of each graph correspond to the floating OSS. For cables, the first 80 units are inter array cables and the last four units represent the export cable installation dates.

The sequence of tasks shown in these figures has no significant impact on the overall duration of the simulated project. With different starting points for each simulated campaign, seasonal effects are captured in the different percentiles. For a real project a different order of campaigns is more reasonable from a financial perspective: First, the OSS and export cables would be installed to enable power production as soon as the first turbine is installed and connected to the OSS. As such, the process of IAC laying can become more integrated and parallel to the floating foundation hook-up, with the potential cost of CLV's waiting frequently for prevailing activities. Alternatively, different approaches like IAC pre-lay could be required.

In the below graphs (Figure 7-19 and Figure 7-20), seasonal impacts can be seen for all sub campaigns. Anchor installation and hook-up seem to be less impacted by bad weather in winter than mooring pre-lay. The cable laying campaign is most impacted by seasonal changes. With these information, further optimisation of the installation campaign can be undertaken, for example considering split campaigns or exclusive use of more benign weather conditions.

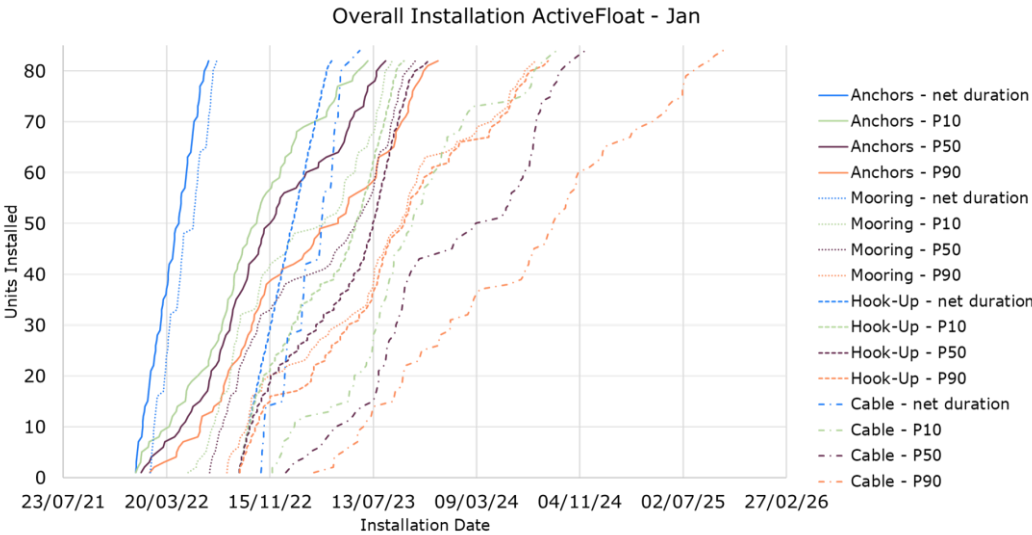


Figure 7-19: S-Curves for overall campaign of ActiveFloat with different probability levels with starting date in January [Source: Ramboll].

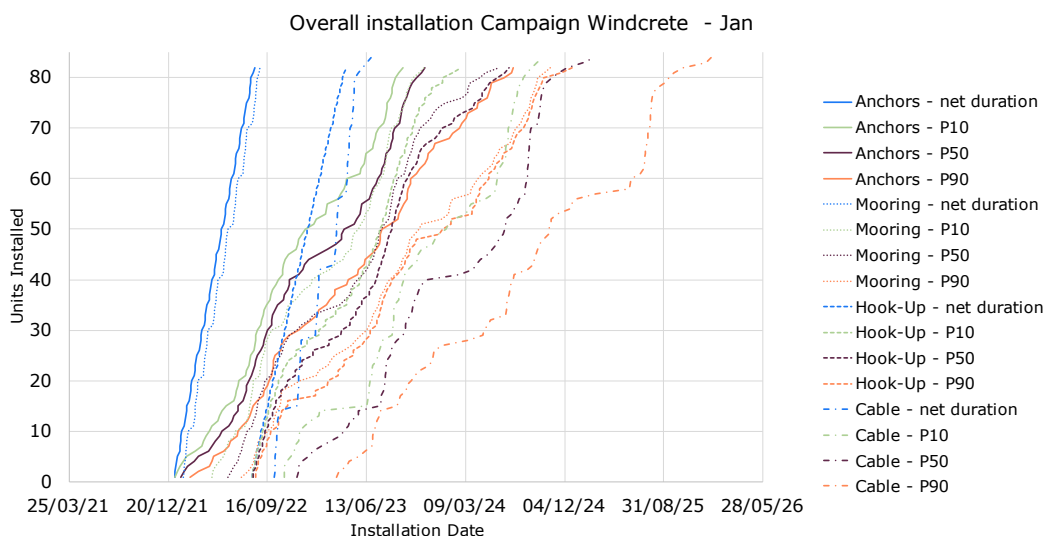


Figure 7-20: S-Curves for overall campaign of Windcrete with different probability levels with starting date in January [Source: Ramboll].

Cumulative overall campaign durations are displayed in Table 7-23. The optimum starting dates differs between the probability levels. For P50, ActiveFloat has the optimum starting point in January but the deviation to the other months is very low. For Windcrete, the optimum starting point is found to be in April and the deviation to the other months is even lower, whereas the overall duration is generally about 10% longer than for ActiveFloat. The small difference in overall campaign durations is probably not the decisive factor when to start the installation because other influences could be more relevant, such as vessel availabilities and supply chain limitations.

Table 7-23 Comparison of overall campaign duration (incl. OSS) for ActiveFloat (left) and Windcrete (right)

ActiveFloat:

Total Campaign Days	01-Jan	01-Apr	01-Jul	01-Oct
WDT Days @P10	984	934	920	1020
WDT Days @P30	1018	983	1010	1070
WDT Days @P50	1051	1086	1075	1088
WDT Days @P70	1246	1226	1146	1282
WDT Days @P90	1371	1284	1294	1430

Windcrete:

Total Campaign Days	01-Jan	01-Apr	01-Jul	01-Oct
WDT Days @P10	1009	985	1059	1077
WDT Days @P30	1088	1100	1119	1104
WDT Days @P50	1147	1145	1148	1154
WDT Days @P70	1288	1252	1211	1343
WDT Days @P90	1466	1440	1447	1477

For the monthly workabilities see Table 7-24 and Table 7-25. April is found as the best start month for the overall campaign for ActiveFloat considering the weather down time days. For Windcrete January is identified as the best start month. With relatively high weather down times compared to the estimated campaign duration of 58% to 78% (ActiveFloat) and 62% to 77% (Windcrete), the campaign schedule would benefit from further adjustments.

Table 7-24 Monthly workability for overall campaign of ActiveFloat.

Overall Campaign	JAN	FEB	MAR	APR	MAY	JUN	JUL	AUG	SEP	OCT	NOV	DEC
Workability: P10	42%	41%	42%	47%	53%	56%	70%	77%	72%	65%	48%	46%
Workability: P30	33%	32%	31%	38%	44%	47%	64%	70%	64%	53%	40%	32%
Workability: P50	26%	24%	24%	30%	35%	40%	58%	63%	58%	44%	31%	23%
Workability: P70	17%	14%	16%	22%	27%	33%	53%	56%	52%	36%	22%	17%
Workability: P90	7%	1%	3%	9%	12%	21%	32%	43%	40%	23%	7%	6%

**Table 7-25 Monthly workability for overall campaign of Windcrete.**

Overall Campaign	JAN	FEB	MAR	APR	MAY	JUN	JUL	AUG	SEP	OCT	NOV	DEC
Workability: P10	37%	37%	37%	46%	49%	49%	66%	74%	67%	57%	44%	40%
Workability: P30	30%	30%	28%	38%	40%	42%	58%	65%	61%	49%	38%	31%
Workability: P50	25%	24%	22%	31%	34%	36%	52%	58%	55%	41%	29%	23%
Workability: P70	18%	15%	15%	24%	27%	32%	47%	51%	49%	35%	22%	18%
Workability: P90	7%	2%	3%	11%	11%	21%	29%	37%	39%	24%	8%	6%

Differentiating between the two parameters overall campaign duration and weather down time days is important, because one day of waiting time results in several weather down time days overall as it counts for each of the four campaign and assets. Longer campaign duration and increased weather down time days for Windcrete compared to ActiveFloat indicate for the later a slight advantage for the proposed installation procedure. Especially lacking the upending process, ActiveFloat seems to be more a plug and play solution from the installation perspective. Anyhow, apart from the different net durations, both concepts perform similar in regards to weather down time days and overall duration relative to their net duration.

From these parameters, two main approaches for further optimisation are proposed:

- Splitting the full campaigns into multiple sub campaigns can overcome long waiting times and reduce the risk of delay of project implementation and asset (vessel) costs.
- Mobilisation of additional assets (vessels) to perform tasks of the WBS in parallel can have beneficial impact on project duration as well.

Feasibility of such approaches and their applicability on each sub-campaign is also driven by a thorough cost analysis.

## 7.3 Cost Modelling and Analysis

### 7.3.1 [Approach](#)

The following section describes the approach to offshore wind cost modelling used in this study. It will cover general modelling limitations for offshore wind cost estimations, the general approach to estimating costs and a description and evaluation of the probabilistic cost modelling approach used in this study.

#### 7.3.1.1 [Modelling Limitations](#)

CAPEX levels of offshore wind farms are highly project and market specific. A robust CAPEX model requires a full technical concept supported by site-specific data that is naturally not available at an early stage in the development process.

Key drivers of CAPEX include site parameters (water depth, soil conditions, wind and wave climate, distance to shore, etc.) and market conditions (regulatory requirements, supply and demand, offtake environment, etc.), which also strongly influence technology choices. Additional uncertainties can arise when considering the risk appetite of the developer, the selected contracting strategy, and the terms and conditions of the construction contracts, which heavily impact CAPEX.

The following general comments and limitations should be considered:

- With global demand expanding rapidly, we anticipate the next years to be a demanding period for offshore wind globally. This will put pressure on the supply chain and have effects on costs which are currently difficult to predict.
- As the market expands, new players will look to enter the market and may offer attractive/strategic pricing to gain market shares. While careful risk/reward evaluation on a case-by-case basis needs to be conducted, this also presents an opportunity.
- Some activities require specialized equipment, experienced staff and/or special vessels. The current supply chain is in some cases limited to a few contractors and thus the costs for such services are very sensitive to supply-demand imbalances.
- With project sizes increasing significantly, it is anticipated that suppliers may choose to focus on key clients with large pipelines and GW-projects.
- The regulatory framework may have local content requirements and hence foster the development of a local supply chain. The cost impacts of a local supply chain are uncertain.

Consequentially, transferring past experience and generic cost estimates to a specific project comes with noteworthy uncertainty. The ongoing, substantial expansion of the global supply market increases this. A project specific market outreach/tender process is required to fully understand the effects the current developments may have on a specific project or package.

#### 7.3.1.2 [Estimating Costs](#)

When estimating the capital expenditure of a project it is important to understand the underlying calculation approach. Any cost calculation can be broken down into the following formula:

$$Costs = \sum_{Cost\ items} \{Project\ Parameter * Specific\ Cost\}$$

The three driving factors of this cost calculation are defined as follows:

- **Cost items** form the structure of the cost calculation:
  - A high number of cost items usually reflects a higher level of detail of the cost estimation. However, the number of cost items cannot be selected freely but is instead determined by the available information, the development phase, and the purpose of the cost estimation. In this context, it is important to acknowledge that a high number of cost items, which are not backed up by sufficient input information, will not increase the value of the cost estimation. Instead, if insufficient information is available to support a detailed number of cost items, the results will tend to indicate a false degree of certainty. This is especially important for early project development phases.
  - When developing a list of cost items, the goal is to identify key cost drivers and to separate them from less dynamic costs.
  - In addition when breaking down cost items, it must be ensured that cost items are of a similar magnitude. Minor aspects of the project might be lumped into a larger cost item, even if very certain cost information is available. For example, even if there is a clear understanding of the fall-arrest system for a wind turbine foundation, it will not be reflected as a separate cost item as it is marginal in comparison to the rest of the structure.
- **Project parameters** define the technical scope of the cost estimation:
  - They describe technical concepts, designs, and scenario considerations.
  - The unit of a cost parameter is usually pre-determined by the cost item definition, ensuring that the driving parameters are captured in the cost estimation. They can describe the number of turbines (scenario), the weights of the foundations (technical design) or the assumed installation duration (technical concept).
- **Specific costs** are based on the unit of the cost parameter and reflect the estimated market situation.

Any cost calculation set up in this manner is bound to a particular framework. This framework defines the applicability of the calculation and the results. Generally, two levels of framework can be identified:

1. The **project scenario** definition:
  - Clearly defined technical and strategic concepts are required within the general objective of the estimation to perform a cost estimation. These clearly defined concepts form the scenario definition. Usually, multiple scenarios are compared against each other in a cost study, each reflected by an independent cost model. A sensitivity analysis of a particular item would form a separate scenario in this context.
  - Key indicator for the project scenario is its structure (the cost item breakdown), which describes the technical solutions and breaks them down into key cost drivers.
  - A cost calculation and its results are only valid for a distinct project scenario. If certain elements of the project are unknown or undefined, either certain assumptions must be made for these elements, or the scope of the cost estimation must be changed.
    - For example: If the foundation type for a wind turbine is not defined, either assumptions have to be made, which foundation type is reflected, or the foundation package needs to be removed from the cost calculation scope.

## 2. The key assumptions:

- Within a project scenario, certain assumptions are made when defining input values for either project parameters or specific costs. These assumptions must be transparent to ensure that the context of the cost calculation and its results is captured. Generally, the results of a cost estimation should never be interpreted without the context of the underlying assumptions.
- Especially for more complex project scenarios, the large amount of assumptions will make them difficult to assess at first sight. A simplified overview like a technical assumption book can support here.

### 7.3.1.3 Probabilistic Methodology

Ramboll uses a probabilistic calculation method to execute concept-level cost models based on the commercially available Excel Add-in @RISK. The main difference to a deterministic calculation method is that both project parameters and specific costs are reflected as input distributions rather than discrete values or even three-point-estimates<sup>3</sup>.

In cost modelling, data is gathered from a variety of sources such as market outreach, internal cost databases or project specific offers as a basis for the model. The inputs from these sources require proper conditioning to assure applicability to the individual project as well as consistency and transparency. Different sources present different cost values, introducing cost uncertainties into the model. Probabilistic cost modelling aims to utilise these uncertainties to develop a statistical range of possible outcomes which accurately captures financial risk. The Monte Carlo method as an advanced sampling technique forms the basis for Ramboll's probabilistic cost modelling by simulating the input data statistically for thousands of fully relevant, albeit hypothetical projects. The final result is a cost model that accurately represents project costs on the full spectrum from P0 to P100<sup>4</sup> and anywhere in between.

The probabilistic method offers key advantages versus a deterministic method:

- A marked advantage of the probabilistic cost modelling in comparison to a deterministic approach is the lower impact of all types of organisational bias when assessing the inputs. An inaccurate assessment of uncertainties is not as influential as an inaccurate assessment of a scalar input parameter unless there is a systematic error across the whole process. This ensures stability of the results where bias is well controlled.
- During the Monte Carlo simulation, each iteration represents a fully independent project, defined by the input parameters yet allocated to any value across the input range. Compiling the data from thousands of iterations shows which situations are most and least likely across the entire project scope.
- Comparing a probabilistic cost calculation with a deterministic cost calculation based on three-point-estimates, where the calculations target an overall lower bound, expected value and upper bound, additional advantages of the probabilistic approach can be identified. To illustrate these, the results of the two calculation methods are illustrated exemplarily and qualitatively in Figure 7-21:

---

<sup>3</sup> Three-point-estimates are a common way of describing uncertain parameters. They are reflected by a set of three values: Lower bound, expected, and upper bound.

<sup>4</sup> P-values are probabilistic parameters, which add context to a probabilistic number. A P0 would indicate that the particular value is fallen below in 0% of the cases. Thus, the parameter is expected to be equal or above the P0 value in 100% of the cases. A P25 for example will be higher. This value is only fallen below in 25% of the cases, while in 75% of the cases, a higher value is expected.

- The deterministic extreme values  $\text{Min}_{\text{det}}$  and  $\text{Max}_{\text{det}}$  reflect the true minimum and maximum results. Within the input's boundaries, there is no possibility for a lower or a higher result. This reflects a situation where all possible aspects of the wind farm development are from a cost perspective ideal or the exact opposite. Both events are virtually impossible. When comparing these to the extreme values of the probabilistic calculation  $\text{Min}_{\text{prob}}$  and  $\text{Max}_{\text{prob}}$ , it is apparent that the results are less extreme. The probabilistic extreme values can be interpreted as a realistic and project specific minimum and maximum value in contrast to the artificial and unrealistically extreme results of a deterministic calculation. Thus,  $\text{Min}_{\text{prob}}$  and  $\text{Max}_{\text{prob}}$  are still highly unlikely events, which describe the single lowest and highest out of thousands of iterations derived from the Monte Carlo calculation. These single iterations are highly sensitive and can scatter if changes are made to the model. They should therefore be interpreted as range indicators rather than robust and realistic events.
- The probabilistic assessment allows for the selection of a representative lower and upper bound for the cost estimation based on the project context and the willingness to take on risk, represented as P-values. For example, the P10 of the results can be considered the lower bound and the P90 the upper bound. This then allows for a classification and assessment of the cost results, which is closer to the expected reality and can be discussed qualitatively. In case a more risk averse approach is selected for the upper bound, a more conservative P-value can be selected, for example a P95 or a P99. In any case, the results are conditioned specifically to the project.

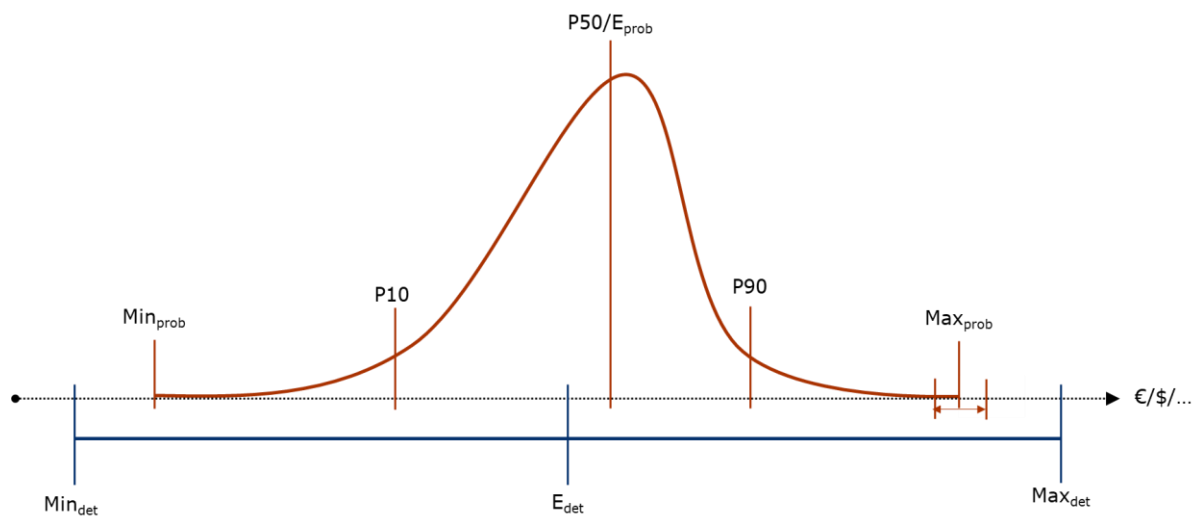


Figure 7-21: Qualitative comparison of the results from a deterministic (blue) and a probabilistic (red) cost estimation [y-axis reflects the probability density for the probabilistic result] [Source: Ramboll].

The probabilistic calculation approach entails particular mathematical features which may not be intuitive and shall be addressed shortly:

- **Summation of P-values:** In a deterministic calculation, the results equal the sum of all packages or cost items below. For example, the overall project costs consist of the sum of all packages: Wind turbines, foundations, substations, cables, etc. This is not the case for the results in probabilistic cost modelling. While the probabilistic model itself reflects precisely these summations, the results must be interpreted differently. Generally, the sum of packages low P-values (e.g. P10) will be lower than the similar P-value



of the project (and respectively higher for high P-values). The reason is that each package individually can reach particularly low cost estimations in single iterations. However in these iterations of the cost model, the other packages are estimated statistically independent from each other. Therefore, the very extreme events of single cost items or packages are levelled out by the other items or packages in the cost calculation as those will be relatively less extreme. While this can be counterintuitive at first, it is one of the key advantages of a probabilistic method versus a deterministic method, as the impossible events of larger numbers of cost items all being estimated to the one extreme at the same time are diminished.

- **Probability correlations:** The modelled uncertainty distributions are not always statistically independent from each other. For example, it is intuitive that if the probability distribution reflecting the specific cost for the fabrication of a jacket foundation resulted in a high value for a certain iteration of a Monte-Carlo simulation, the value for the specific cost for the fabrication of a pin-pile should not be a very low value. Both specific costs are based on welding operations, and it is likely that if welding is more expensive, this is true for both cost items. These dependencies can be modelled as correlations in the probabilistic cost model to ensure that different cost items are not levelling each other out by creating unrealistic, single iterations. From experience, it can be stated that the effect of including these correlations remains marginal unless a high share of cost items entail correlations. Especially for full offshore wind projects, the packages are sufficiently independent so that the inclusion of correlations does not change the results drastically. In addition to that, when adding correlations, it must be ensured that a clear understanding of the interdependencies between the items exists. Including a correlation incorrectly will result in a skewed result, where both the bias and the cause are not easily identifiable.

The main methodology steps behind the probabilistic modelling in the Ramboll cost model are as follows:

- In probabilistic cost modelling, inputs are developed as probability distributions reflecting the uncertainties derived from a range of different sources. This applies to both project parameters and specific costs. For example, for a jacket foundation structure, there are uncertainties attached to both the fabrication price per ton (specific cost) and the mass (project parameter). The first step is therefore to define the input distributions as they are usually unknown. Ramboll has developed a process to develop the distributions based on the quantitative and qualitative input from the different sources.
- From the different sources, three intuitively understandable values are derived for the cost parameter or specific cost: Minimum, most likely, and maximum. These three values correlate to the generic three-point-estimate (lower bound, expected, upper bound) and add an additional qualitative weighting. Especially when retrieving the values from expert opinions, the objective is to identify the extreme values that the expert could envision for the particular item.
- These three values form the basis for the probability distribution definition taking into account an additional qualitative assessment of the certainty attached to the most likely value. Based on this assessment one of the following distributions (visualized in Figure 7-22) is selected:
  - Flat distribution: The uniform distribution represents a clearly defined range, but no value is considered to be more likely than any other, meaning all values are equally likely to occur.
  - Partial triangle distribution: The partial triangle distribution represents a moderate confidence level in the expected value. In this case, the most likely value is given a modest statistical preference represented by a 50% higher probability density in comparison to minimum and maximum value.

- Full triangle distribution: The Full Triangle distribution represents a high confidence level in the expected value. In this case, the most likely value is given a strong statistical preference represented by a 100% higher probability density in comparison to the minimum and maximum values
- An additional qualitative assessment of the initial three values is performed. Based on the classification of the certainty attached to the minimum and maximum value, a drop-off zone is added to either side of the main distribution function to allow for the very small possibility of unexpectedly favourable or detrimental conditions to occur. This area of the distribution function captures the uncertainty attached to the range of input values in order to avoid defining the range of values as a true P0 and P100. This would reflect zero probability of the presence of values outside of the defined range. The drop-off zone is defined by an independent probabilistic function based on the confidence level of the input range.

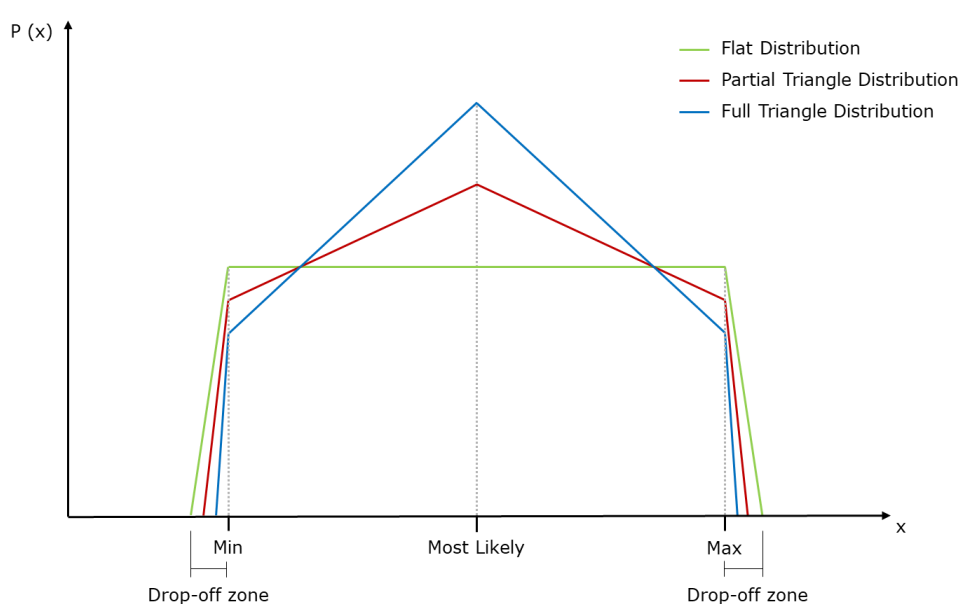


Figure 7-22: Overview of distributions used in probabilistic modelling [Source: Ramboll].

### 7.3.2 Project Scenarios

This cost study estimates and compares the capital expenditure (CAPEX) for the marine operations of the T&I strategies presented in the previous chapters. The two scenarios reflected in this study are based on the two reference floating foundations.

Table 7-26: Overview of scenarios for the cost estimation.

Scenario	Reference Design	Foundation Type	WTG Rating	Number of WTG	Site Location	Additional Operations
Scenario 1	ActiveFloat	Semi-Submersible	15 MW	80	Morro Bay, USA	-
Scenario 2	Windcrete	Spar	15 MW	80	Morro Bay, USA	Upending of spar

The scope for the cost estimation in this study is limited to the capital expenditure resulting from the **marine operations** for the installation phase including floater (WTG and OSS) installation, inter-array cable installation

and export cable installation are reflected in the cost estimation. The wind turbine integration is not part of the cost estimation.

Other costs, such as project management, port lease or supply are not reflected in this cost model. Also excluded are commercial elements such as financing, insurance or contingency.

### 7.3.3 Key Assumptions

The following sections outline the key assumptions taken for this study.

#### 7.3.3.1 Model Assumptions

Installation and weather durations are based on the weather downtime analysis described in section 7.2. In the analysis, different campaign starting points are investigated (section 7.2.4.2). The overall campaigns are conducted over all four seasons independently from the starting point due to the significant durations of the installation works (Table 7-23). As the uncertainty related to the forecasted installation costs and vessel day rates is considerable in comparison to the variance in installation durations depending on the start month, only one campaign duration has been investigated in this study. To do so, the four different campaign results are aggregated in one generic campaign result. Based on Ramboll engineering expertise this generic campaign configuration is conditioned according to the procedure described in section 7.3.1.3 and based on the results of the weather downtime analysis.

For the purpose of the CAPEX estimation, it is not distinguished between the wind turbine floaters and the OSS floaters. Both utilise the same set of installation vessels and are conducted sequentially, therefore it is assumed that they are installed as part of one larger campaign. Based on the input evaluation, an expected share of the installation costs is determined. This share is calculated based on the relative durations for the different vessels. These are then weighted according to the expected vessel day rates. The results are described in Table 7-27.

**Table 7-27: Expected cost share of FOWT and OSS out of the floater installation.**

	Scenario 1: ActiveFloat	Scenario 2: Windcrete
<b>Cost Share FOWT</b>	87.5 %	86.8 %
<b>Cost Share OSS</b>	12.5 %	13.2 %

The cost inputs for vessel day rates etc. are retrieved from Ramboll’s international cost database and global market expertise.

#### 7.3.3.2 Parameters and Project Specific Assumptions

The same set of parameters:

- Installation duration and weather downtime;
- Vessel requirements;
- Mobilisation and demobilisation cycles;

and project specific assumptions:

- Installation durations and weather downtime are reflected as described in section 7.3.3.1;
- Vessel rates are estimated for the utilised vessels as described in section 5.1 to 5.3 . Estimations are based on generic vessel configuration and Ramboll expertise and market insight;

are applied for the cost assessment of the campaigns (anchor installation, mooring line pre-lay, hook-up of floating foundation and power cable installation).

### 7.3.3.3 [Scope of Marine Operations](#)

The scope considered in cost modelling of each of the different campaigns is summarised for the different assets below. The floater installation also covers the installation of the anchors, the mooring line deployment and the hook-up at the final location.

#### Floating Foundation Installation:

- Installation of FOWT and floating OSS
- Scope covers all marine operations as described in the work breakdowns in the sections 5.1 to 5.3 except for step C07 (turbine integration for Windcrete, scenario 2). It entails but is not limited to:
  - Operation of the installation / transport vessel spread for the assumed period (incl. personnel, fuel, other operational costs)
  - Provision of sea fastening and installation tools
  - Required aux. vessels
  - Loading and float out
  - Transit
  - Preparation works (incl. seabed preparation, boulder removal, UXO surveying and identification)
  - Anchor installation (incl. lift and lowering, self-penetration and suction operations, lifting tool removal)
  - Mooring line deployment (incl. chain-fibre connection, connection to anchor)
  - Hook-up (incl. mooring line recovery, connecting mooring line, tensioning, ballasting, upending if required)

#### Inter-Array Cable Installation:

- Installation of inter-array cables
- Scope covers all marine operations as described in the work breakdowns in section 5.4. It entails but is not limited to:
  - Operation of the installation / transport vessel spread for the assumed period (incl. personnel, fuel, other operational costs)
  - Provision of sea fastening and installation tools
  - Required aux. vessels
  - Loading
  - Transit
  - Preparation works (incl. seabed preparation, boulder removal, UXO surveying and identification)
  - Cable laying (incl. connection to cable anchors)
  - Cable pull-ins/-outs (incl. connection to floating foundation, installation of ancillaries)

#### Export Cable Installation:

- Installation of export cables
- Scope covers all marine operations as described in the work breakdowns in section 5.4. It entails but is not limited to:
  - Operation of the installation / transport vessel spread for the assumed period (incl. personnel, fuel, other operational costs)
  - Provision of sea fastening and installation tools
  - Required aux. vessels
  - Loading
  - Transit

- Preparation works (incl. seabed preparation, boulder removal, UXO surveying and identification)
- Cable laying (incl. connection to cable anchors)
- Cable pull-outs /shore landings (incl. installation of ancillaries, cable cutting, cable sealing)

### 7.3.4 CAPEX Results From Marine Operations

The following section outlines the results from the CAPEX estimation resulting from the marine operations.

#### 7.3.4.1 Interpreting the Results

In this section, multiple P-values are referred to when analysing the resulting cost estimates. These P-values reflect different confidence levels of the resulting cost numbers as described in section 7.3.1.3. The **low and high range** reflected in the results are comparing the P50 value and the range between the single lowest and highest iteration (P0 and P100). They reflect what deviation to the P50 value is expected in a very optimistic or pessimistic scenario. Naturally, the spread of the project CAPEX result will be lower than for each package, as the packages level each other out.

The results allow for a classification of the project CAPEX estimation based on the AACE (Association for the Advancement of Cost Engineering) Cost Estimate Classification Matrix (AACE International Recommended Practice No. 18R-97) [21].

#### 7.3.4.2 Scenario 1 for ActiveFloat

The following table breaks down the CAPEX estimation for the marine operations of scenario 1, the ActiveFloat semi-submersible floater. Comparing the ranges for the floater and the power cable installation, it is apparent that the ranges for the cable installation are much higher than for the floater installation. A key reason here is the higher variability of the operational duration in comparison to those of the floater installation campaign as described in section 7.2.4.

**Table 7-28: Scenario 1 (ActiveFloat) CAPEX estimations for marine operations.**

	P10	P50	P90	Low Range	High Range
<b>Total CAPEX</b>	279.1 MEUR	313.4 MEUR	348.7 MEUR	-25.3 %	26.3 %
<b>Floater Installation</b>	174.4 MEUR	195.4 MEUR	216.3 MEUR	-25.7 %	25.9 %
<b>Inter-Array Cable Inst.</b>	69.0 MEUR	95.3 MEUR	124.1 MEUR	-46.4 %	48.7 %
<b>Export Cable Inst.</b>	17.2 MEUR	22.0 MEUR	27.3 MEUR	-41.8 %	46.8 %

The results of the Monte-Carlo simulation for the total CAPEX for scenario 1 are shown in Figure 7-23.

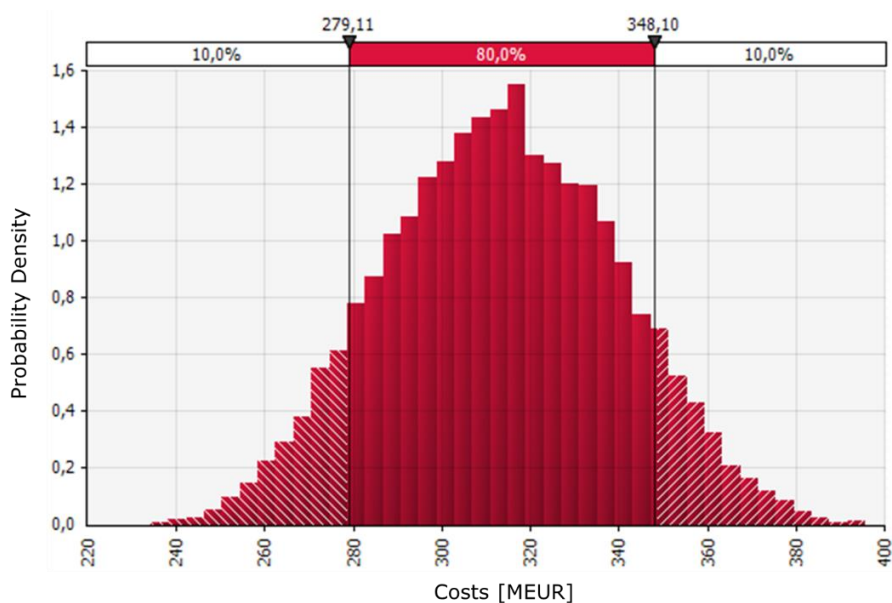


Figure 7-23: Scenario 1 (ActiveFloat) total CAPEX results of Monte-Carlo simulation [Source: Ramboll].

### 7.3.4.3 Scenario 2 for Windcrete

The following table breaks down the CAPEX estimation for the marine operations of scenario 2, the Windcrete spar buoy floater. Similarly to the results of scenario 1 (ActiveFloat), the ranges for the power cable installation are higher than those of the floater installation. The reasons are similar as for scenario 1.

Table 7-29: Scenario 2 (Windcrete) CAPEX estimations for marine operations.

	P10	P50	P90	Low Range	High Range
<b>Total CAPEX</b>	365.9 MEUR	409.9 MEUR	453.6 MEUR	-24.4 %	26.3 %
<b>Floater Installation</b>	242.1 MEUR	271.6 MEUR	300.9 MEUR	-26.3 %	26.1 %
<b>Inter-Array Cable Inst.</b>	81.7 MEUR	113.2 MEUR	147.6 MEUR	-46.5 %	48.9 %
<b>Export Cable Inst.</b>	18.9 MEUR	24.3 MEUR	30.3 MEUR	-42.4 %	46.9 %

The results of the Monte-Carlo simulation for the total CAPEX for scenario 2 are shown in Figure 7-23.

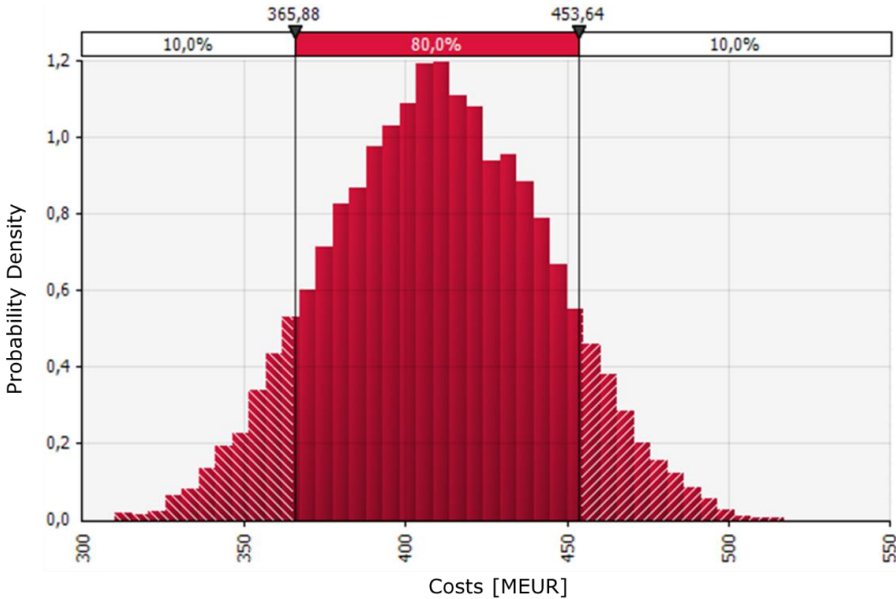


Figure 7-24: Scenario 2 (Windcrete) total CAPEX results of Monte-Carlo simulation [Source: Ramboll].

7.3.4.4 Comparison

Table 7-30 and Figure 7-25 summarise the results of the total CAPEX estimation for scenarios 1 (ActiveFloat) and 2 (Windcrete).

Table 7-30: Comparison of total CAPEX estimations for marine operations.

	P10	P50	P90	Low Range	High Range
<b>Scenario 1: ActiveFloat</b>	279.1 MEUR	313.4 MEUR	348.7 MEUR	-25.3 %	26.3 %
<b>Scenario 2: Windcrete</b>	365.9 MEUR	409.9 MEUR	453.6 MEUR	-24.4 %	26.3 %

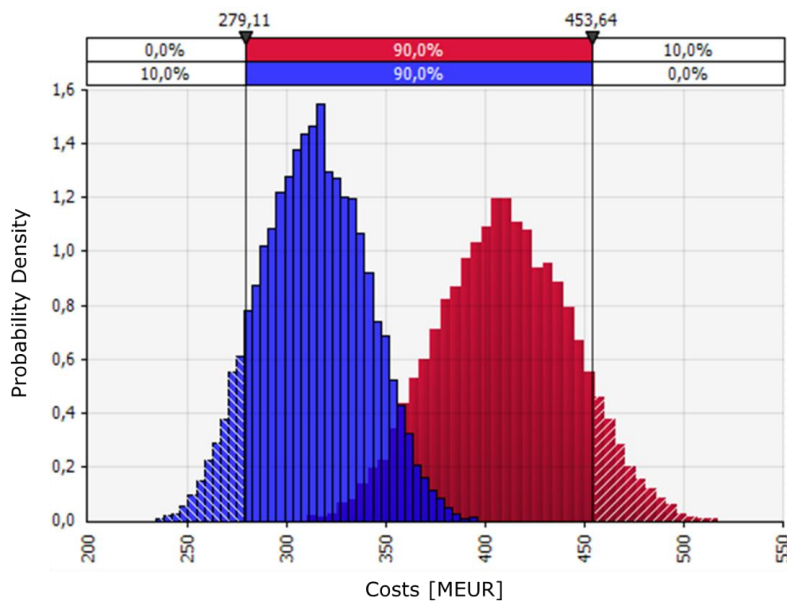


Figure 7-25: Comparison of total CAPEX results of Monte-Carlo simulation (Scenario 1 in blue, Scenario 2 in red) [Source: Ramboll].

Comparing the two resulting CAPEX estimates and the probability distributions, it can be concluded that higher costs are expected for scenario 2 (Windcrete). The P50 CAPEX estimate for the marine operations are for scenario 2 approximately 30.8 % higher than for scenario 1. Taking into account the shape of the probability distributions, it can also be stated that the costs for scenario 2 are also object to higher uncertainties. The shape describes a flatter curve, spreading out values over a wider range. Though the relative spread is due to the higher P50 value slightly lower than for scenario 1, the range confirms this observation from the comparison of the two probability distributions.

Breaking down the total CAPEX estimations to the package level, the key driver for the higher costs of scenario 2 can be identified. Figure 7-26 shows that for the P50 results, there is not a large deviation for the power cable packages between scenarios 1 and 2. However, the floater package (including anchor installation, mooring deployment and floater hook-up) entails significantly higher expected costs for scenario 2. The main reason here is the significantly higher durations, likely due to additional time required for the upending of the structures.

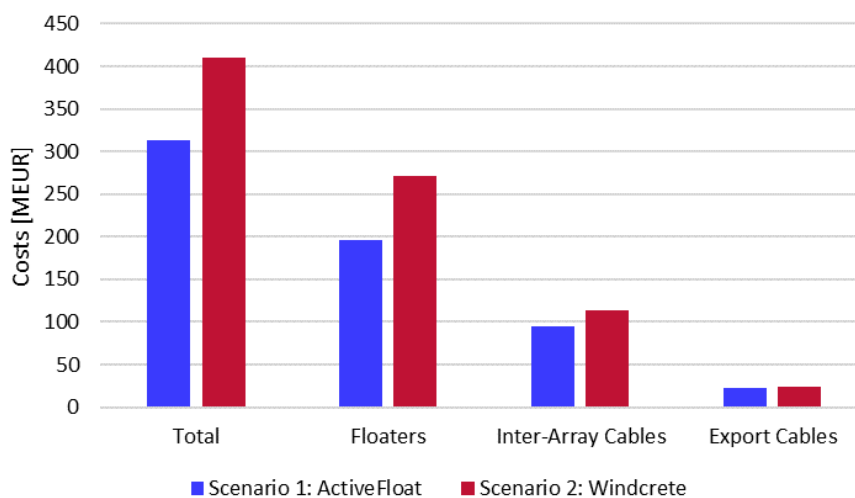


Figure 7-26: P50 CAPEX results per scenario and package [Source: Ramboll].



A similar view on this topic is shown when comparing the CAPEX share of the different packages out of the two scenario's CAPEX estimations. For scenario 2, the share of the floater installation package is increased in comparison to scenario 1. Both power cable packages' share on the other hand, is reduced for scenario 2.

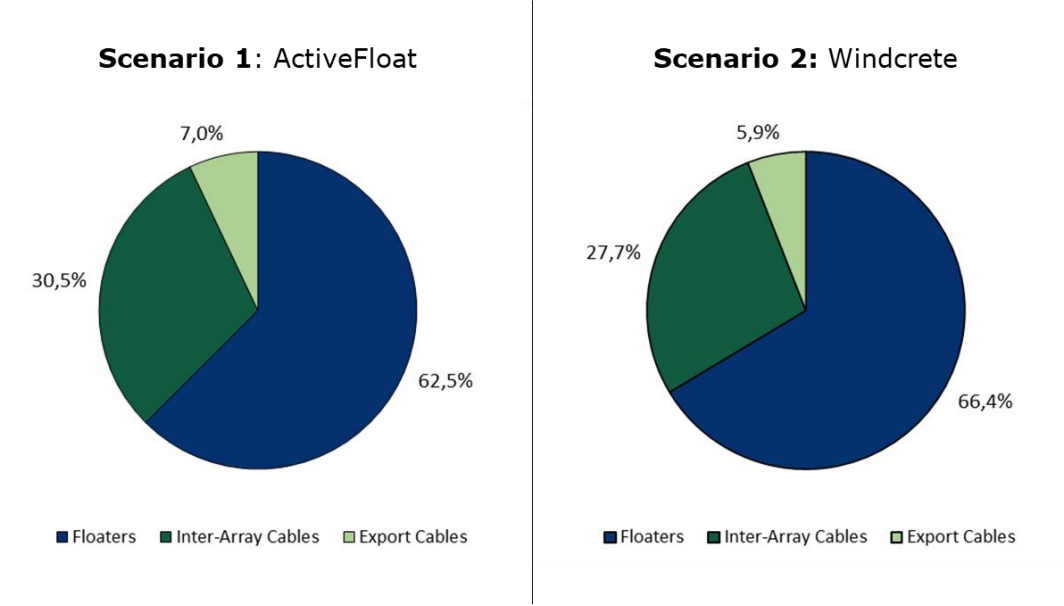


Figure 7-27: P50 CAPEX shares per scenario and package [Source: Ramboll].

7.3.5 Conclusion

The results of the probabilistic cost estimation of marine operations related to the installation identify scenario 1, the semi-submersible ActiveFloat, as relatively seen the advantageous. All P-values are below the respective results for scenario 2. In addition to that the resulting probability distribution indicates slightly higher certainty attached to the cost estimation for scenario 1.

This said, it must be mentioned that the cost estimations for both scenarios are subject to significant uncertainties at this point. It has been clearly shown that longer installation durations directly impact the estimated CAPEX, with the longer installation duration for the floaters being the main difference between the two scenarios. The resulting costs must be put into the context of an overall CAPEX estimation also considering supply and other aspects of the project.

Based on the calculation, the CAPEX estimates qualify for an Estimate Class 4 categorisation according to AACE's Cost Estimate Classification Matrix (AACE International Recommended Practice No. 18R-97) [21]. This makes sense in the light of the extensive development works related to the T&I concept as presented in this study.

## 8 Conclusion and Perspective

This document aimed to present a reference for the transportation and installation strategy for the COREWIND project. The reference floating offshore wind farm contains of 80 units at 15 MW rating with the substructure type of either semi-submersible (ActiveFloat) or spar buoy (Windcrete) and two floating OSS. The COREWIND installation site selected for this analysis is Morro Bay, which is located at the West Coast of the USA. The water depths in this area are varying between 400 to 900 m.

Further objective of this document was to provide the operational workability for selected critical operation steps during the different T&I campaigns (anchor installation, mooring line pre-lay, floating foundation hook-up), which could be considered in the quantification of weather downtime and project costs. In chapter 5, selected T&I procedures and method statements were presented. After defining the T&I methods the operational limits of temporary marine operations in terms of allowable Hs-Tp combinations were assessed in chapter 6 to define input conditions for the quantification of weather downtime and project costs using the weather downtime analysis.

**Table 8-1: Overview of T&I analyses.**

Study	Objective	Analysis	Tool	Outcome
<b>1 – Temporary marine operations (Chapter 6)</b>	Towing	Towing analysis	In-house Python	Required tug capacity and tug number; sailing speed
	Anchor installation	Simplified lifting analysis (through wave zone)	Ansys AQWA, OrcaFlex, Excel	Workability Hs-Tp combination
	Hook-up	Force allocation calculation	In-house Python	Tug capacity and heading control
<b>2 – Sequential weather downtime analysis (Chapter 7)</b>	Weather downtime, cost estimation	Work breakdown analysis, probabilistic cost model	Shoreline, Excel	Estimated project duration, operation costs

After conducting the preliminary studies, the transportation and installation durations and costs using sequential weather downtime analyses were evaluated in Chapter 7. From the assessment of a pre-defined work breakdown the probability of down time due to sea state conditions was calculated.

Based on the results above, the following conclusions were drawn:

- The overall transport workability was influenced by the vessel capacity and the size of the components to be transported onboard.
- Crane capacity and vessel motion limits impacted the choice of an offshore installation vessel.
- The use of more transport and installation vessels decreases the T&I operation duration. However, the economic profit of using several vessels simultaneously was affected.
- Weather and impact on workabilities:
  - o Seasonal varying metocean conditions highly impacted the weather downtime analysis at Morro Bay. Deviations in available weather time series for Morro Bay highlighted the importance of suitable metocean assessments for all sites and passages which are mandatory for robust and reliable calculations.

- High probabilities for large Hs and Tp values resulting from swell components in the range of operational limits for required assets lead to increased weather down time days and reduced workabilities.
- Workabilities were drastically reduced compared to commercial offshore wind sites in western Europe or Asia. Best performing months at Morro Bay were comparable to winter months with worst workabilities for European or Asian sites.
- Work breakdown and critical marine operations:
  - The proposed anchor installation and hook-up procedures turned out to be less impacted by bad weather than the mooring prelay procedure and cable laying. Strong deviations were seen between medium or good workabilities in summer months and winter months where only little or no work could be performed.
  - During anchor installation, overboarding and positioning of the anchor was found to be the most critical operation with regard to operational limits.
  - For the mooring prelay campaign, the mooring line connection to the anchor was driving the weather downtimes as it was limited by the weather envelope of the vessel and the maximum possible heave compensation.
  - Windcrete required a sheltered area with sufficient water depth for the erection process, which was highly restricted in regards to weather limits. Finding this area south of Santa Cruz island was crucial to enabling these operations.
  - For the floating foundation hook-up campaign, mooring line recovery and on-deck connection of top chain and fibre rope were limiting the works, especially in regards to swell induced Tp values.
  - Cable pull-in with the interaction of two or more floating assets was the most restricted operation of the cable laying due to on-deck operations and initiation wire recovery at the CLV.
- Based on this study, ActiveFloat turns out to experience less absolute weather downtime days and requires less overall installation duration than Windcrete, mainly driven by the additional upending process for Windcrete. Even though this seems to indicate a slight advantage of ActiveFloat from the installation perspective, both investigated concepts perform similar relative to their weather downtime days and overall duration relative to the outlined net duration.
- Upending analysis (Windcrete spar only):
  - The initial position of 10 deg upending angle was found to be the most critical in terms of motions. Also, the weather windows with respect to slack loads in the sling showed restrictions for wave periods of 9 and 12 s. Generally, further investigation through experimental comparison and the consideration of second-order drift loads will give a better understanding of the implications on the operational limits of the upending process.

Future works can investigate the following aspects:

- Splitting installation campaigns to only operate in months with more benign weather conditions could help reducing waiting times but not the overall duration. One key aspect could be the balance between reduced costs from idling days against additional mobilisation/demobilisation costs.
- Increasing the amount of mobilised assets would reduce the overall installation duration. Key aspects to be considered might be increased requirements to ports and supply chains compared to earlier project delivery phases.
- Investigation of larger vessels or innovative assets with increased weather limits for specific operations like e.g. cable pull-in, anchor installation or mooring line to anchor connection to overcome weather induced down times.

- The connection of bottom chain and anchor might benefit from innovative concepts to avoid the need for surface piercing operations. Even though heave compensation already has positive impact on the workability, subsea operations with e.g. heavy work class ROV or other subsea solutions are required.

The cost assessment of the marine operations leads to the following considerations:

- It is expected that the ActiveFloat concept entails a relatively seen less cost-intensive installation campaign than Windcrete. This is the expectation for the all P-values. The relative cost reduction of ActiveFloat in comparison to Windcrete is approximately 30%. Main cost driver is the operational durations for the two concepts.
- The CAPEX assessment shows that approximately two thirds of the costs are tied to the floater installation of wind turbines and OSS (including anchor installation, mooring line deployment and floater hook-up), while the power cable installation (IAC and export) accounts for one third of the costs.
- The uncertainty attached to the two concepts' CAPEX estimations is very similar at this point. Additional clarifications regarding vessel requirements could be utilised to confirm this understanding for the current scope.
- The cost assessment focussed on the marine operations only. It is proposed to include other cost factors like the wind turbine integration or the port requirements into the cost assessment as well to get a more holistic understanding of the expected CAPEX and the sensitivities for the two scenarios.

**Disclaimer**

*The authors cannot make any representations or warranties of any kind, express, or implied about the completeness, accuracy or reliability of the information and related graphics. Any reliance placed on this information is at own risk and in no event shall the authors be held liable for any loss, damage including without limitation indirect or consequential damage or any loss or damage whatsoever arising from reliance on same.*

*The outlined input parameters shall not be used as a basis for a specific commercial project, as they will vary from case to case. The information is not intended to serve as an exhaustive list of all relevant parameters for a specific project. The report is based on a comprehensive assessment and the authors do not recommend or promote any technology, software or methodology above one another*

## 9 References

- [1] M.-A. Schwarzkopf, F. Borisade, D. Matha, M. D. Kallinger, M. Y. Mahfouz, R. D. Vicente and S. Muñoz, "COREWIND, Deliverable D4.1, Identification of floating-wind-specific O&M requirements and monitoring technologies," 2020.
- [2] M. Chemineau, F. Castillo, V. Arramounet, P. Trubat, C. Molins, F. Vigarà, G. de Guglielmo, C. Cortés, M. Y. Mahfouz, Q. Pan, T. Bailey, M. Schilling, F. Borisade and X. Ren, "COREWIND, Deliverable D2.2, Design analysis and optimization of mooring and anchoring system for floating wind turbines," 2022.
- [3] F. Vigarà, L. Cerdán, R. Durán, S. Muñoz, M. Lynch, S. Doole, C. Molins, P. Trubat and R. Guanche, "COREWIND, Deliverable D1.2, Design basis," 2020.
- [4] J. Verma, J. I. Rapha, J. L. Domínguez and V. Ferreira, "COREWIND, D6.1 General frame of the analysis and description of the new FOW assessment app," 2020.
- [5] M.-A. Schwarzkopf, F. Borisade, J. Espelage, E. Johnston, R. D. Vicente, S. Muñoz, P. Hylland, W. He, J. Urbano, F. J. Comas, A. Arribas, M. S. Rodríguez and S. F. Ruano, "COREWIND, Deliverable D4.2, Floating Wind O&M Strategies Assessment," 2021.
- [6] M. Y. Mahfouz, M. Salari, S. Hernández, F. Vigarà, C. Molins, P. Trubat, H. Bredmose and A. Pegalajar-Jurado, "COREWIND, Deliverable D1.3, Public design and FAST models of the two 15MW floater-turbine concepts," 2020.
- [7] T. J. & H. A. M. Larsen, "How 2 HAWC2, the user's manual," *Risø National Laboratory*, 2007.
- [8] N. G. Jacobsen, "waves2foam manual.," *Deltares, The Netherlands*, 570., 2017.
- [9] P. Troman, A. Anaturk and Hagemeyer, "A New Model For the Kinematics Of Large Ocean Waves- Application As a Design Wave," *ISOPE-I-91-154*, 1991.
- [10] S. Doole, J. I. Rapha, F. Castillo, F. Borisade and M. S. Rodríguez, "COREWIND, Deliverable D3.2, Analysis and optimisation of dynamic cabling design for floating offshore wind farms," 2022.
- [11] "Shoreline," Shoreline AS, [Online]. Available: <https://www.shoreline.no/>. [Accessed 26 08 2021].
- [12] DOE, "DOE's Water Power Technology Office's (WPTO) US Wave dataset," [Online]. Available: <https://registry.opendata.aws/wpto-pds-us-wave/>. [Accessed 02 12 2022].
- [13] NREL, "Marine Energy Atlas," [Online]. Available: <https://maps.nrel.gov/marine-energy-atlas/download/big-data>. [Accessed 02 12 2022].
- [14] UCAR, "Research Data Archive, NCEP Climate Forecast System Reanalysis (CFSR) Selected Hourly Time-Series Products, January 1979 to December 2010," [Online]. Available: <https://rda.ucar.edu/datasets/ds093.1/>. [Accessed 02 12 2022].

- [15] BOEM, "Ocean Reports," [Online]. Available: <https://marinecadastre.gov/oceanreports>. [Accessed 02 12 2022].
- [16] USACE, "Coastal Ocean Data System- CODS: Wave Information Study Work Unit (WIS)," [Online]. Available: [https://wis.erdc.dren.mil/wis\\_project\\_overview.html](https://wis.erdc.dren.mil/wis_project_overview.html). [Accessed 02 12 2022].
- [17] Shoreline, "How to add weather files to a case," [Online]. Available: <https://design.support.shoreline.no/support/solutions/articles/80000756191-how-to-add-weather-files-to-a-case#era5>. [Accessed 02 12 2022].
- [18] Copernicus, "ERA5 hourly data on single levels from 1959 to present," [Online]. Available: <https://cds.climate.copernicus.eu/cdsapp#!/dataset/reanalysis-era5-single-levels?tab=overview>. [Accessed 02 12 2022].
- [19] ECMWF, "ERA5: data documentation," [Online]. Available: <https://confluence.ecmwf.int/display/CKB/ERA5%3A+data+documentation#ERA5:datadocumentation-Introduction>. [Accessed 02 12 2022].
- [20] C. Stefanakos, "Intercomparison of Wave Reanalysis based on ERA5 and WW3 Databases," in *Proceedings of the Twenty-ninth (2019) International Ocean and Polar Engineering Conference*, Honolulu, Hawaii, USA, 2019.
- [21] AACE International, Recommended Practice No. 18R-97, Cost Estimate Classification System - As applied in engineering, procurement and construction for the process industries, 2005.